Wave propagation methods for hyperbolic problems on mapped grids

A France-Taiwan Orchid Project Progress Report 2008-2009

Keh-Ming Shyue

Department of Mathematics

National Taiwan University

Taiwan

Talk objective

- Review a body-fitted mapped grid approach for numerical approximation of hyperbolic balance laws in multi-D with complex geometries
- Present numerical results for problems arising from
  - Compressible inviscid gas flow
  - Barotropic cavitating flow
  - Shallow granular avalanches

Mathematical model

Consider a hyperbolic balance laws of the form

$$\frac{\partial}{\partial t} q\left(\vec{x}, t\right) + \sum_{j=1}^{N} \frac{\partial}{\partial x_j} f_j\left(q, \vec{x}\right) = \psi(q)$$

in a general multidimensional domain

- $\vec{x} = (x_1, x_2, \ldots, x_N)$: spatial vector, t: time
- $q \in \mathbb{R}^m$: vector of m state quantities
- $f_j \in \mathbb{R}^m$: flux vector, $\psi \in \mathbb{R}^m$: source terms

Model is assumed to be hyperbolic, where $\sum_{j=1}^{N} \alpha_j \left(\partial f_j / \partial q\right)$ is diagonalizable with real e-values $\forall \alpha_j \in \mathbb{R}$

Mathematical model (Cont.)

In a body-fitted mapped grid approach, we introduce a coordinate change $\vec{x} \mapsto \vec{\xi}$ via

$$\vec{\xi} = (\xi_1, \xi_2, \ldots, \xi_N), \qquad \xi_j = \xi_j(\vec{x})$$

that transform a physical domain Ω to a logical one $\hat{\Omega}$, see below when $N = 2$,

physical domain

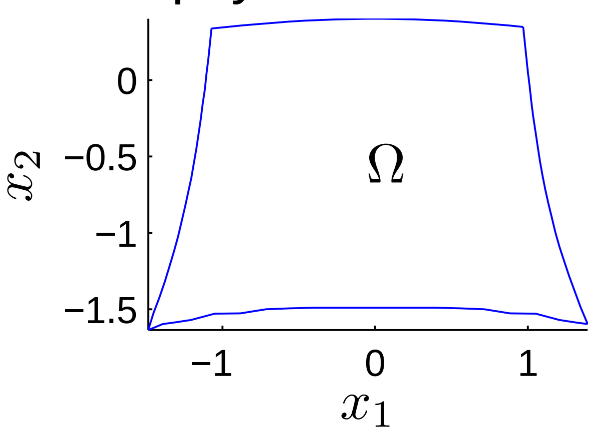

mapping

$$\longrightarrow$$

$$\xi_1 = \xi_1(x_1, x_2)$$
$$\xi_2 = \xi_2(x_1, x_2)$$

logical domain

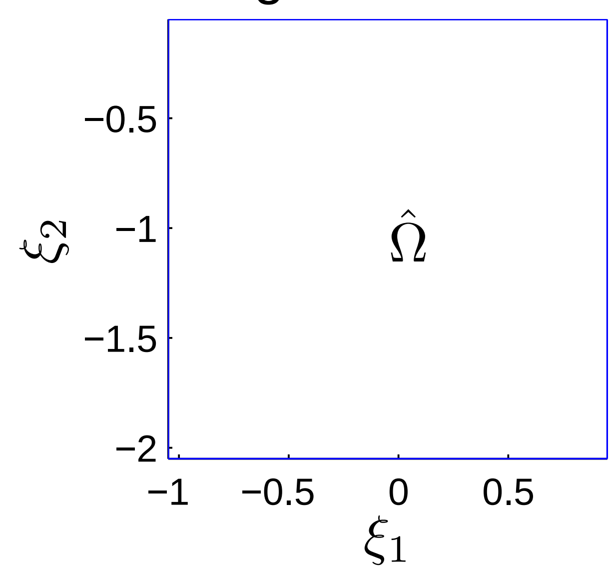

Mathematical model (Cont.)

In a body-fitted mapped grid approach, we introduce a coordinate change $\vec{x} \mapsto \vec{\xi}$ via

$$\vec{\xi} = (\xi_1, \xi_2, \ldots, \xi_N)\,, \qquad \xi_j = \xi_j(\vec{x})$$

that transform a physical domain Ω to a logical one $\hat{\Omega}$, and so equations into the form

$$\frac{\partial q}{\partial t} + \sum_{j=1}^{N} \frac{\partial \tilde{f}_j}{\partial \xi_j} = \psi(q)$$

with

$$\tilde{f}_j = \sum_{k=1}^{N} f_k \frac{\partial \xi_j}{\partial x_k}$$

Mathematical model (Cont.)

Basic coordinate mapping relations in $N = 3$ are

$$\begin{pmatrix} 1 & 0 & 0 & 0 \\ 0 & \partial_{x_1}\xi_1 & \partial_{x_2}\xi_1 & \partial_{x_3}\xi_1 \\ 0 & \partial_{x_1}\xi_2 & \partial_{x_2}\xi_2 & \partial_{x_3}\xi_2 \\ 0 & \partial_{x_1}\xi_3 & \partial_{x_2}\xi_3 & \partial_{x_3}\xi_3 \end{pmatrix} = \frac{1}{J} \begin{pmatrix} J & 0 & 0 & 0 \\ 0 & J_{11} & J_{21} & J_{31} \\ 0 & J_{12} & J_{22} & J_{32} \\ 0 & J_{13} & J_{23} & J_{33} \end{pmatrix}$$

where $J = |\partial(x_1, x_2, x_3)/\partial(\xi_1, \xi_2, \xi_3)| = \text{det}\,(\partial(x_1, x_2, x_3)/\partial(\xi_1, \xi_2, \xi_3))$,

$$J_{11} = \left|\frac{\partial(x_2, x_3)}{\partial(\xi_2, \xi_3)}\right|, \quad J_{21} = \left|\frac{\partial(x_1, x_3)}{\partial(\xi_3, \xi_2)}\right|, \quad J_{31} = \left|\frac{\partial(x_1, x_2)}{\partial(\xi_2, \xi_3)}\right|,$$

$$J_{12} = \left|\frac{\partial(x_2, x_3)}{\partial(\xi_3, \xi_1)}\right|, \quad J_{22} = \left|\frac{\partial(x_1, x_3)}{\partial(\xi_1, \xi_3)}\right|, \quad J_{32} = \left|\frac{\partial(x_1, x_2)}{\partial(\xi_3, \xi_1)}\right|,$$

$$J_{13} = \left|\frac{\partial(x_2, x_3)}{\partial(\xi_1, \xi_2)}\right|, \quad J_{23} = \left|\frac{\partial(x_1, x_3)}{\partial(\xi_2, \xi_1)}\right|, \quad J_{33} = \left|\frac{\partial(x_1, x_2)}{\partial(\xi_1, \xi_2)}\right|.$$

Compressible Euler equations

- Cartesian coordinate case

$$\frac{\partial}{\partial t}\begin{pmatrix}\rho\\ \rho u_i\\ E\end{pmatrix}+\sum_{j=1}^{N}\frac{\partial}{\partial x_j}\begin{pmatrix}\rho u_j\\ \rho u_i u_j+p\delta_{ij}\\ Eu_j+pu_j\end{pmatrix}=\begin{pmatrix}0\\ -\rho\partial_{x_i}\phi\\ -\rho\vec{u}\cdot\nabla\phi\end{pmatrix}, \quad i=1,\ldots,N$$

- Generalized coordinate case

$$\frac{\partial}{\partial t}\begin{pmatrix}\rho\\ \rho u_i\\ E\end{pmatrix}+\sum_{j=1}^{N}\frac{\partial}{\partial \xi_j}\begin{pmatrix}\rho U_j\\ \rho u_i U_j+p\partial_{x_i}\xi_j\\ EU_j+pU_j\end{pmatrix}=\begin{pmatrix}0\\ -\rho\partial_{x_i}\phi\\ -\rho\vec{u}\cdot\nabla\phi\end{pmatrix}$$

ρ: density, $p=p(\rho,e)$: pressure , e: internal energy

$E=\rho e+\rho\sum_{j=1}^{N}u_j^2/2$: total energy, ϕ: gravitational potential

$U_j=\partial_t\xi_j+\sum_{i=1}^{N}u_i\partial_{x_i}\xi_j$: contravariant velocity in ξ_j-direction

Finite volume approximation

Employ finite volume formulation of numerical solution

$$Q^n_{ijk} \approx \frac{1}{\Delta\xi_1 \Delta\xi_2 \Delta\xi_3} \int_{C_{ijk}} q(\xi_1, \xi_2, \xi_3, t_n)\, dV$$

that gives approximate value of cell average of solution q over cell C_{ijk} at time t_n (sample case in $2D$ shown below)

physical domain

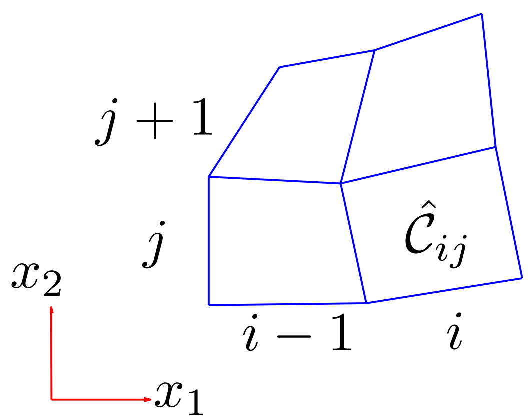

mapping

$$\longleftarrow$$

$$x_1 = x_1(\xi_1, \xi_2)$$
$$x_2 = x_2(\xi_1, \xi_2)$$

logical domain

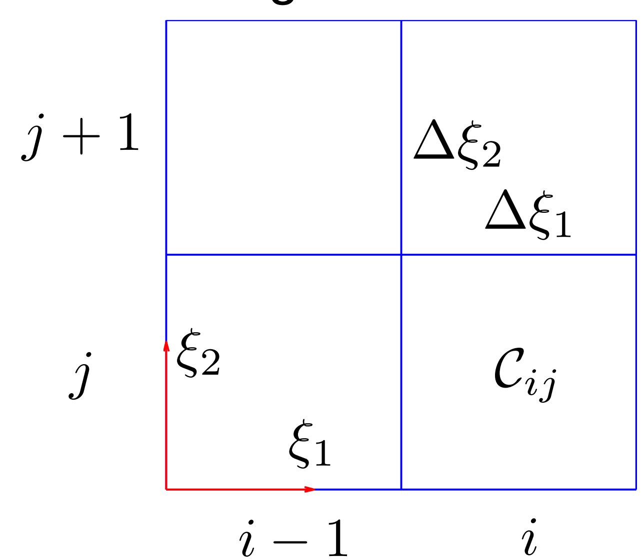

Finite volume (Cont.)

In three dimensions $N = 3$, equations to be solved take

$$\frac{\partial q}{\partial t} + \sum_{j=1}^{N} \frac{\partial \tilde{f}_j}{\partial \xi_j} = \psi(q)$$

A simple dimensional-splitting method based on wave propagation approach of LeVeque *et al.* is used, *i.e.*,

- Solve one-dimensional Riemann problem normal at each cell interfaces
- Use resulting jumps of fluxes (decomposed into each wave family) of Riemann solution to update cell averages
- Introduce limited jumps of fluxes to achieve high resolution

Finite volume (Cont.)

Basic steps of a dimensional-splitting scheme

- ξ_1-sweeps: solve

$$\frac{\partial q}{\partial t} + \frac{\partial \tilde{f}_1}{\partial \xi_1} = 0 \quad \text{updating} \quad Q^n_{ijk} \text{ to } \quad Q^*_{ijk}$$

- ξ_2-sweeps: solve

$$\frac{\partial q}{\partial t} + \frac{\partial \tilde{f}_2}{\partial \xi_2} = 0 \quad \text{updating} \quad Q^*_{ijk} \text{ to } \quad Q^{**}_{ijk}$$

- ξ_3-sweeps: solve

$$\frac{\partial q}{\partial t} + \frac{\partial \tilde{f}_3}{\partial \xi_3} = 0, \quad \text{updating} \quad Q^{**}_{ijk} \text{ to } \quad Q^{n+1}_{ijk}$$

Finite volume (Cont.)

Consider ξ_1-sweeps, for example,

- First order update is

$$Q^*_{ijk} = Q^n_{ijk} - \frac{\Delta t}{\Delta \xi_1}\left[\left(\mathcal{A}_1^+ \Delta Q\right)^n_{i-1/2,jk} + \left(\mathcal{A}_1^- \Delta Q\right)^n_{i+1/2,jk}\right]$$

with the fluctuations

$$(\mathcal{A}_1^+ \Delta Q)^n_{i-1/2,jk} = \sum_{m:(\lambda_{1,m})^n_{i-1/2,jk}>0} (\mathcal{Z}_{1,m})^n_{i-1/2,jk}$$

and

$$(\mathcal{A}_1^- \Delta Q)^n_{i+1/2,jk} = \sum_{m:(\lambda_{1,m})^n_{i+1/2,jk}<0} (\mathcal{Z}_{1,m})^n_{i+1/2,jk}$$

$(\lambda_{1,m})^n_{\iota-1/2,jk}$ & $(\mathcal{Z}_{1,m})^n_{\iota-1/2,jk}$ are in turn wave speed and f-waves for the mth family of the 1D Riemann problem solutions

Finite volume (Cont.)

- High resolution correction is

$$Q^*_{ijk} := Q^*_{ijk} - \frac{\Delta t}{\Delta \xi_1}\left[\left(\tilde{\mathcal{F}}_1\right)^n_{i+1/2,jk} - \left(\tilde{\mathcal{F}}_1\right)^n_{i-1/2,jk}\right]$$

with $$(\tilde{\mathcal{F}}_1)^n_{i-1/2,jk} = \frac{1}{2}\sum_{m=1}^{m_w}\left[\text{sign}\left(\lambda_{1,m}\right)\left(1 - \frac{\Delta t}{\Delta \xi_1}\left|\lambda_{1,m}\right|\right)\tilde{\mathcal{Z}}_{1,m}\right]^n_{i-1/2,jk}$$

$\tilde{\mathcal{Z}}_{\iota,m}$ is a limited value of $\mathcal{Z}_{\iota,m}$

It is clear that this method belongs to a class of upwind schemes, and is stable when the typical CFL (Courant-Friedrichs-Lewy) condition:

$$\nu = \frac{\Delta t \max_m\left(\lambda_{1,m}, \lambda_{2,m}, \lambda_{3,m}\right)}{\min\left(\Delta \xi_1, \Delta \xi_2, \Delta \xi_3\right)} \le 1,$$

Smooth vortex flow: accuracy test

- Compressible Euler equations with ideal gas law
- Initial condition for vortex is set by

$$
\begin{aligned}
\rho &= \left(1 - \frac{25(\gamma-1)}{8\gamma\pi^2}\exp\left(1-r^2\right)\right)^{1/(\gamma-1)}, \\
p &= \rho^\gamma, \\
u_1 &= 1 - \frac{5}{2\pi}\exp\left(\left(1-r^2\right)/2\right)\left(x_2-5\right), \\
u_2 &= 1 + \frac{5}{2\pi}\exp\left(\left(1-r^2\right)/2\right)\left(x_1-5\right), \\
r &= \sqrt{(x_1-5)^2+(x_2-5)^2}
\end{aligned}
$$

- $\|E_z\|_{1,\infty} = \|z_{\text{comput}} - z_{\text{exact}}\|_{1,\infty}$: discrete 1- or maximum-norm for state variable z

Smooth vortex flow: accuracy test

- Density contours on a 40×40 grid at time $t = 10$

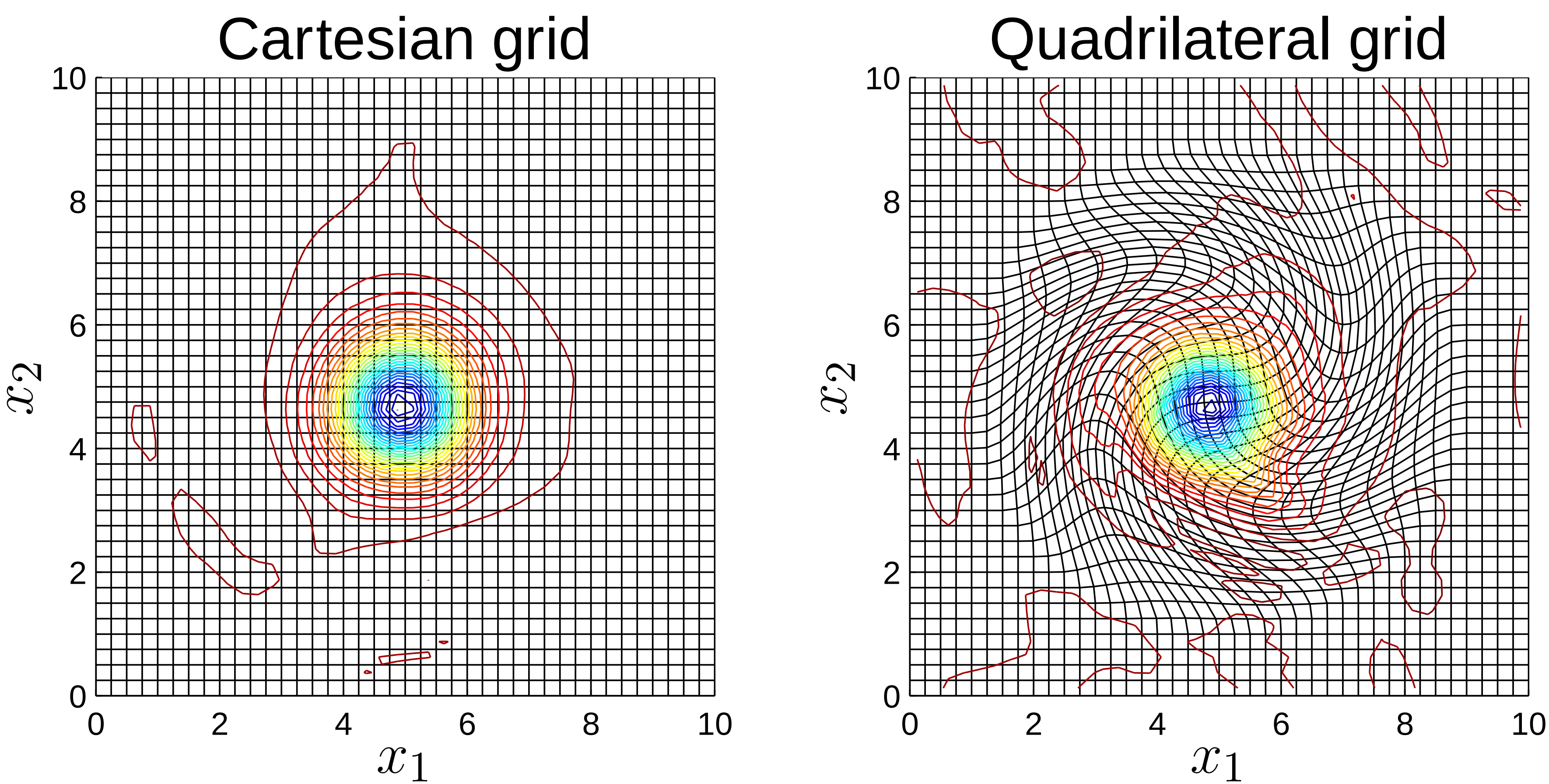

Smooth vortex flow: accuracy test

- Cartesian grid results

Mesh size	40×40	80×80	160×160	320×320	Order
$\Vert E_\rho \Vert_1$	$7.0710(-1)$	$1.9186(-1)$	$4.7927(-2)$	$1.1941(-2)$	1.97
$\Vert E_p \Vert_1$	$8.5264(-1)$	$2.3594(-1)$	$5.9209(-2)$	$1.4721(-2)$	1.96
$\Vert E_{u_1} \Vert_1$	$2.3716(00)$	$6.1437(-1)$	$1.5298(-1)$	$3.8204(-2)$	1.99
$\Vert E_{u_2} \Vert_1$	$1.9377(00)$	$4.7673(-1)$	$1.1773(-1)$	$2.9262(-2)$	2.02
$\Vert E_\rho \Vert_\infty$	$1.4587(-1)$	$3.8860(-2)$	$9.5936(-3)$	$2.3179(-3)$	2.00
$\Vert E_p \Vert_\infty$	$1.8528(-1)$	$5.0122(-2)$	$1.2401(-2)$	$3.0285(-3)$	1.98
$\Vert E_{u_1} \Vert_\infty$	$3.9934(-1)$	$1.0488(-1)$	$2.4857(-2)$	$6.1654(-3)$	2.01
$\Vert E_{u_2} \Vert_\infty$	$2.0948(-1)$	$5.5860(-2)$	$1.3506(-2)$	$3.3386(-3)$	2.00

Smooth vortex flow: accuracy test

- Quadrilateral grid results

Mesh size	40×40	80×80	160×160	320×320	Order
$\|E_\rho\|_1$	$1.1921(00)$	$4.1732(-1)$	$1.6058(-1)$	$7.0078(-2)$	1.36
$\|E_p\|_1$	$1.4984(00)$	$5.3128(-1)$	$2.1063(-1)$	$9.3740(-2)$	1.33
$\|E_{u_1}\|_1$	$2.7085(00)$	$8.5937(-1)$	$2.8118(-1)$	$1.0743(-1)$	1.56
$\|E_{u_2}\|_1$	$2.3014(00)$	$7.4990(-1)$	$2.7248(-1)$	$1.1608(-1)$	1.44
$\|E_\rho\|_\infty$	$1.8793(-1)$	$6.2063(-2)$	$1.9104(-2)$	$7.0730(-3)$	1.59
$\|E_p\|_\infty$	$2.2841(-1)$	$7.2502(-2)$	$2.1285(-2)$	$7.9266(-3)$	1.63
$\|E_{u_1}\|_\infty$	$4.0762(-1)$	$1.3207(-1)$	$4.2383(-2)$	$1.5737(-2)$	1.57
$\|E_{u_2}\|_\infty$	$2.6456(-1)$	$9.0362(-2)$	$2.7416(-2)$	$1.2385(-2)$	1.50

Shock waves over circular array

- A Mach 1.42 shock wave in water over a circular array

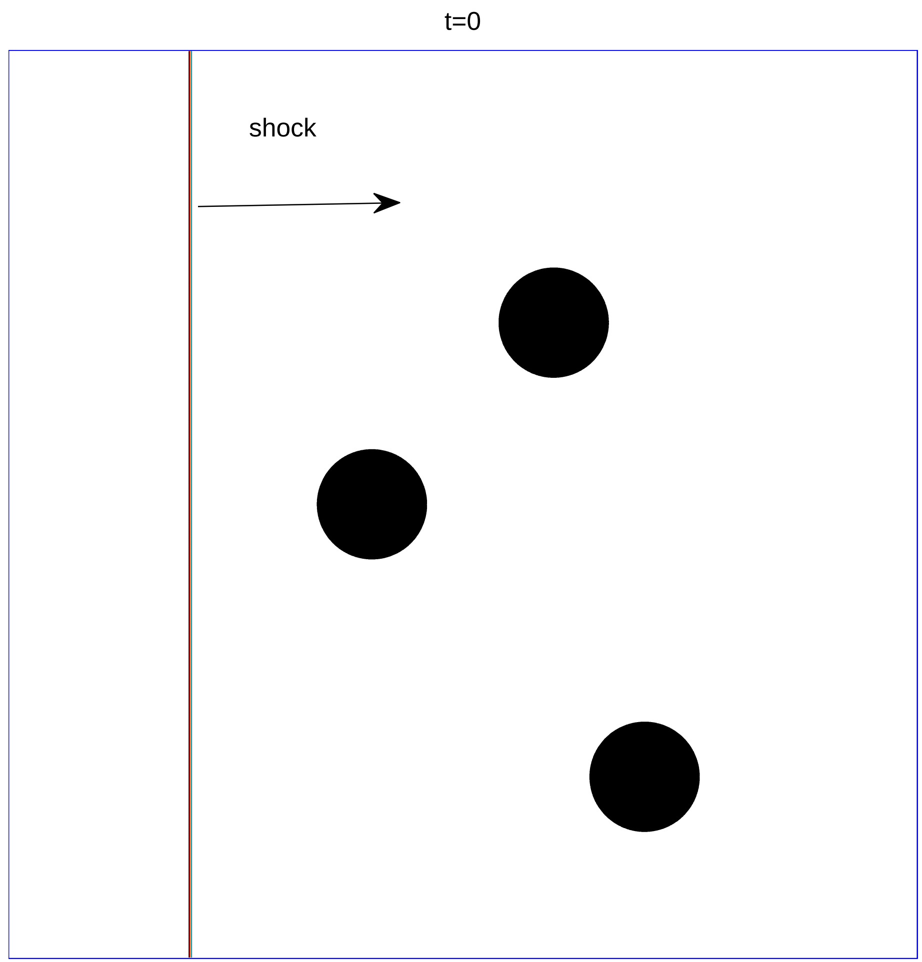

Shock waves over circular array

- Grid system

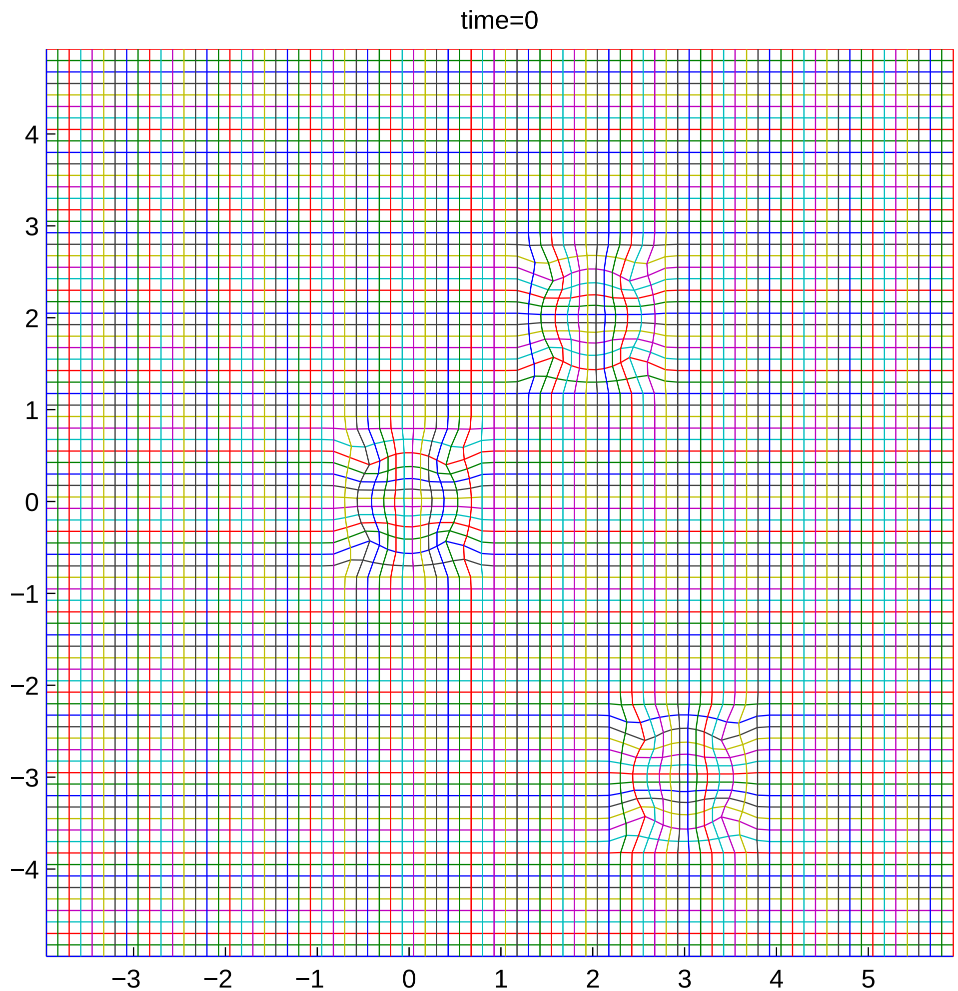

Shock waves over circular array

- Contours for density

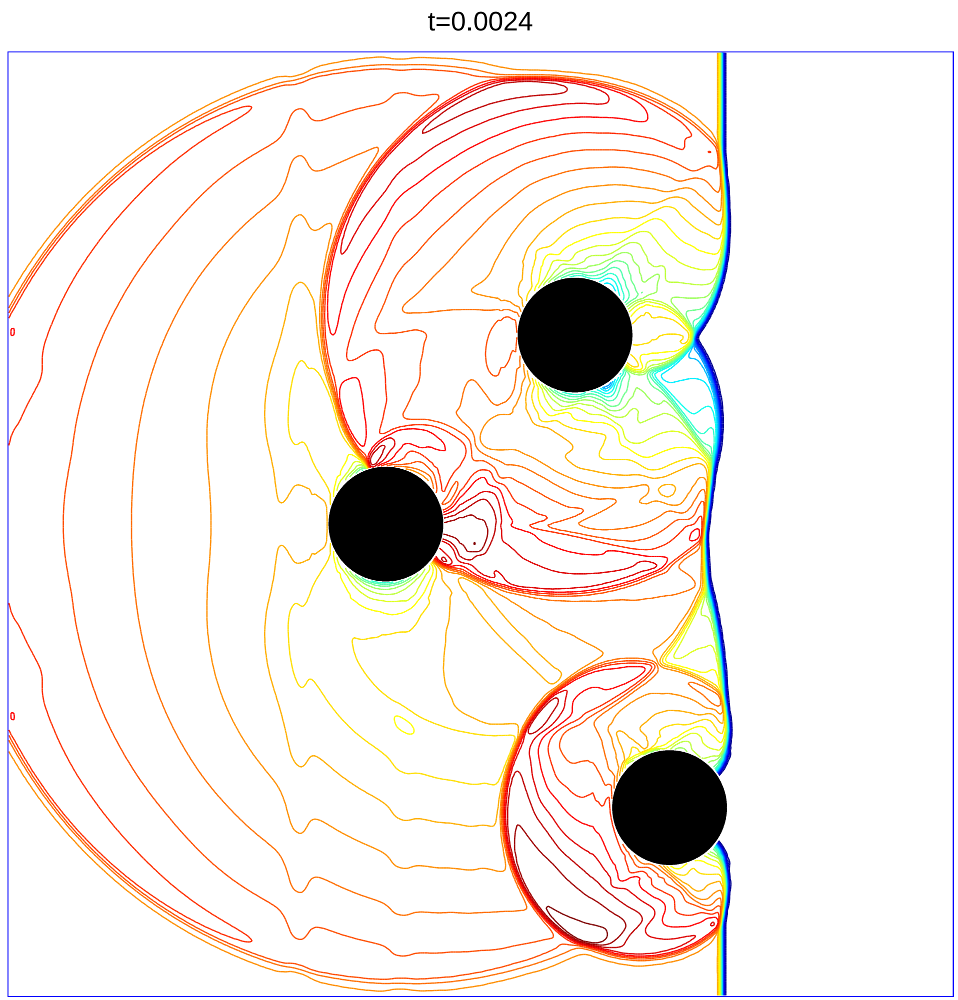

Steady state shock tracking

- A Mach 3 compressible gas flow over a 20^o ramp
- Exact shock location (an oblique shock with 37.8^o) is inserted into underlying grid for computation

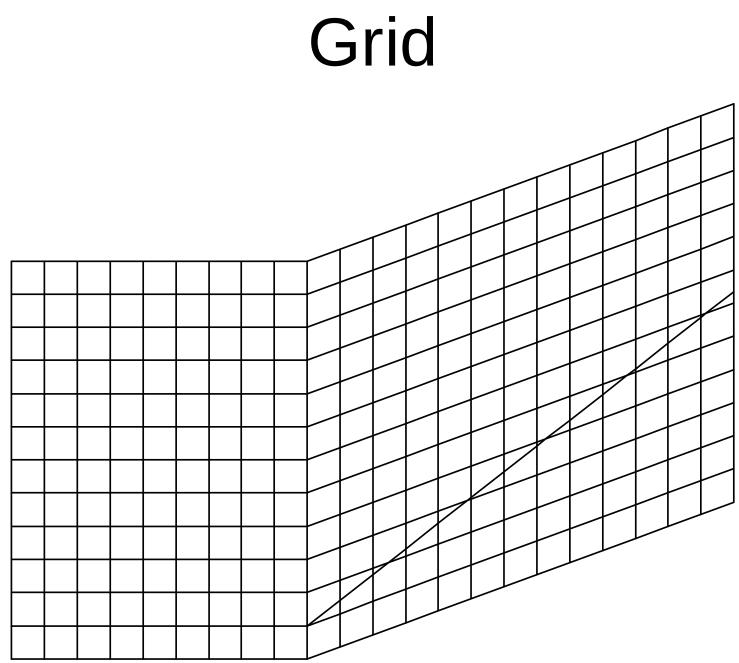

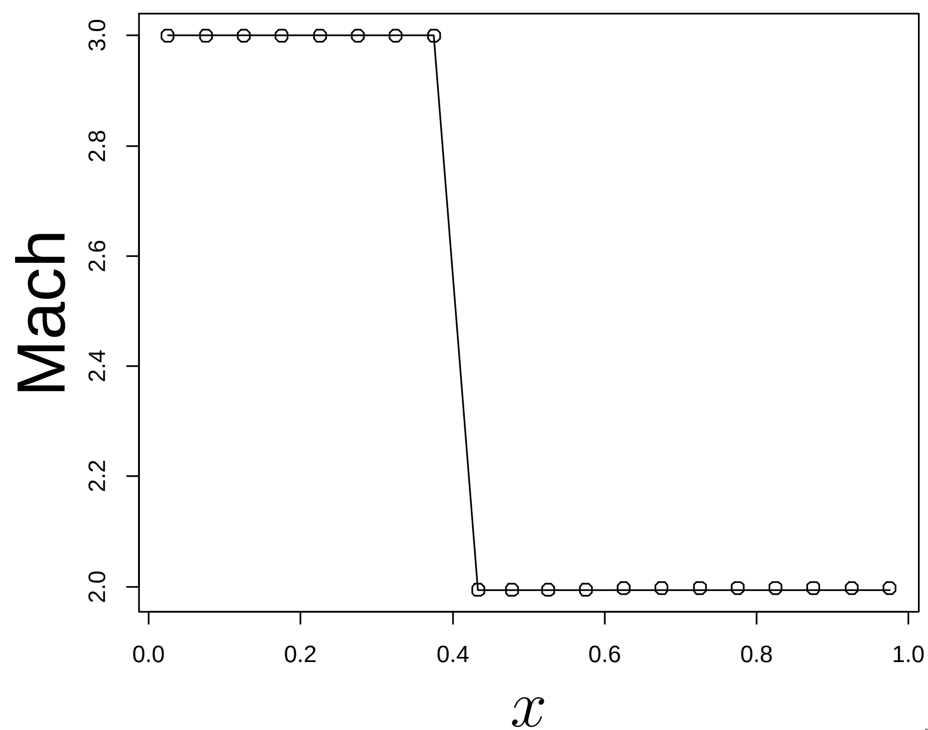

Compressible Multiphase Flow

- Homogeneous equilibrium pressure & velocity across material interfaces
- Volume-fraction based model equations (Shyue JCP '98, Allaire *et al.* JCP '02)

$$\frac{\partial}{\partial t}(\alpha_i \rho_i) + \frac{1}{J}\sum_{j=1}^{N_d} \frac{\partial}{\partial \xi_j}(\alpha_i \rho_i U_j) = 0, \quad i = 1, 2, \ldots, m_f$$

$$\frac{\partial}{\partial t}(\rho u_i) + \frac{1}{J}\sum_{j=1}^{N_d} \frac{\partial}{\partial \xi_j}(\rho u_i U_j + p J_{ji}) = 0, \quad i = 1, 2, \ldots, N_d,$$

$$\frac{\partial E}{\partial t} + \frac{1}{J}\sum_{j=1}^{N_d} \frac{\partial}{\partial \xi_j}(E U_j + p U_j) = 0,$$

$$\frac{\partial \alpha_i}{\partial t} + \frac{1}{J}\sum_{j=1}^{N_d} U_j \frac{\partial \alpha_i}{\partial \xi_j} = 0, \quad i = 1, 2, \ldots, m_f - 1;$$

Moving cylindrical vessel

- Initial setup

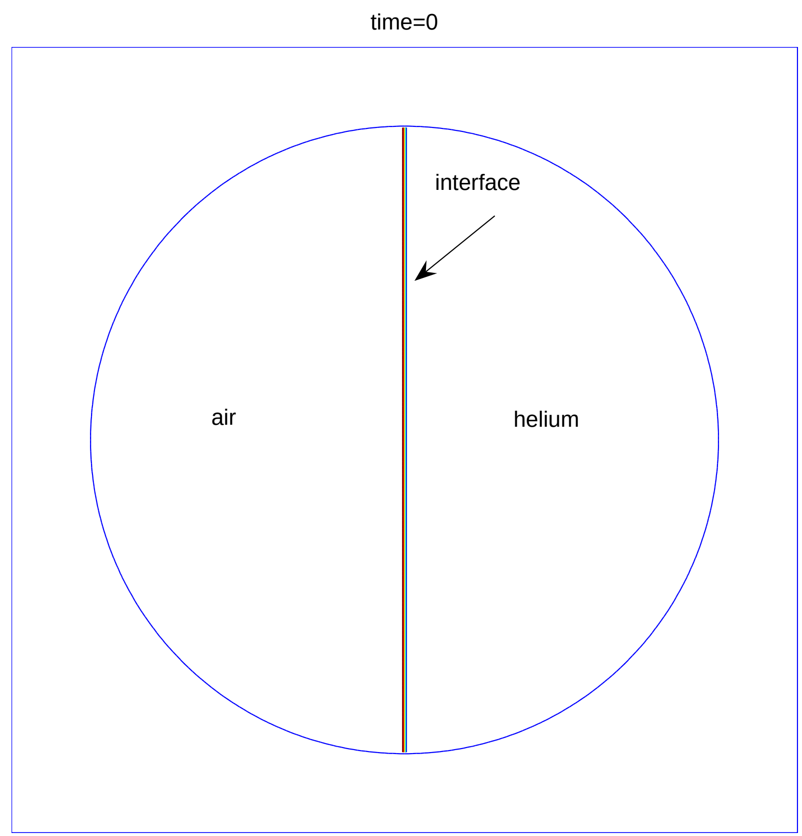

Moving cylindrical vessel

- Solution at time $t = 0.25$

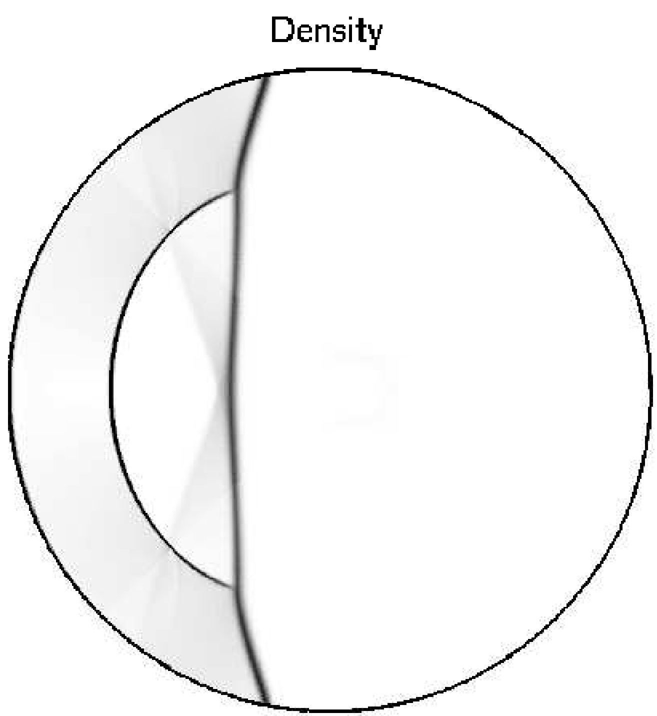

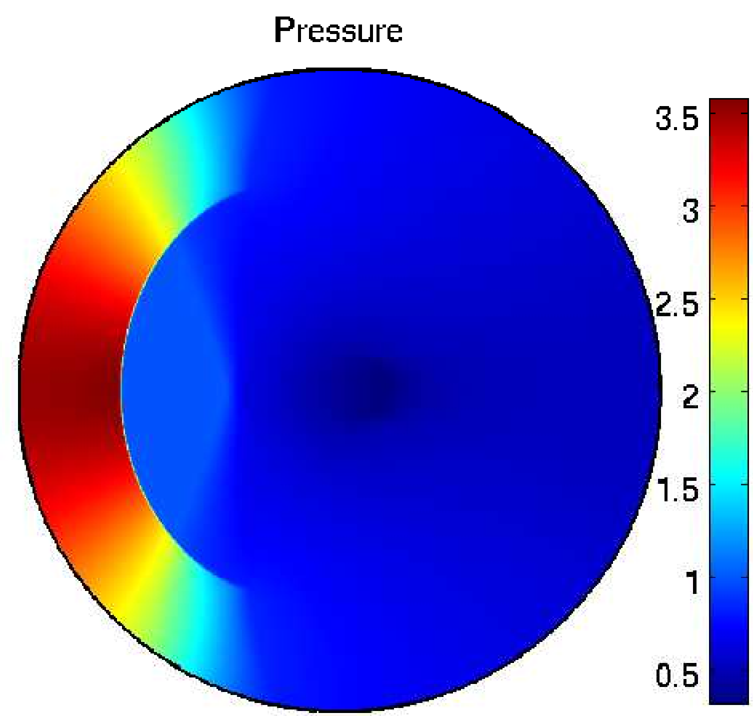

Moving cylindrical vessel

- Solution at time $t = 0.5$

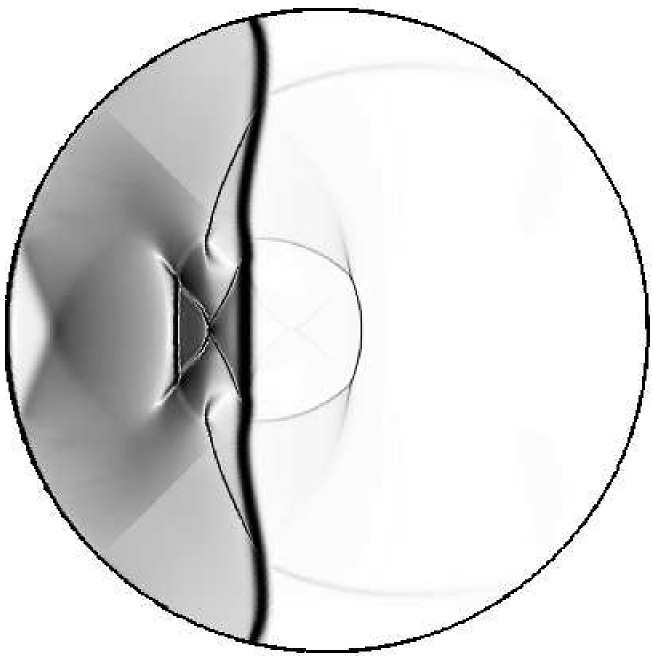

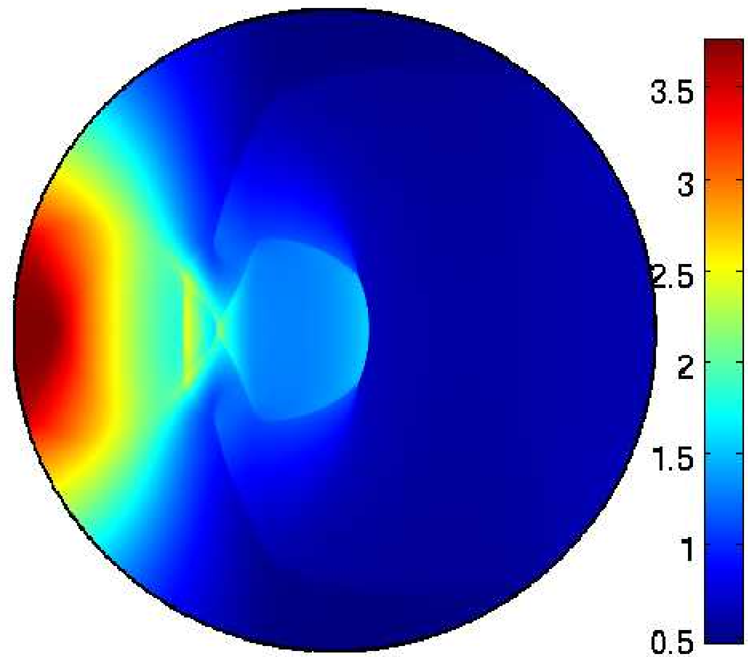

Moving cylindrical vessel

- Solution at time $t = 0.75$

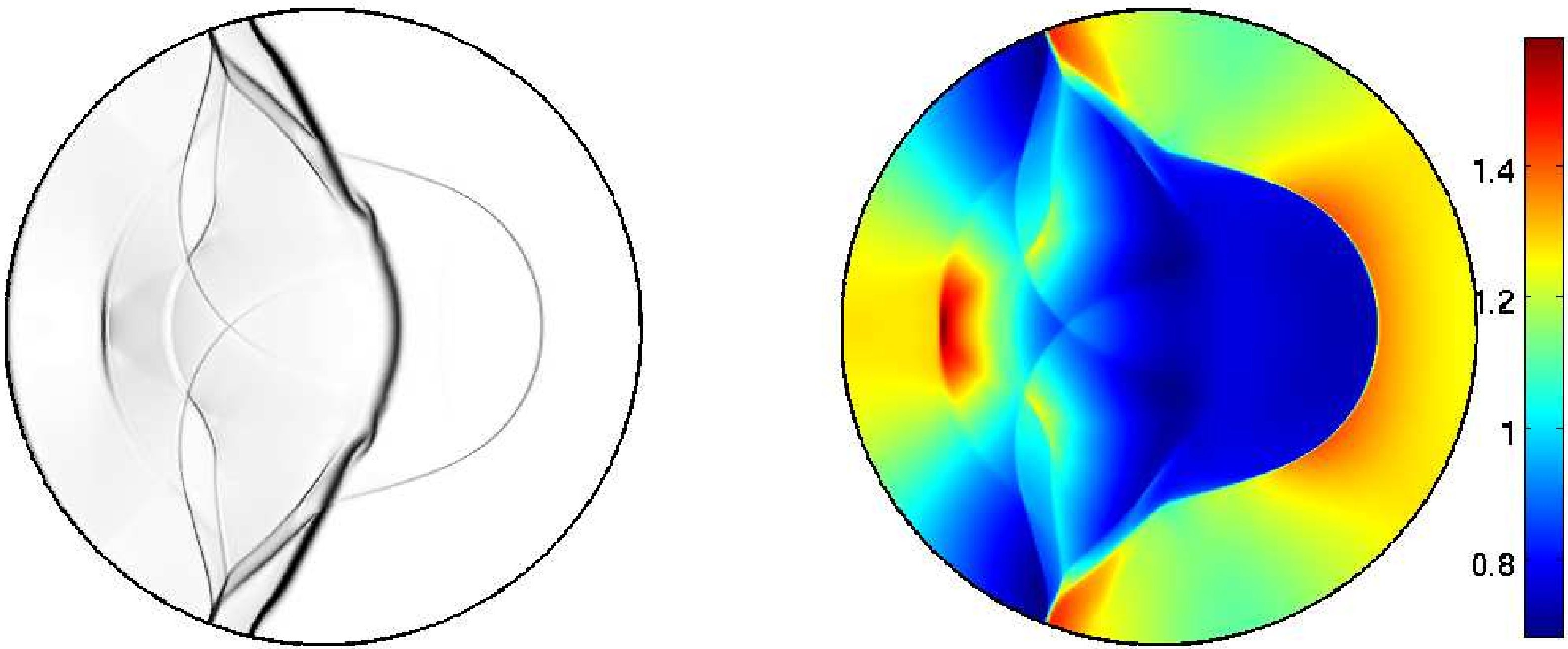

Moving cylindrical vessel

- Solution at time $t = 1$

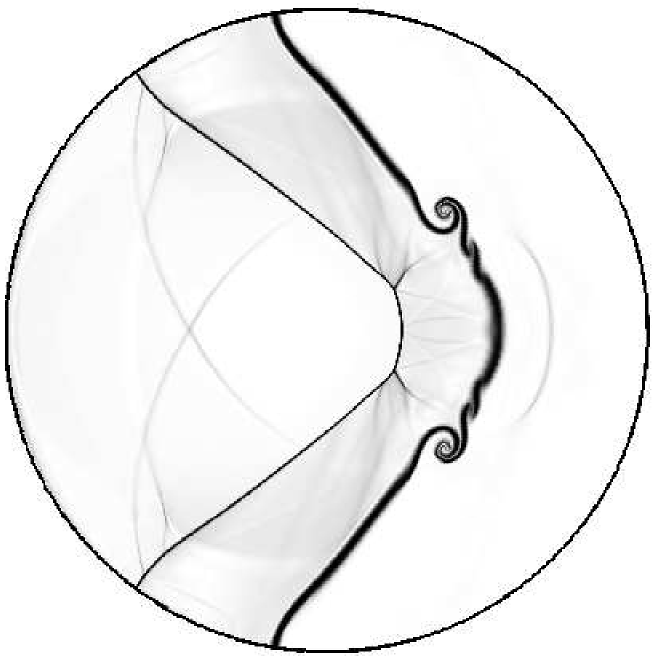

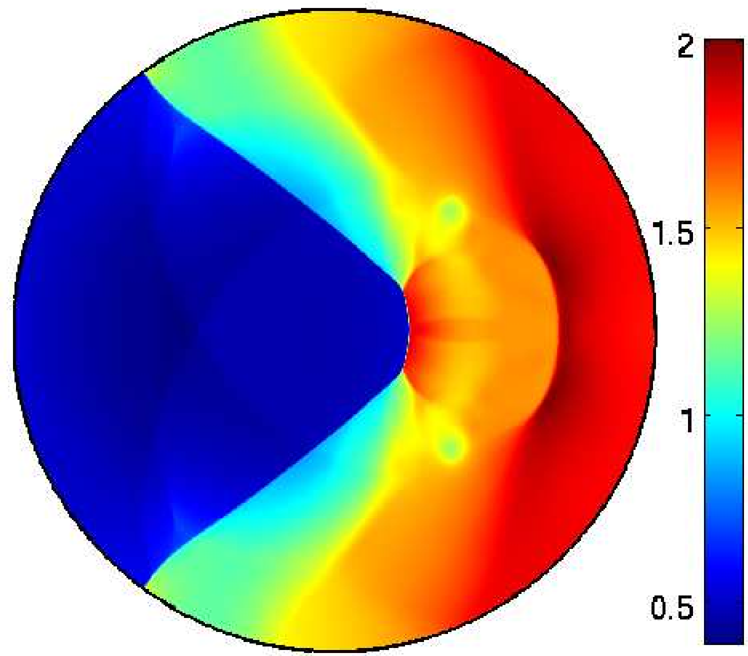

Moving cylindrical vessel

- cross-sectional plot along boundary

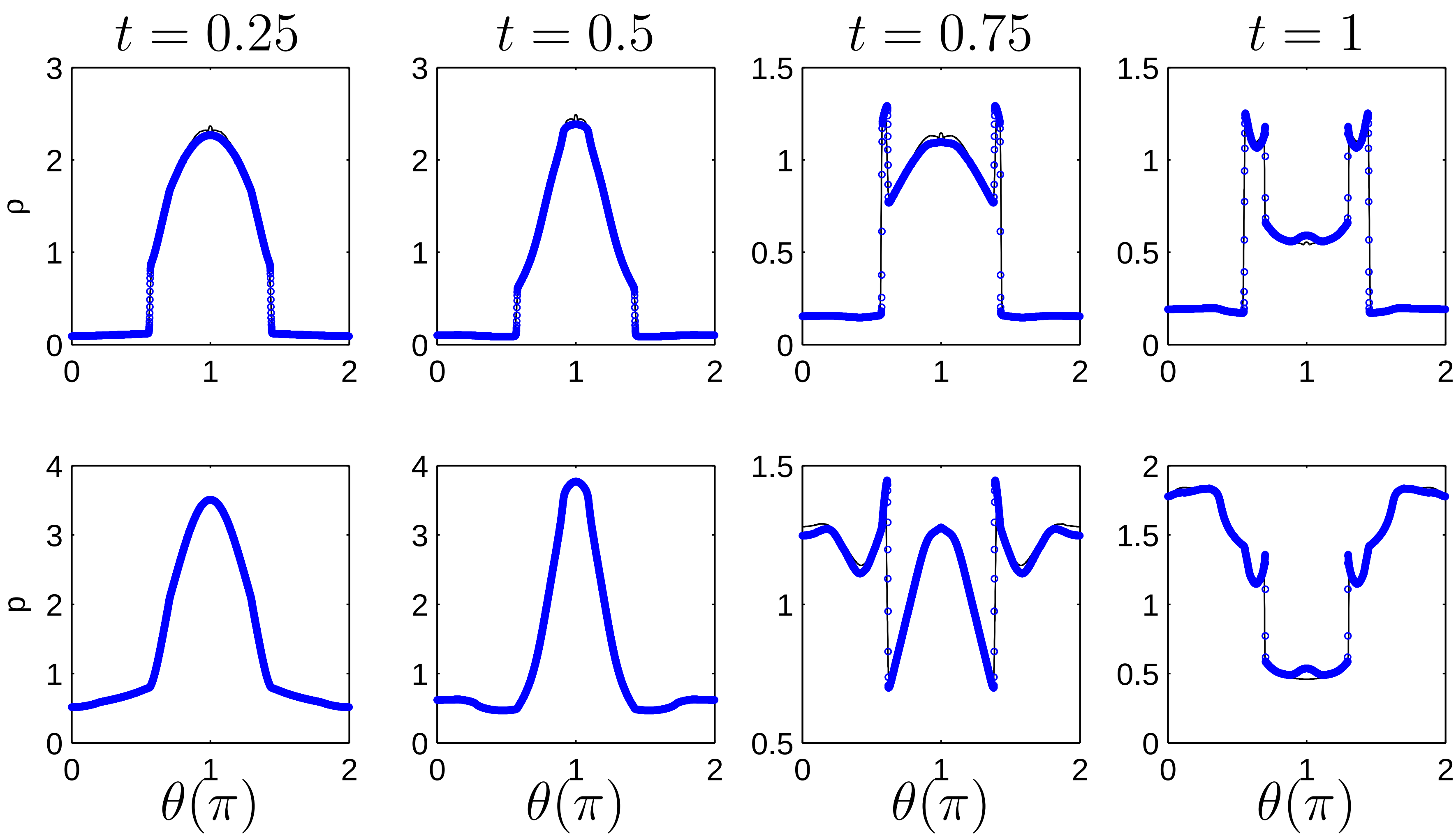

Barotropic cavitating flow

- A relaxation model of Saurel *et al.* (JCP '090

$$\frac{\partial}{\partial t}\left(\alpha_1\rho_1\right) + \sum_{j=1}^{N} \frac{\partial}{\partial x_j}\left(\alpha_1\rho_1 u_j\right) = 0,$$

$$\frac{\partial}{\partial t}\left(\alpha_2\rho_2\right) + \sum_{j=1}^{N} \frac{\partial}{\partial x_j}\left(\alpha_2\rho_2 u_j\right) = 0,$$

$$\frac{\partial}{\partial t}\left(\rho u_i\right) + \sum_{j=1}^{N} \frac{\partial}{\partial x_j}\left(\rho u_i u_j + p\delta_{ij}\right) = 0, \quad i = 1, \ldots, N$$

$$\frac{\partial \alpha_1}{\partial t} + \sum_{j=1}^{N} u_j \frac{\partial \alpha_1}{\partial x_j} = \frac{1}{\mu}\left(p_1\left(\rho_1\right) - p_2\left(\rho_2\right)\right)$$

Each phasic pressure p_ι satisfies $p_\iota(\rho) = \left(p_0 + \mathcal{B}\right)\left(\rho/\rho_0\right)^\gamma - \mathcal{B}$
Mixture pressure p satisfies $p = \alpha_1 p_1 + \alpha_2 p_2, \quad \mu$parameter

Mixture speed of sound

- Wood formula (stiffness in $\bar{c}$ vs. α)

$$\frac{1}{\rho \bar{c}^2} = \frac{\alpha}{\rho_{\text{w}} c_{\text{w}}^2} + \frac{1-\alpha}{\rho_{\text{g}} c_{\text{g}}^2}$$

$$\rho_{\text{w}} = 10^3 \text{kg/m}^3, \quad c_{\text{w}} = 1449.4 \text{m/s}, \quad \rho_{\text{g}} = 1.0 \text{kg/m}^3, \quad c_{\text{g}} = 374.2 \text{m/s}$$

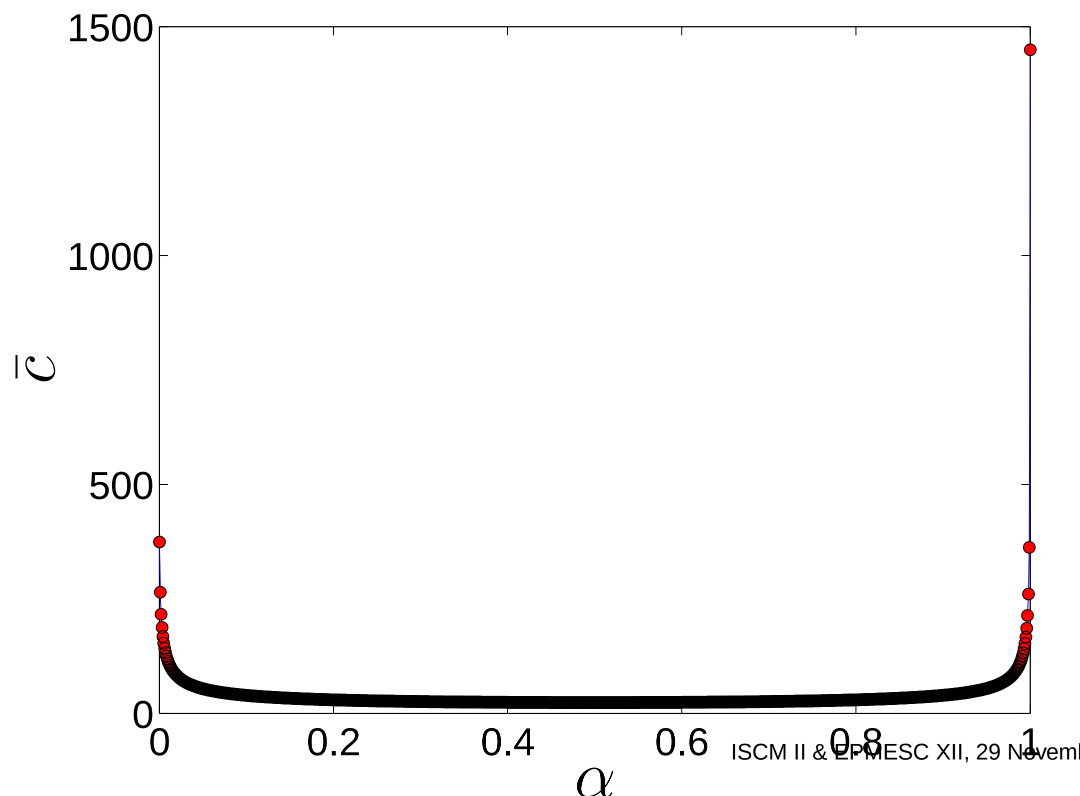

Cavitation test: 1D

- Homogeneous gas-liquid mixture with $\alpha_{\mathrm{g}} = 10^{-2}$

Cavitation test: 1D

- Formation of cavitating gas bubble

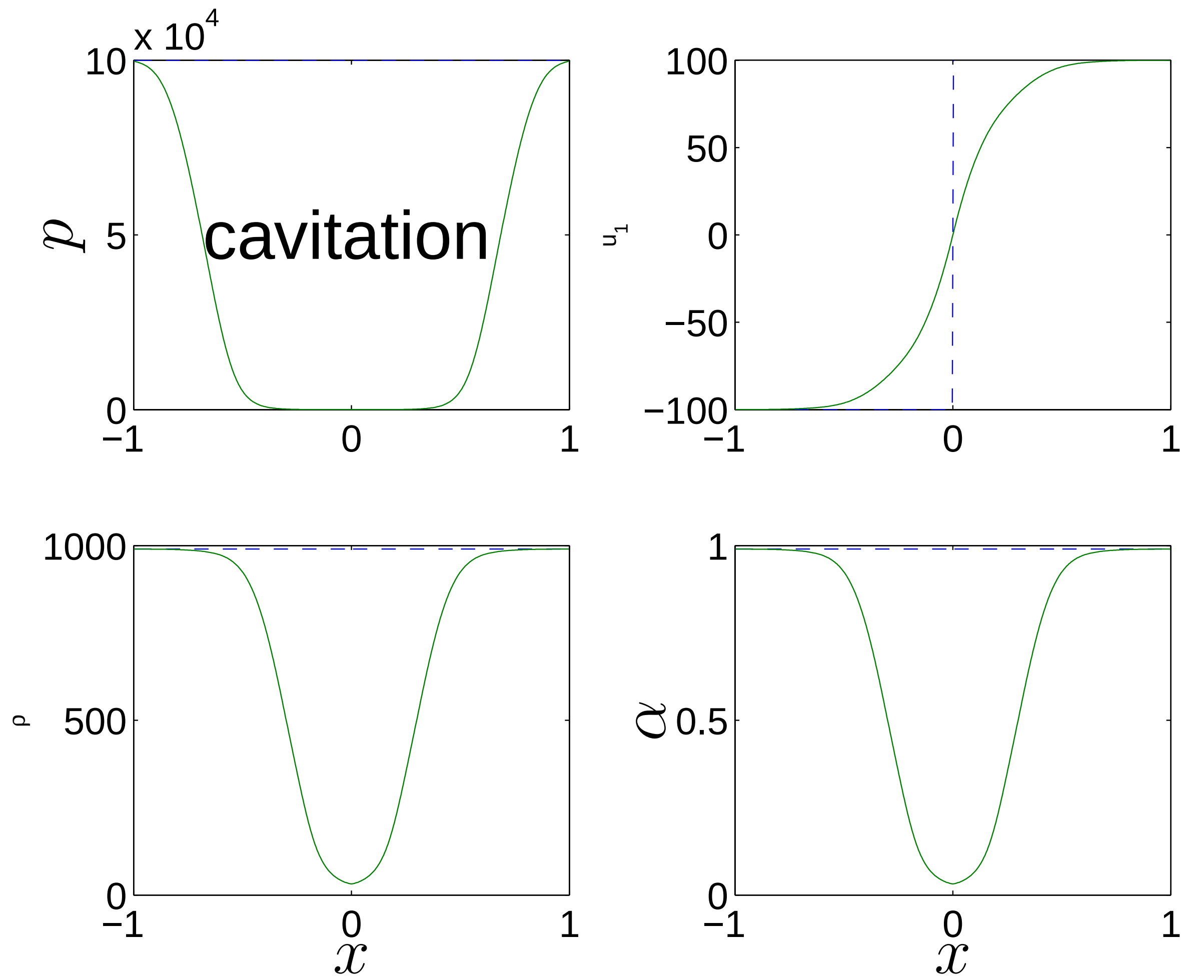

Cavitation test: 2D steady state

- Uniform gas-liquid mixture with speed 600m /s over a circular region

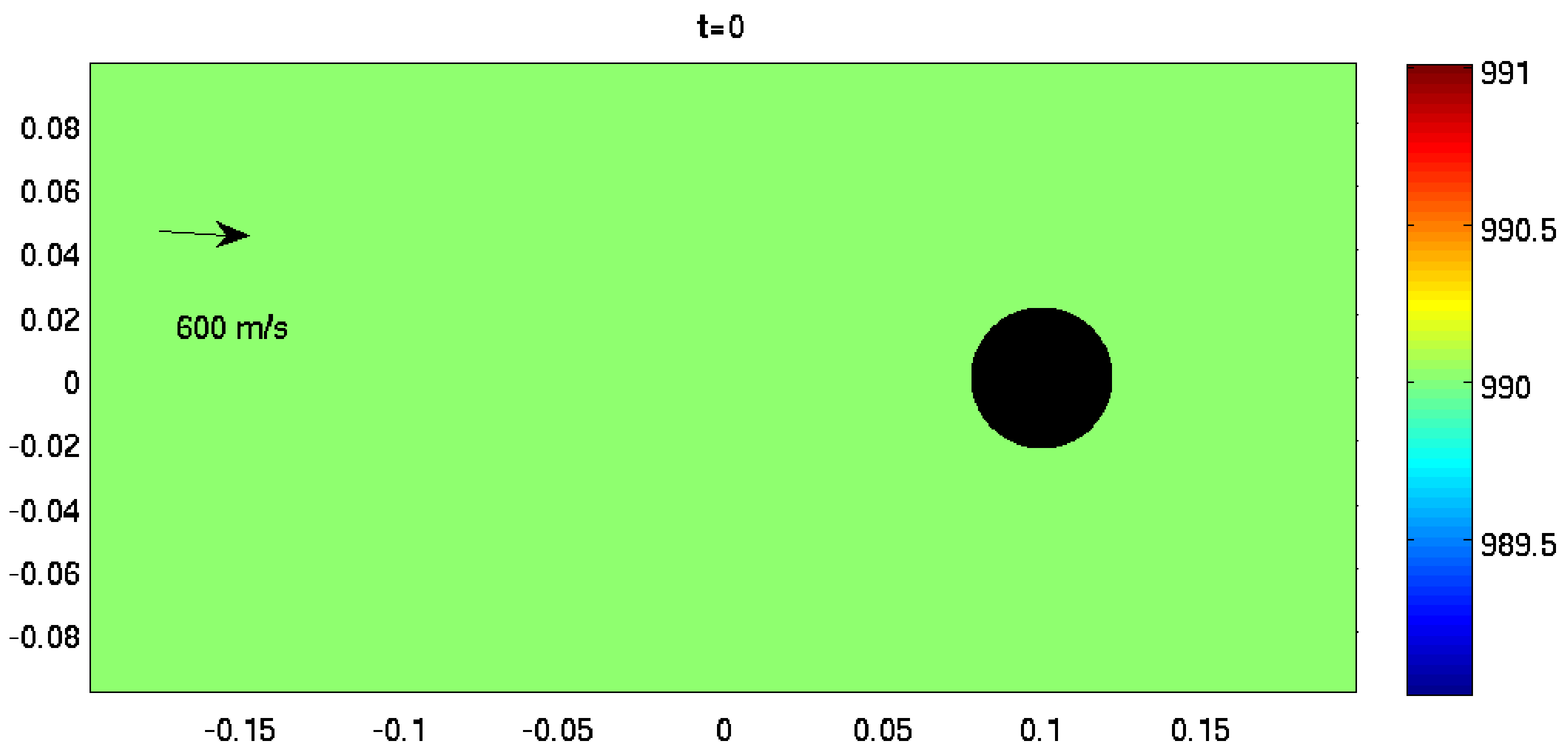

Cavitation test: 2D steady state

- Pseudo colors of volume fraction
  - Formation of cavitation zone (Onset–shock induced, diffusion, . . . ?)

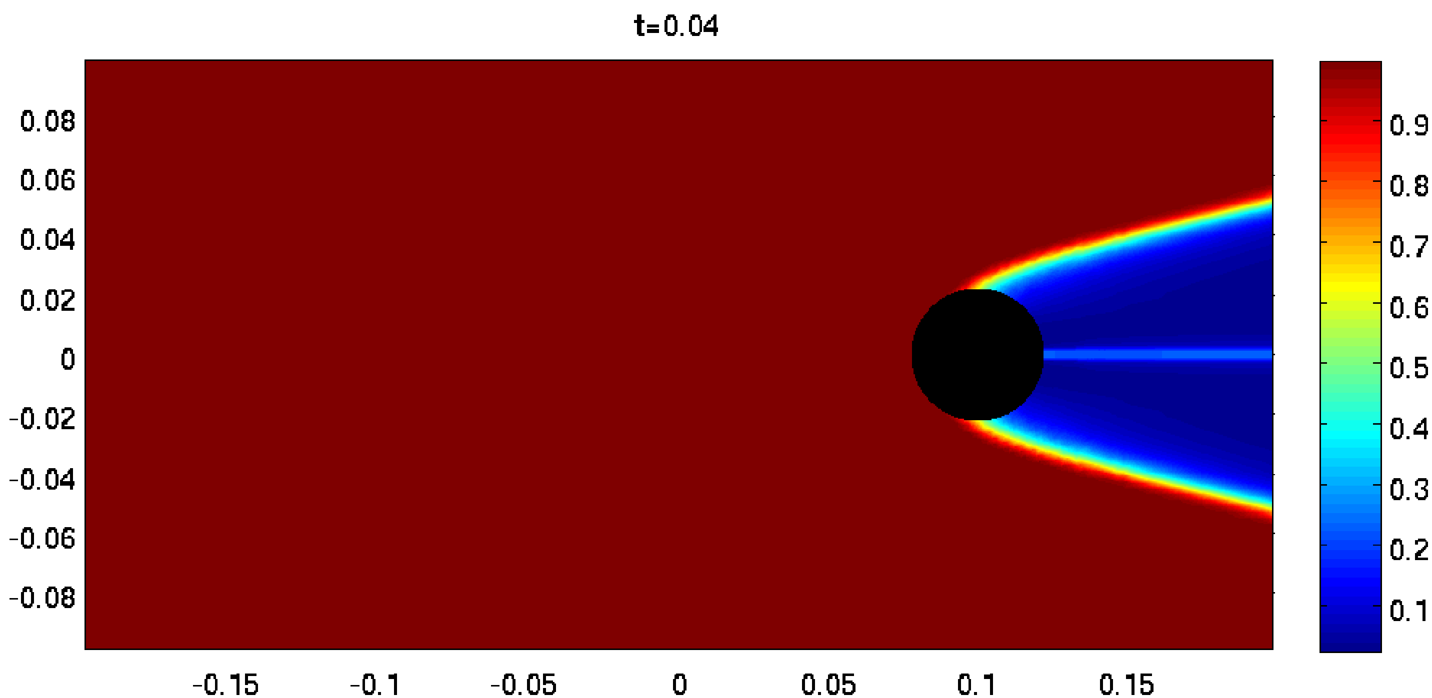

Cavitation test: 2D steady state

- Pseudo colors of pressure
  - Smooth transition across liquid-gas phase boundary

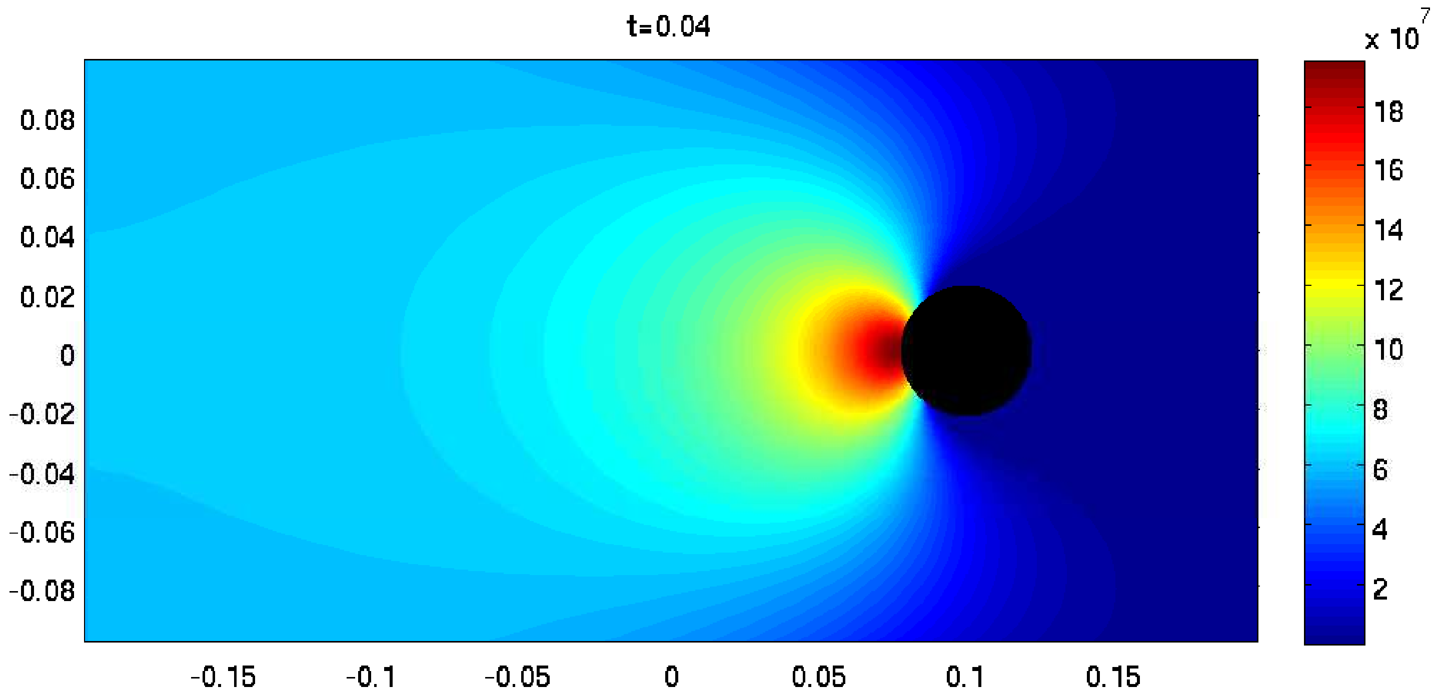

Cavitation test: 2D steady state

- Pseudo colors of volume fraction: 2 circular case
  - Convergence of solution as the mesh is refined ?

t=0.05

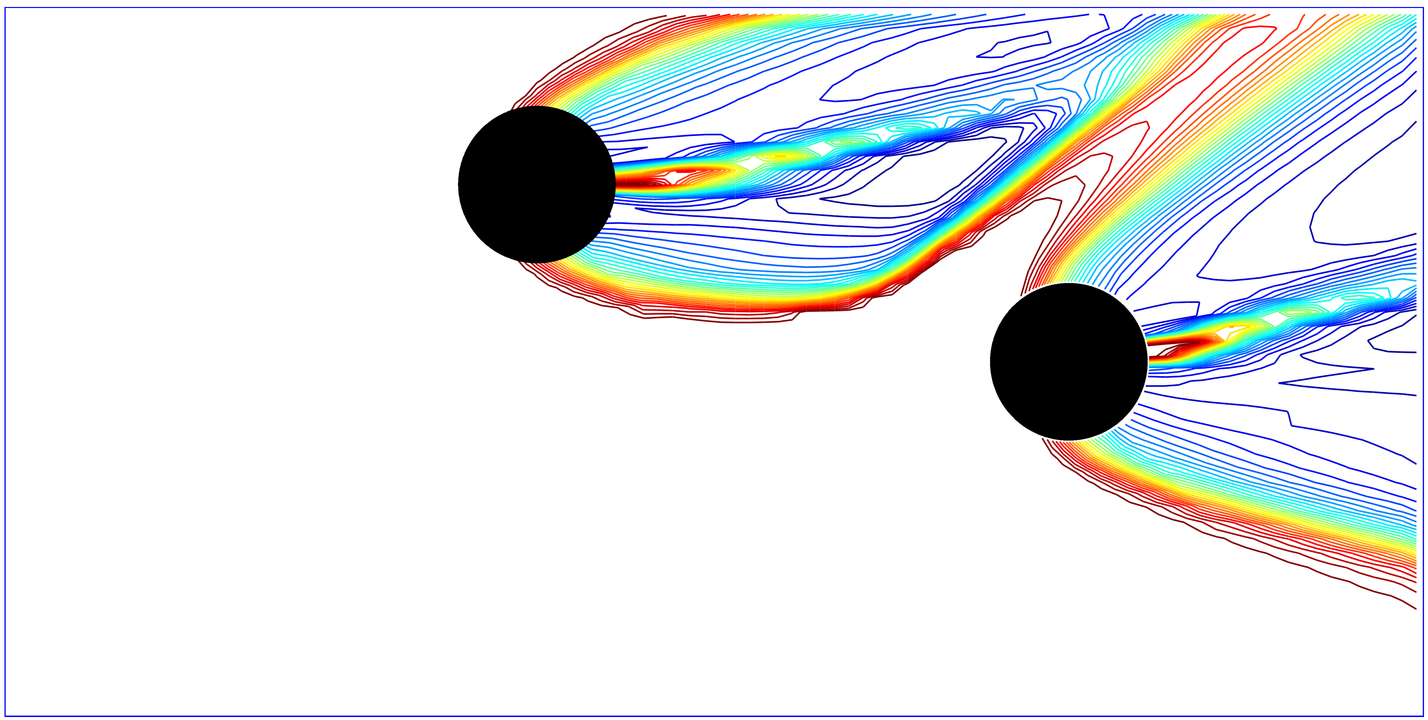

Shallow granular avalanches

- Depth-average Savage-Hutter equations

$$\frac{\partial h}{\partial t} + \sum_{j=1}^{N} \frac{\partial}{\partial x_j}(hu_j) = 0,$$

$$\frac{\partial}{\partial t}(hu_i) + \sum_{j=1}^{N} \frac{\partial}{\partial x_j}\left(hu_iu_j + \frac{1}{2}\beta_x h^2 \delta_{ij}\right) = h\psi_i, \quad i = 1, \ldots, N,$$

where Mohr-Coulomb closure is used with

$$\beta_x = K_x \cos\zeta,$$

$$K_x = \begin{cases} K_x^- & \text{if } \nabla\cdot\vec{u} > 0 \\ K_x^+ & \text{if } \nabla\cdot\vec{u} < 0, \end{cases} \qquad K_x^{\pm} = \frac{2}{\cos^2\phi}\left(1 \pm \sqrt{1 - \frac{\cos^2\phi}{\cos^2\delta}}\right) - 1,$$

$$\psi_i = \sin\zeta\,\delta_{1i} - \frac{u_i}{|\vec{u}|}\tan\delta\left(\cos\zeta + \kappa u_1^2\right) - \cos\zeta\frac{\partial \mathcal{B}}{\partial x_i}$$

Earth pressure coefficients

- Jump discontinuity on K_x, $|K_x^+ - K_x^-| \neq 0$ (see below where $\delta = 30^o$ is used as a reference)

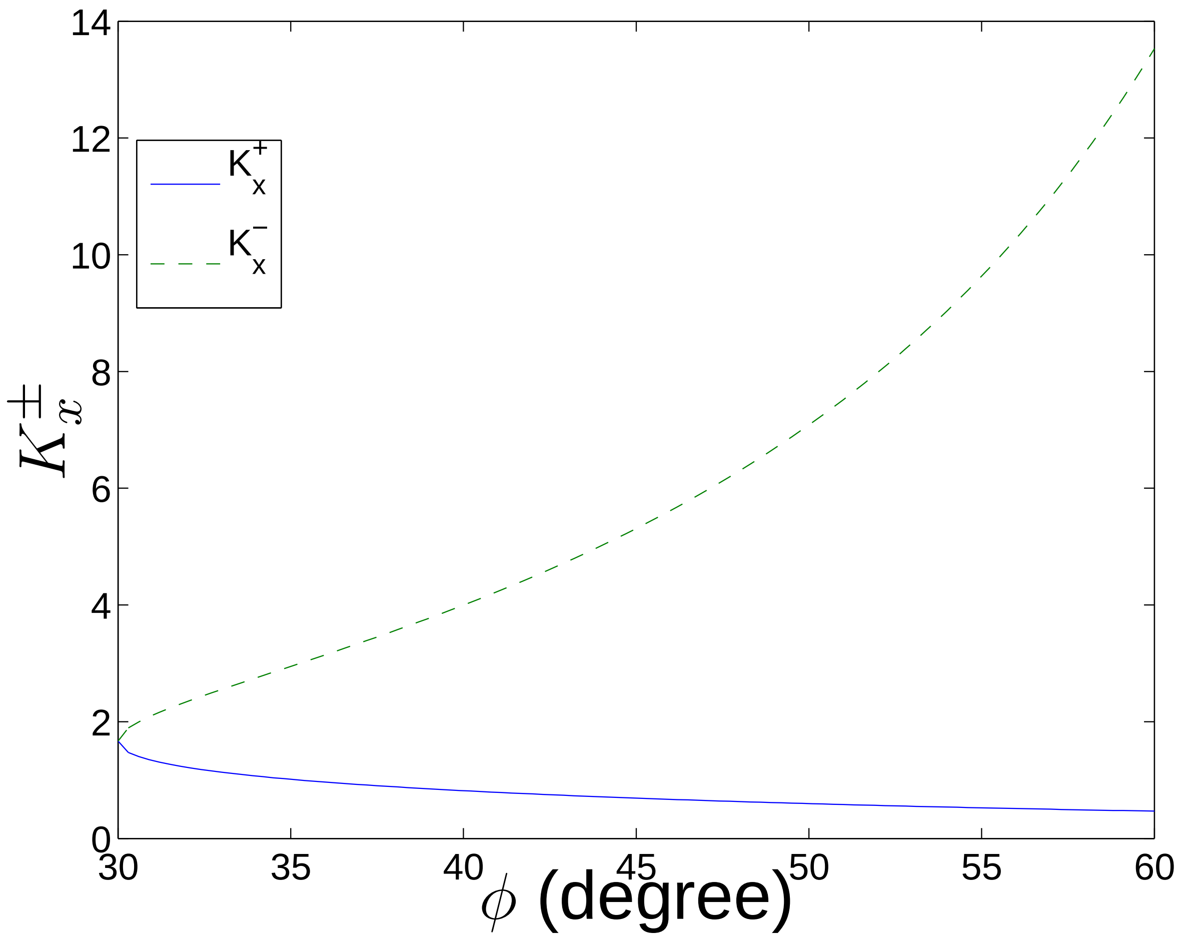

Avalanche on an inclined channel

- Hemispherical granular material
- Parameters: $\zeta = 35^o$, $\phi = 30^o$, $\delta = 30^o$

$t = 0$

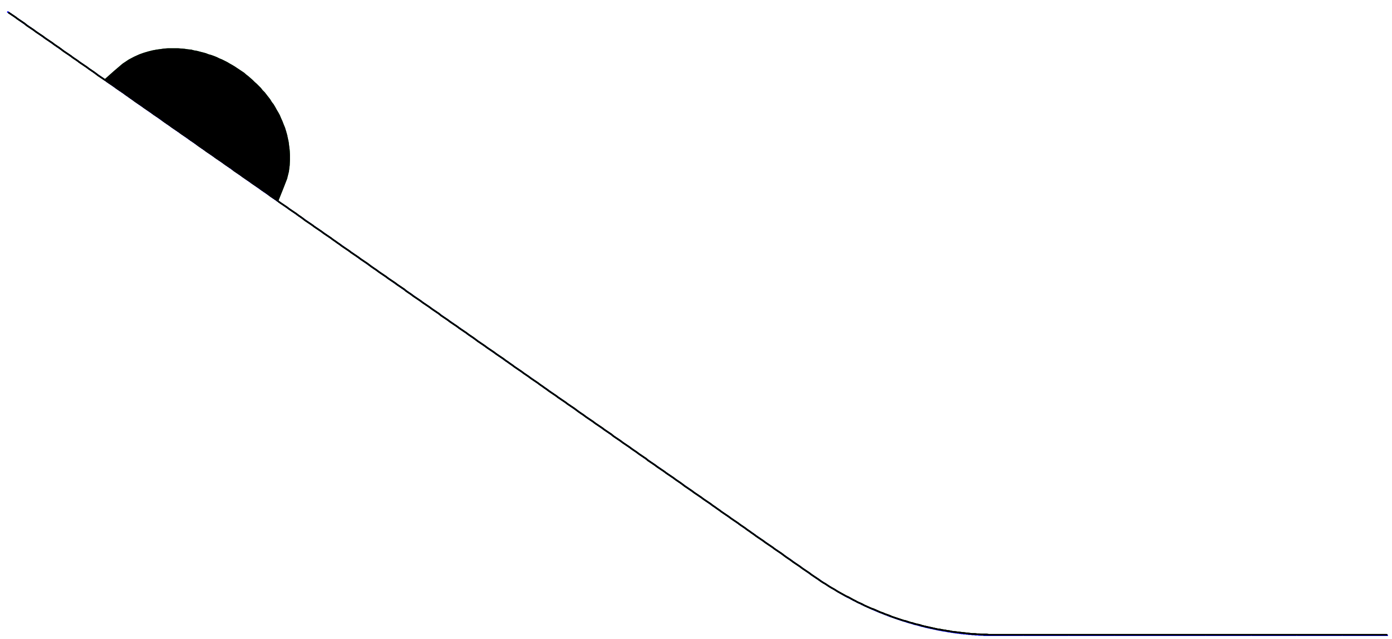

Avalanche on an inclined channel

- Contour plots for granular height (normal to channel)

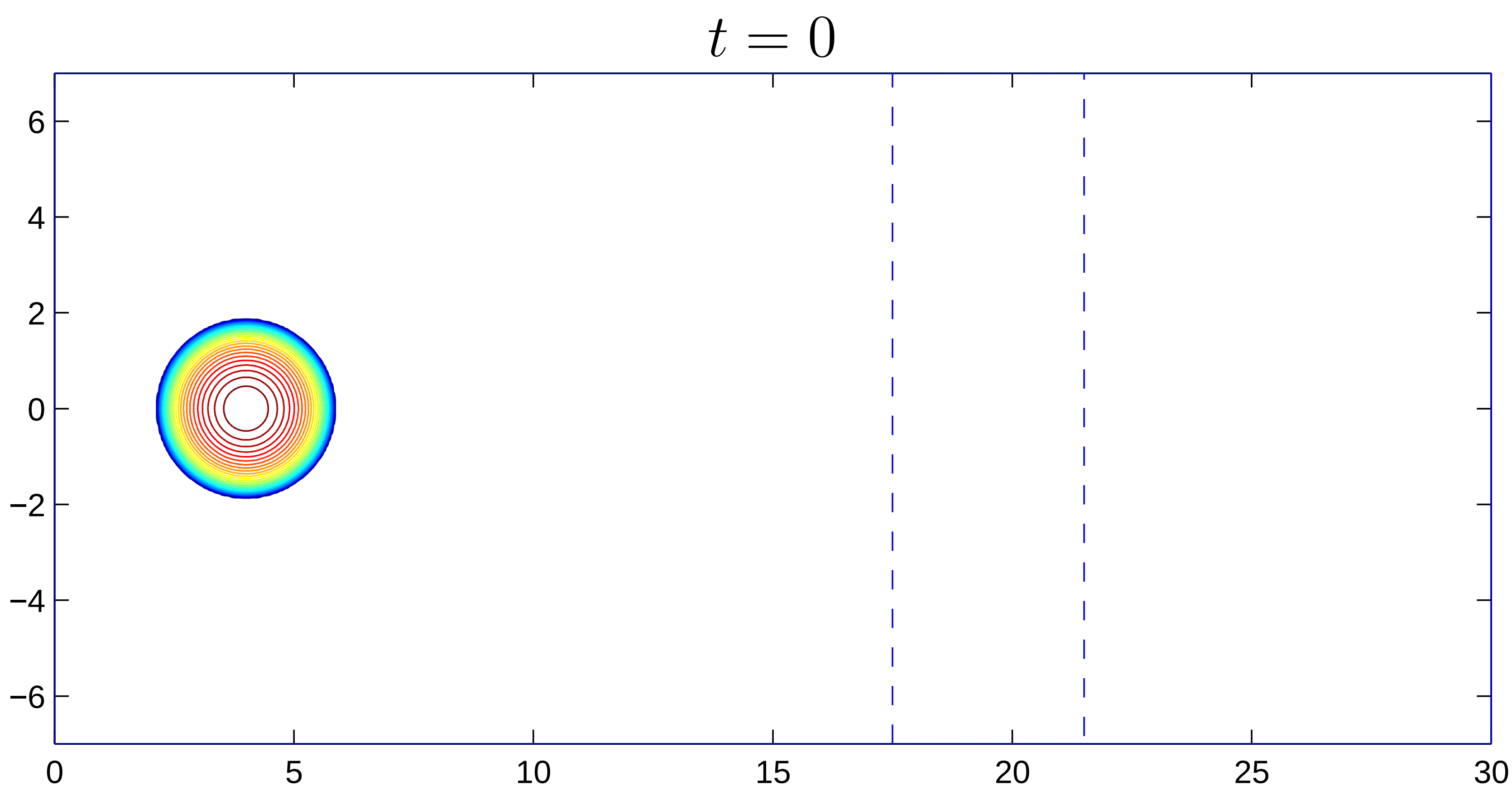

Avalanche on an inclined channel

- Down-flow phase

$t = 3$

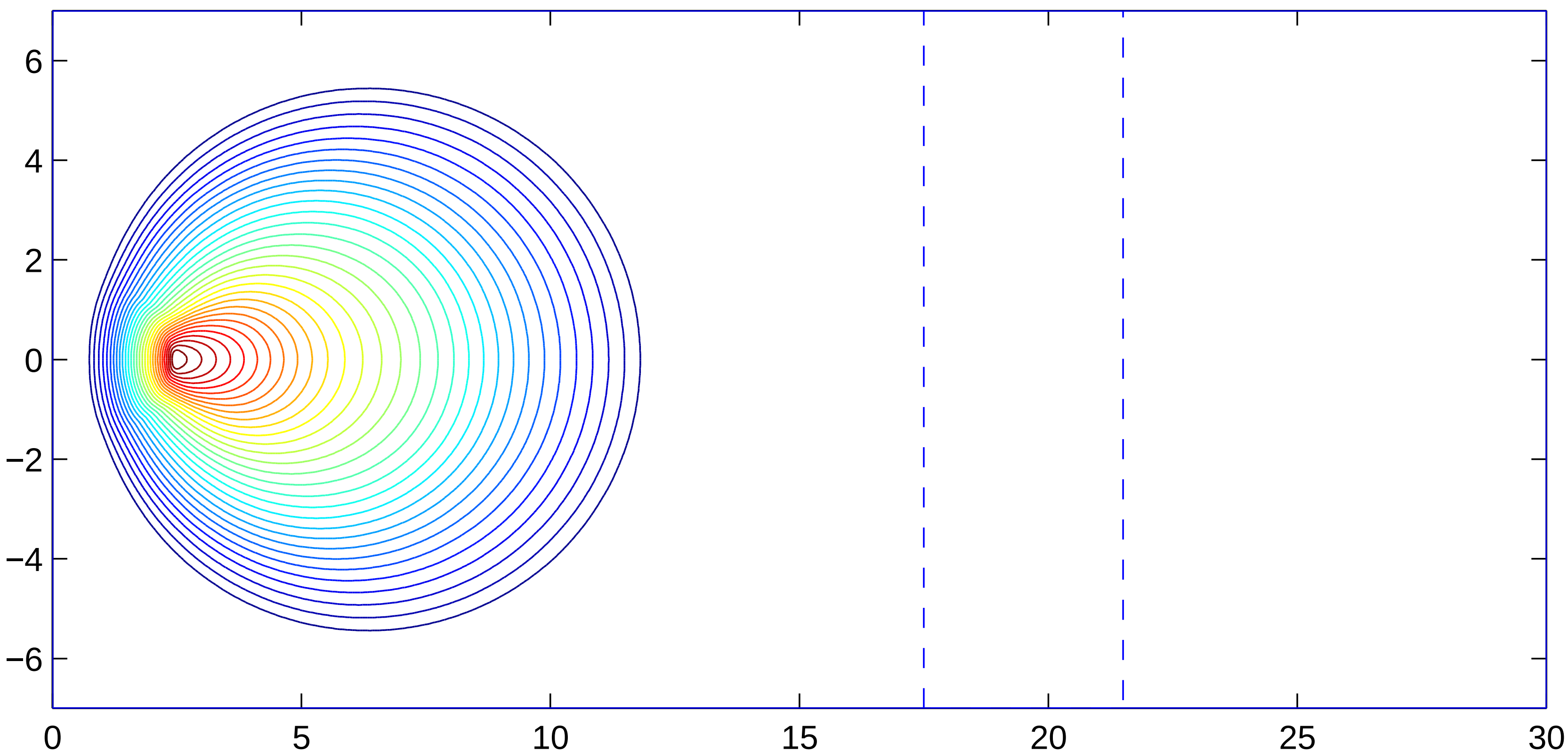

Avalanche on an inclined channel

- Down-flow phase

$t = 6$

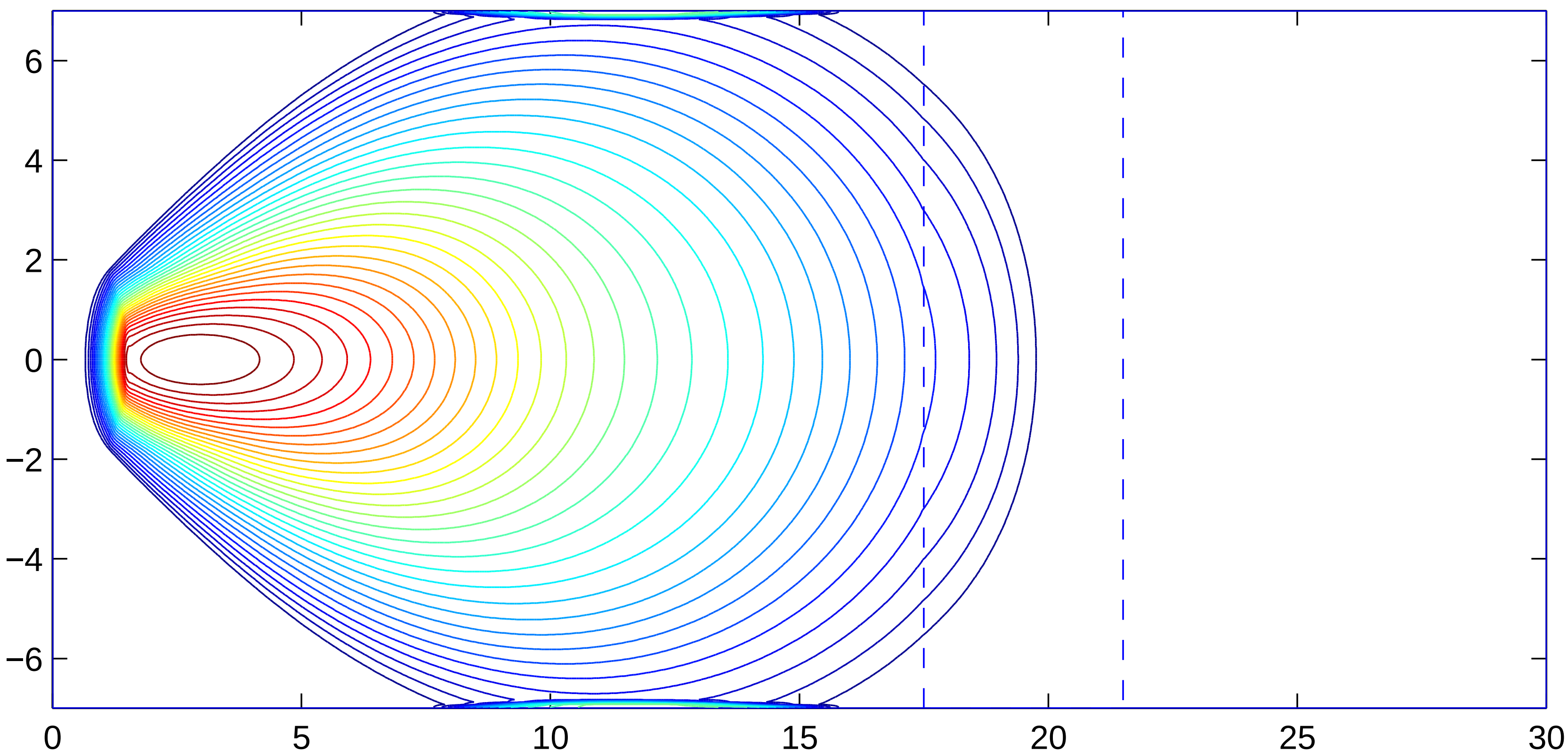

Avalanche on an inclined channel

- Down-flow phase

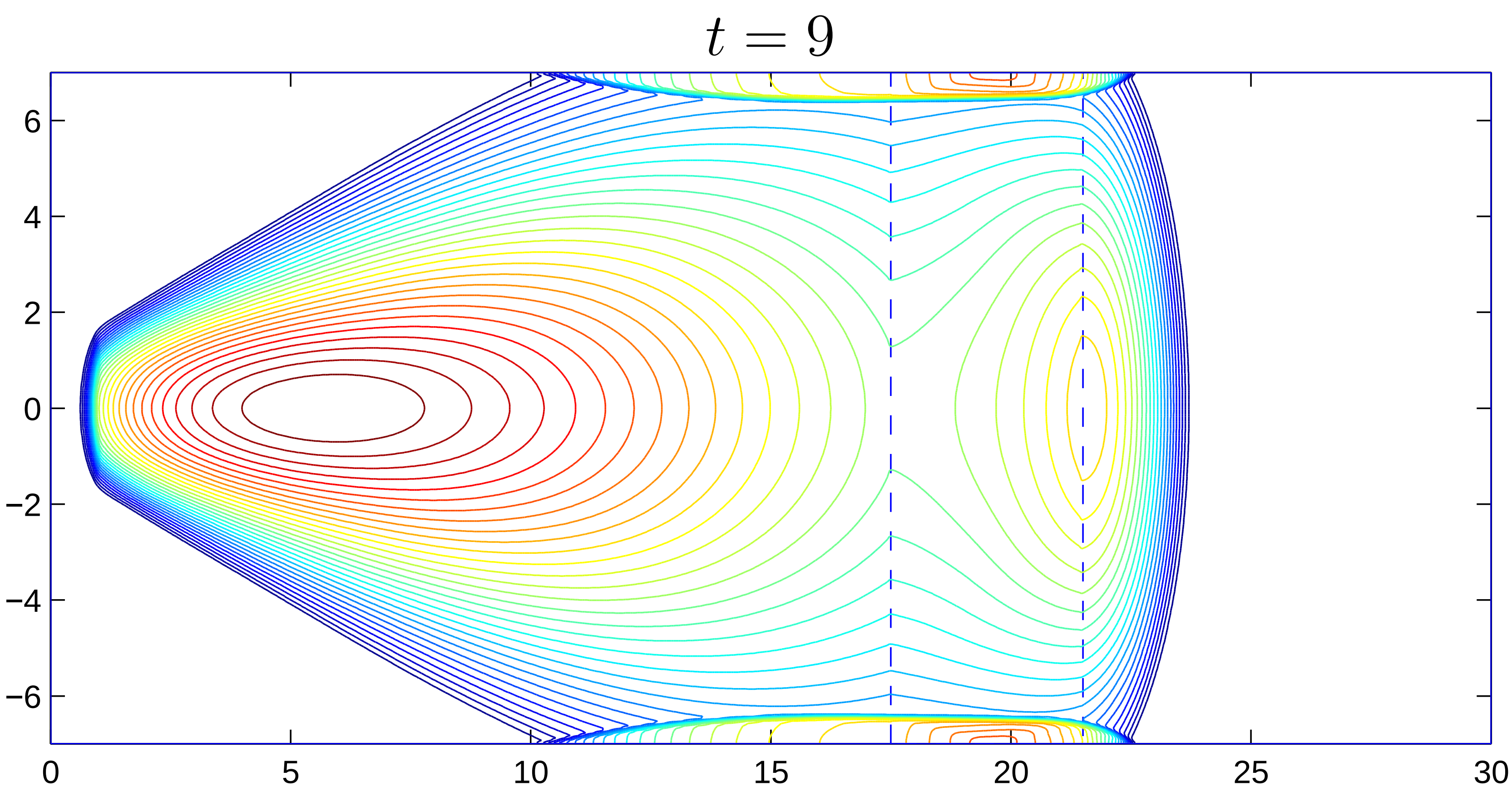

Avalanche on an inclined channel

- Deposit phase

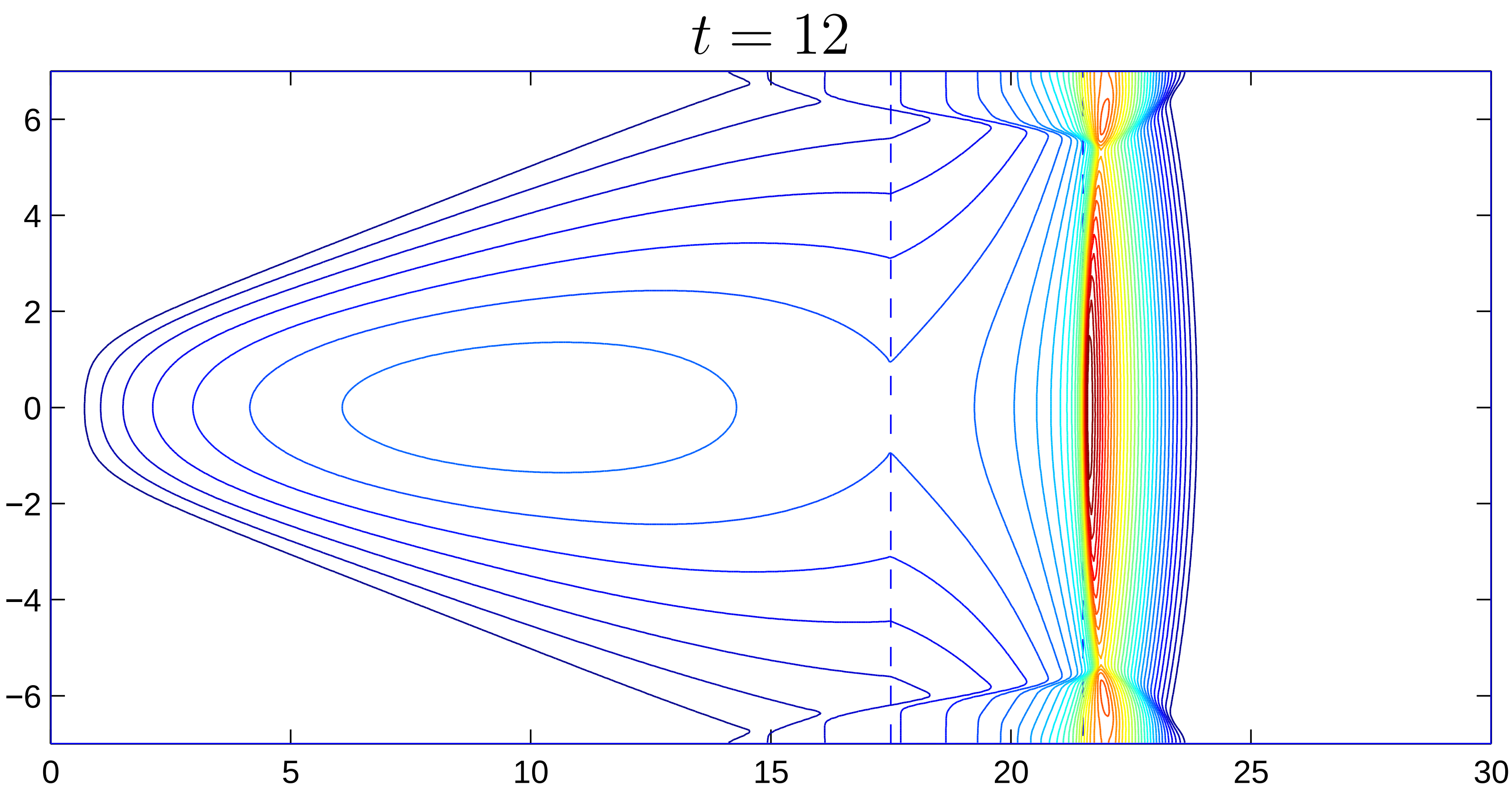

Avalanche on an inclined channel

- Deposit phase

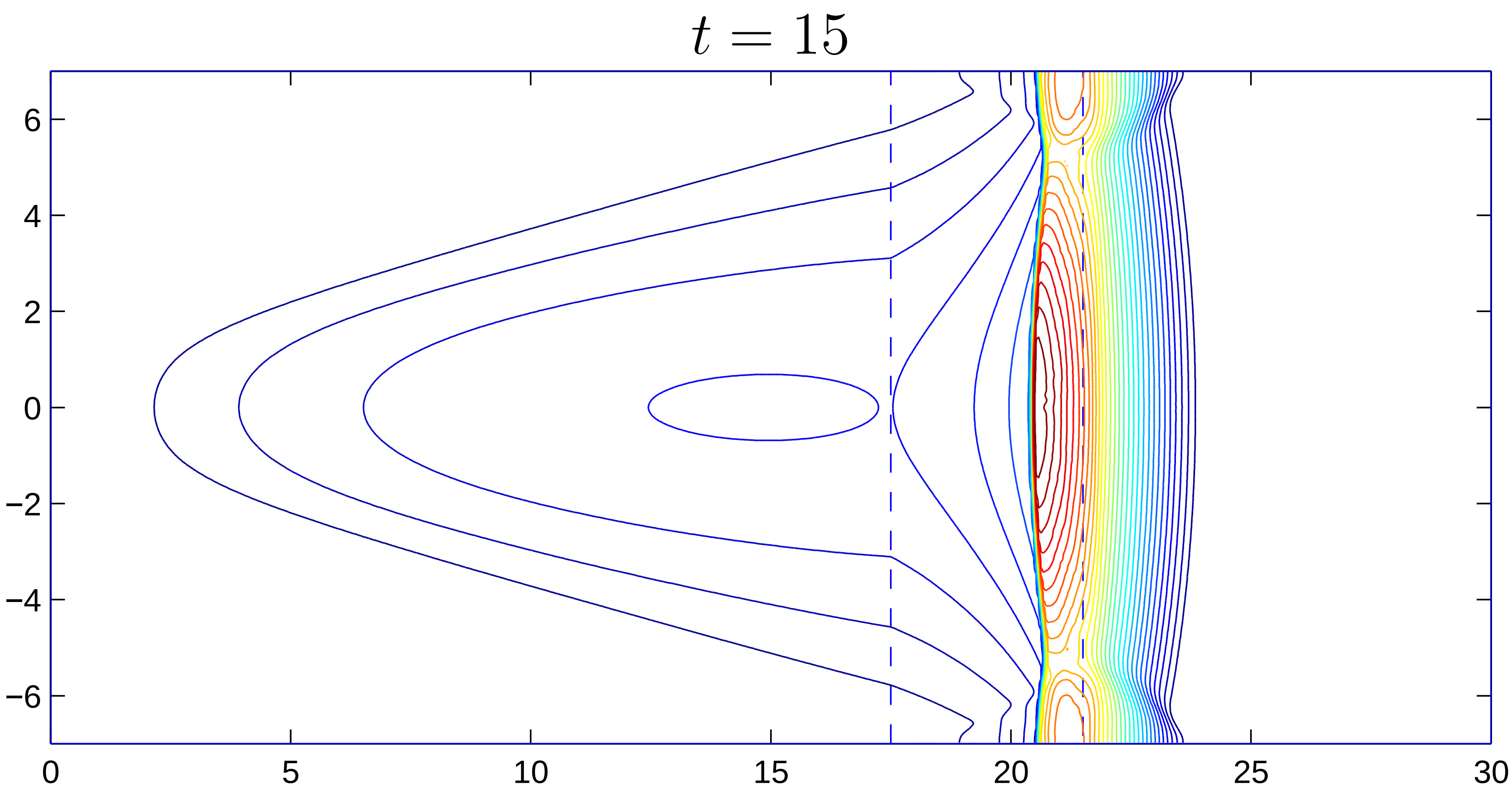

Avalanche on an inclined channel

- Deposit phase

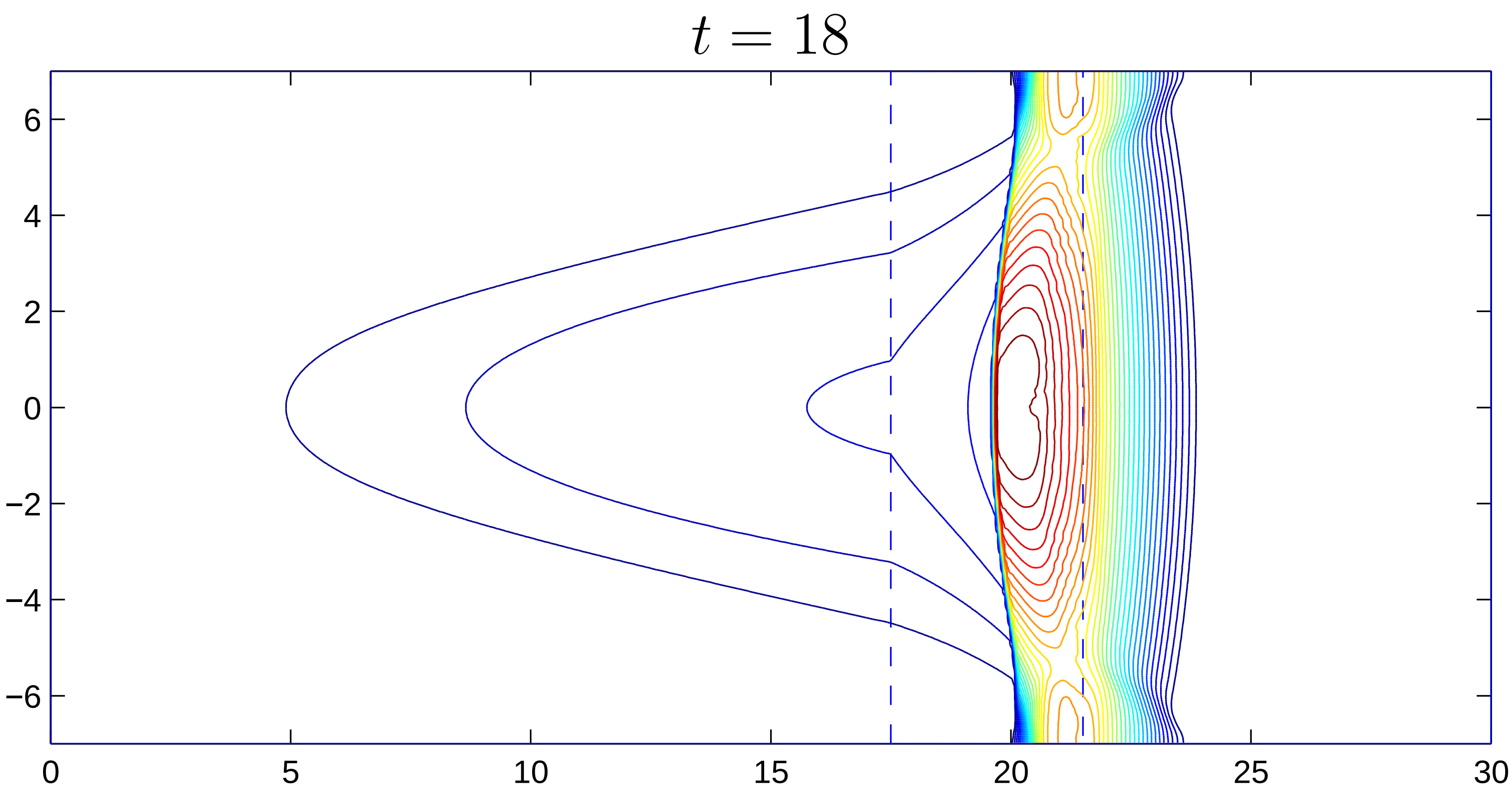

Avalanche on an inclined channel

- Deposit phase

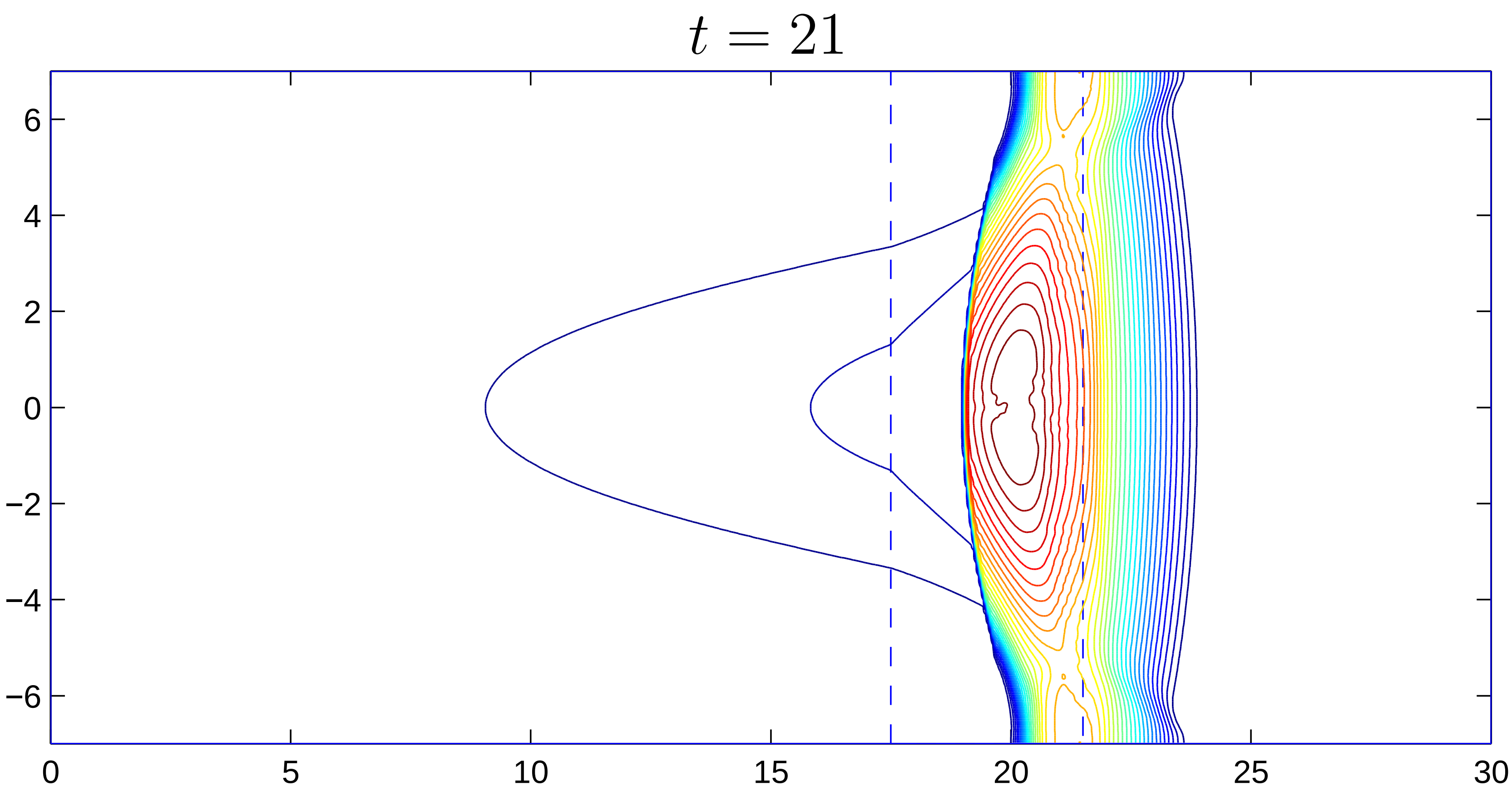

Avalanche on an inclined channel

- Deposit phase

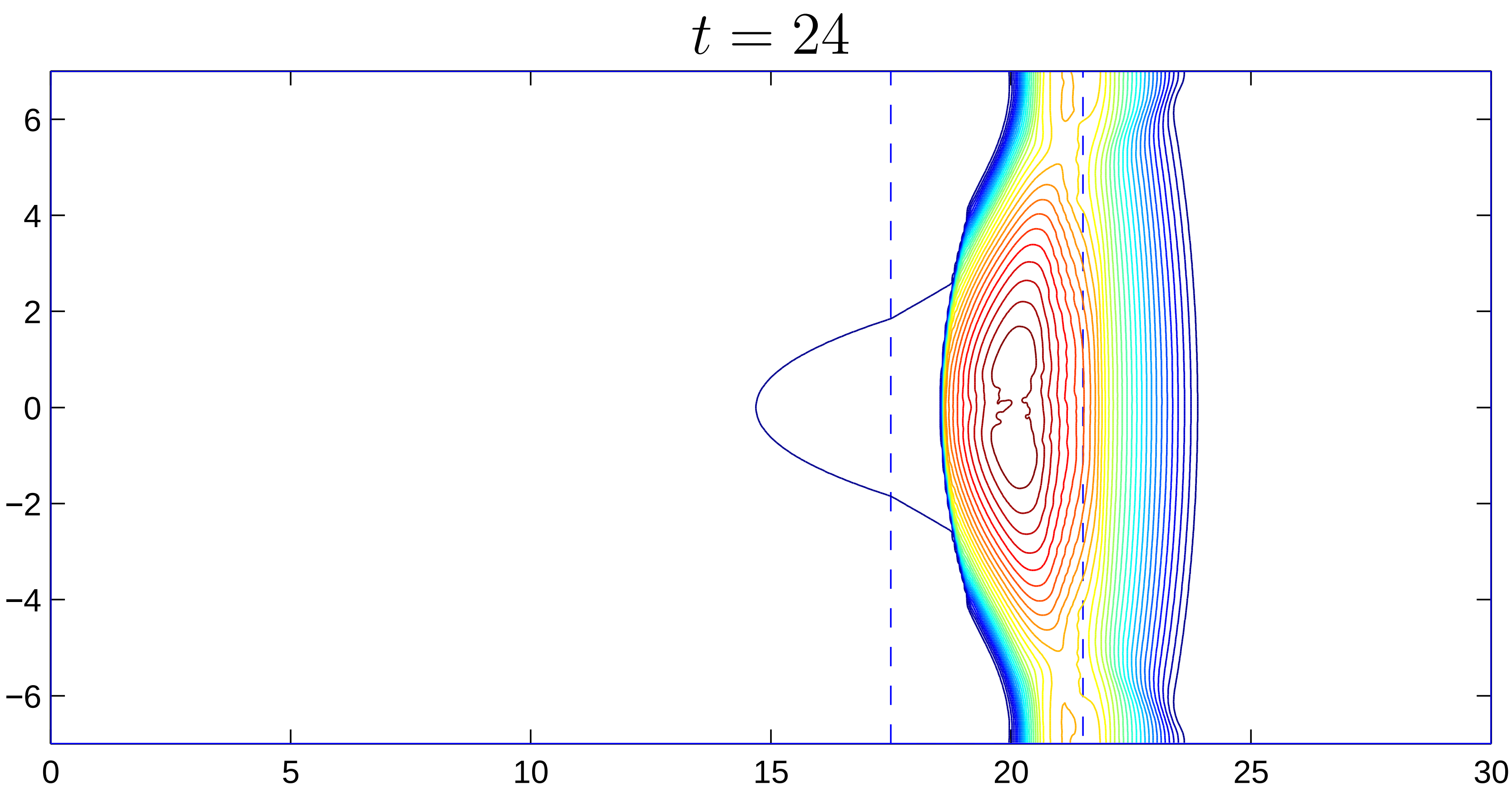

Avalanche on an inclined channel

- Cross-sectional plot along the channel

$$t = 0$$

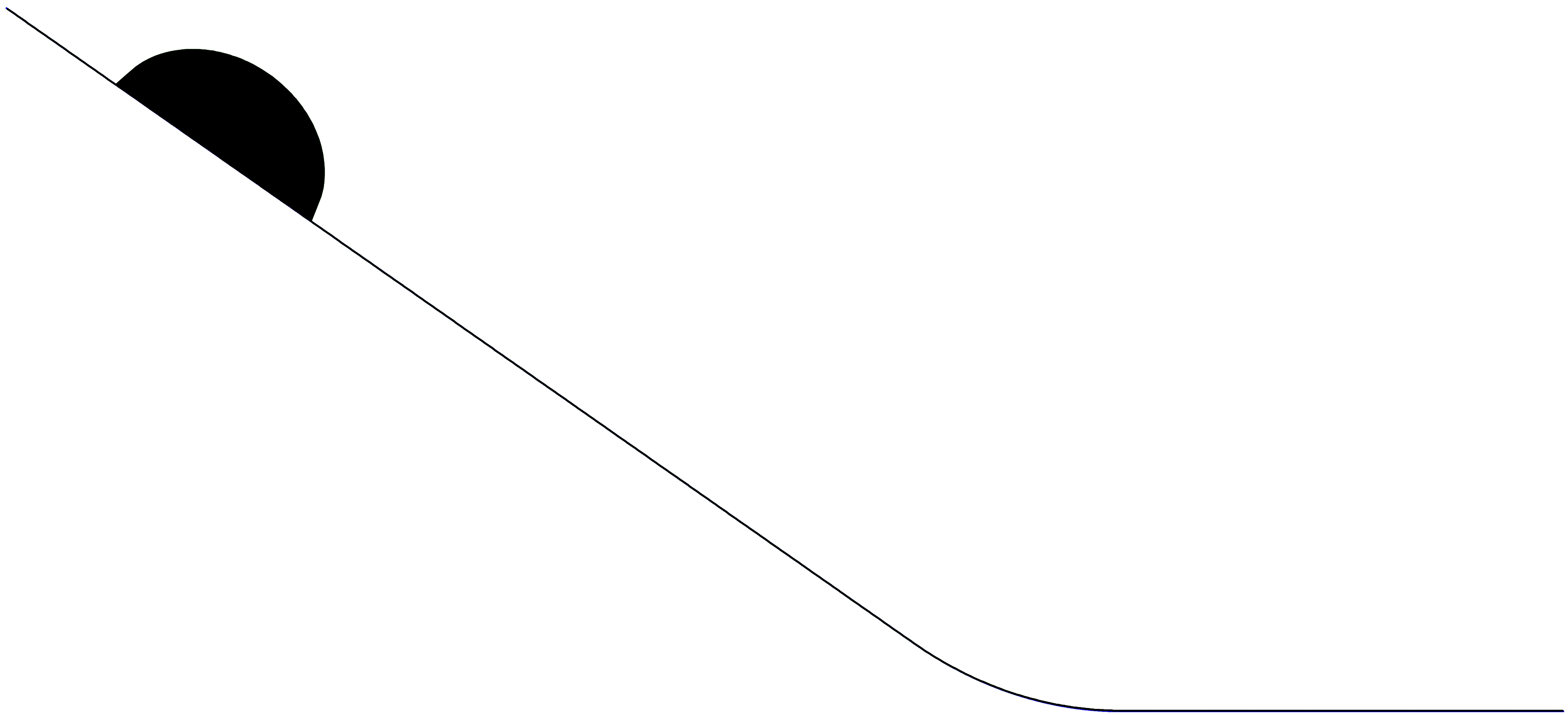

Avalanche on an inclined channel

- Down-flow phase

$$t = 3$$

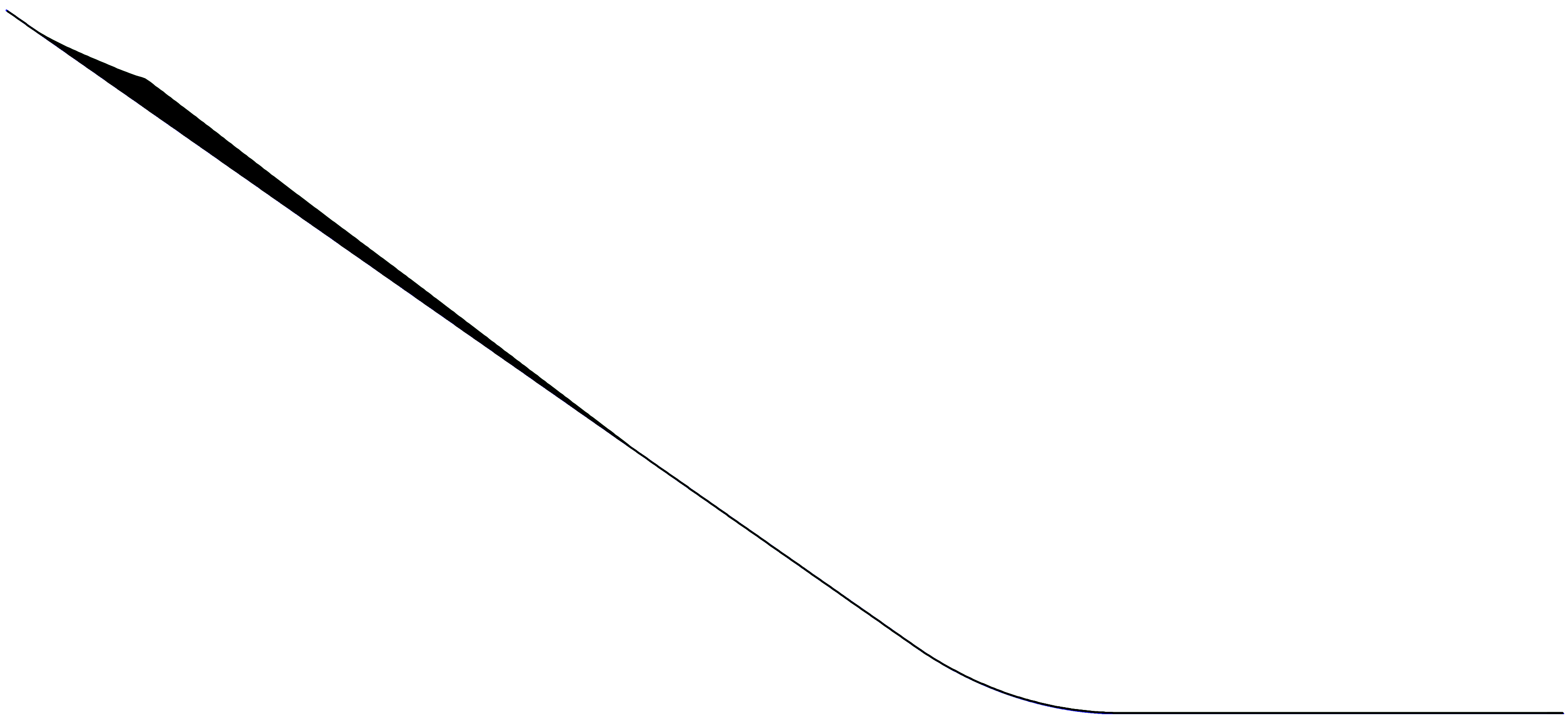

Avalanche on an inclined channel

- Down-flow phase

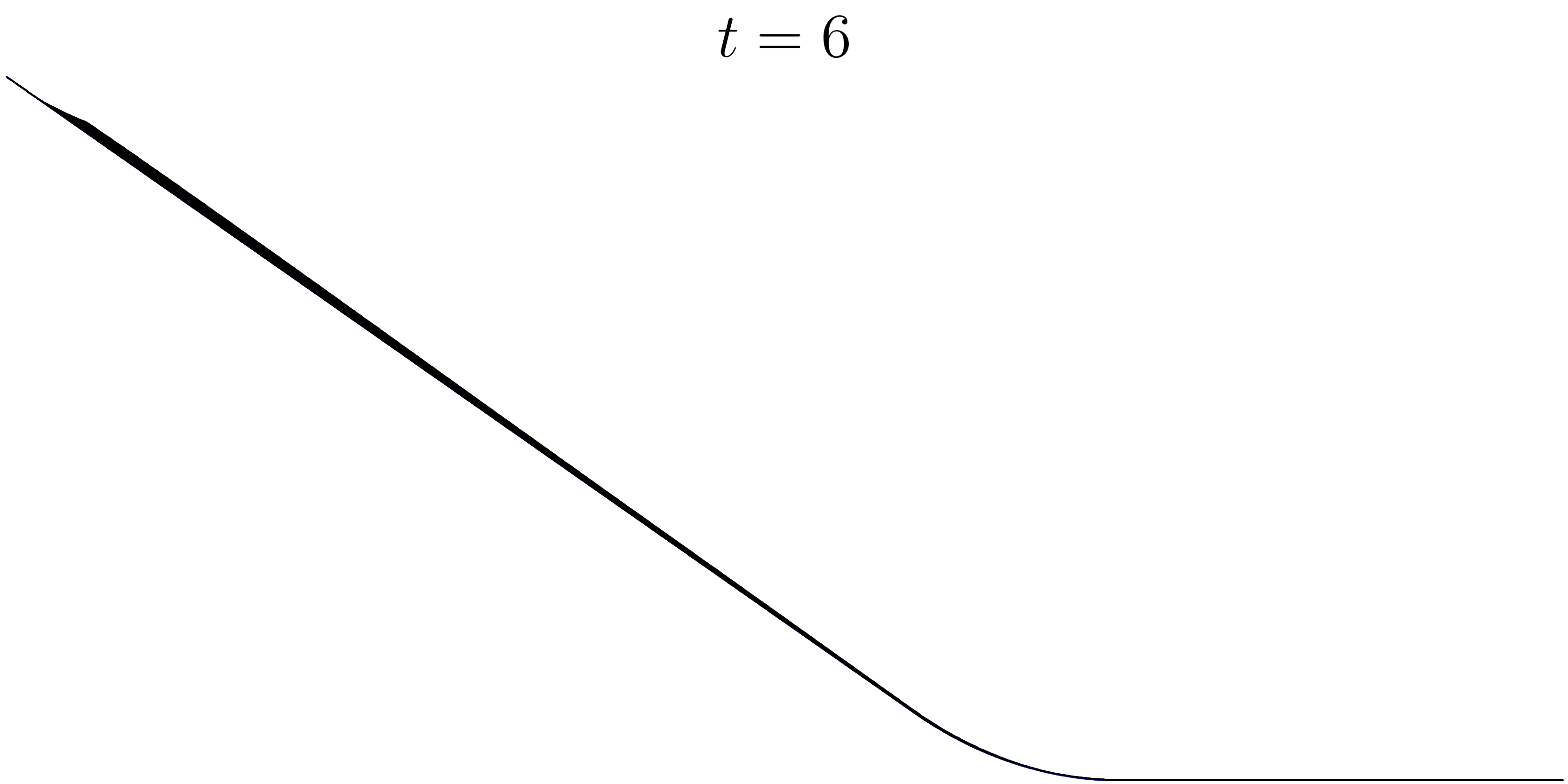

Avalanche on an inclined channel

- Down-flow phase

$$t = 9$$

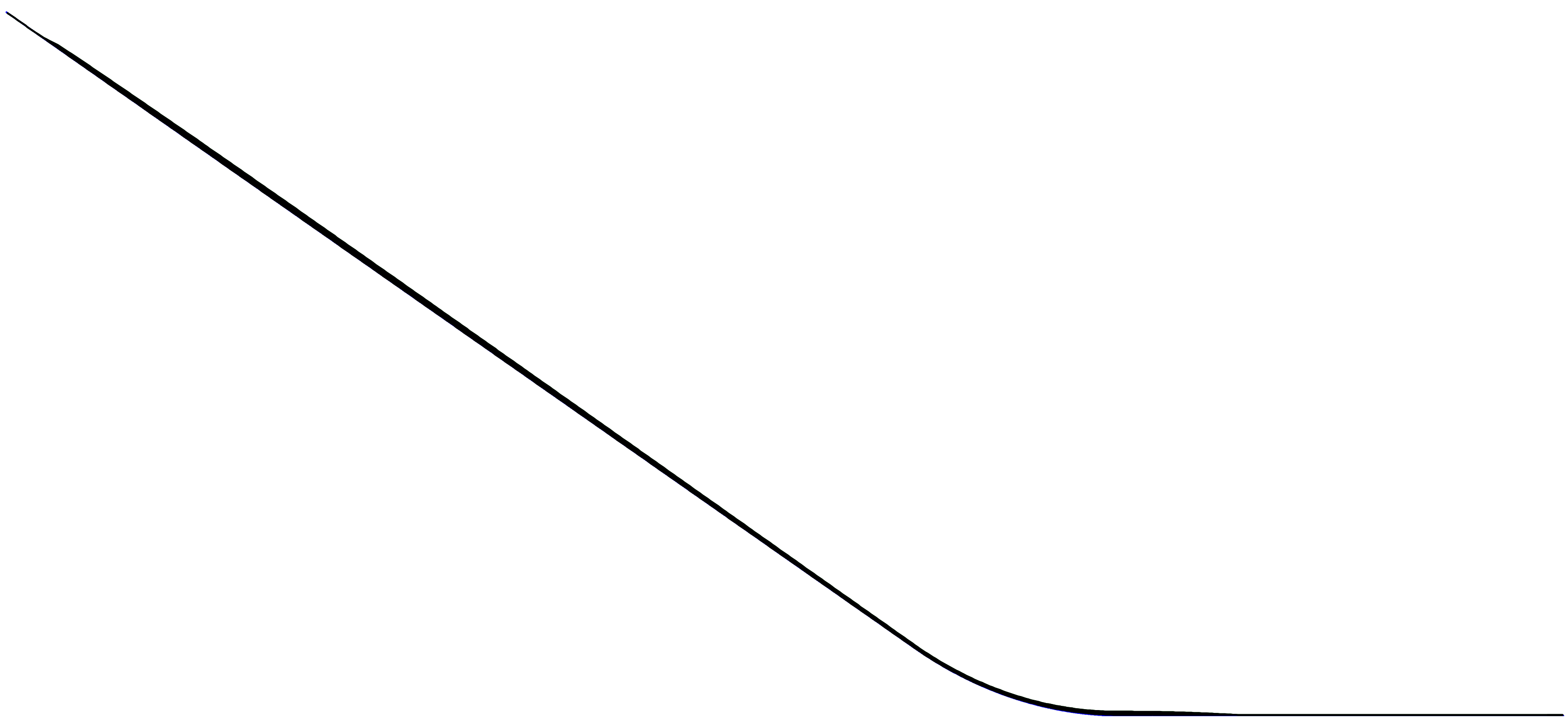

Avalanche on an inclined channel

- Deposit phase

$$t = 12$$

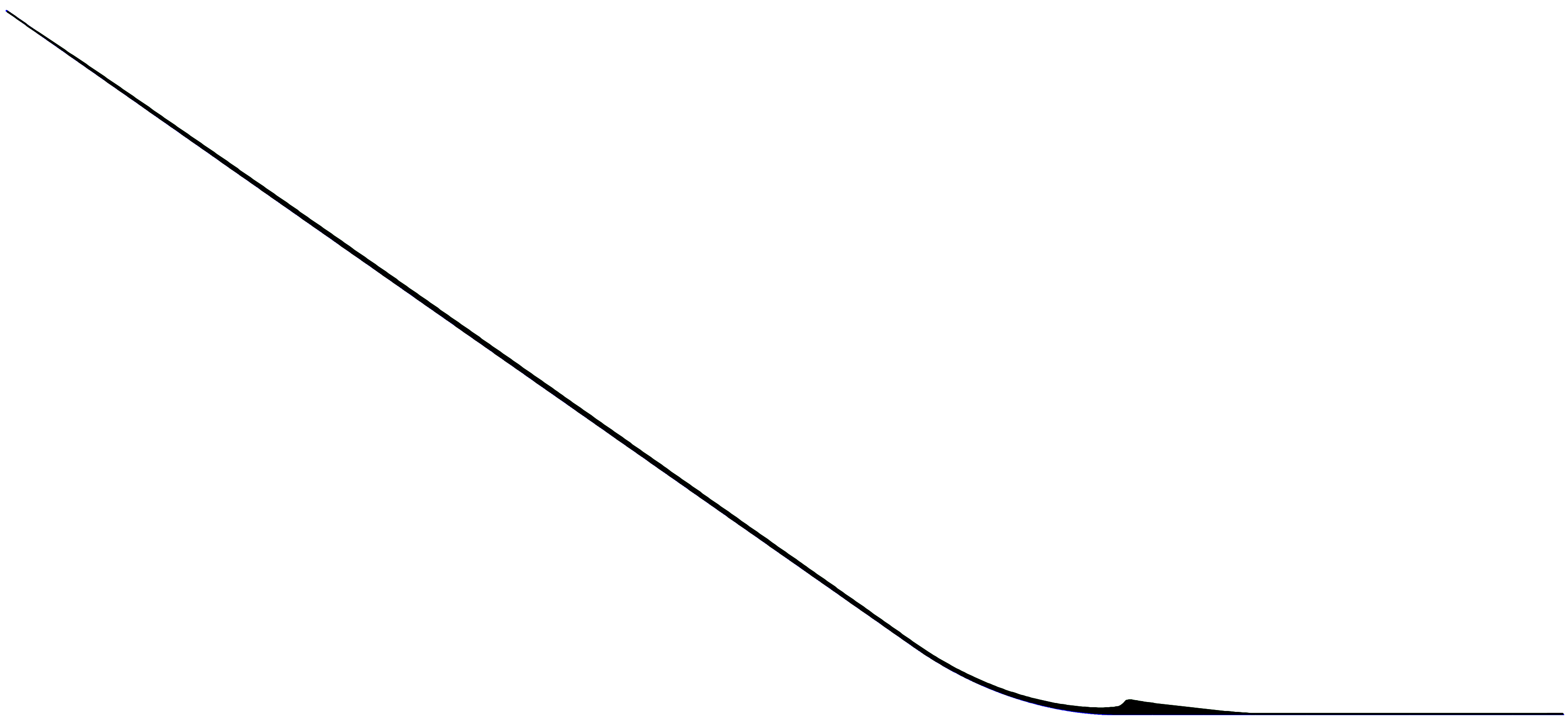

Avalanche on an inclined channel

- Deposit phase

$$t = 15$$

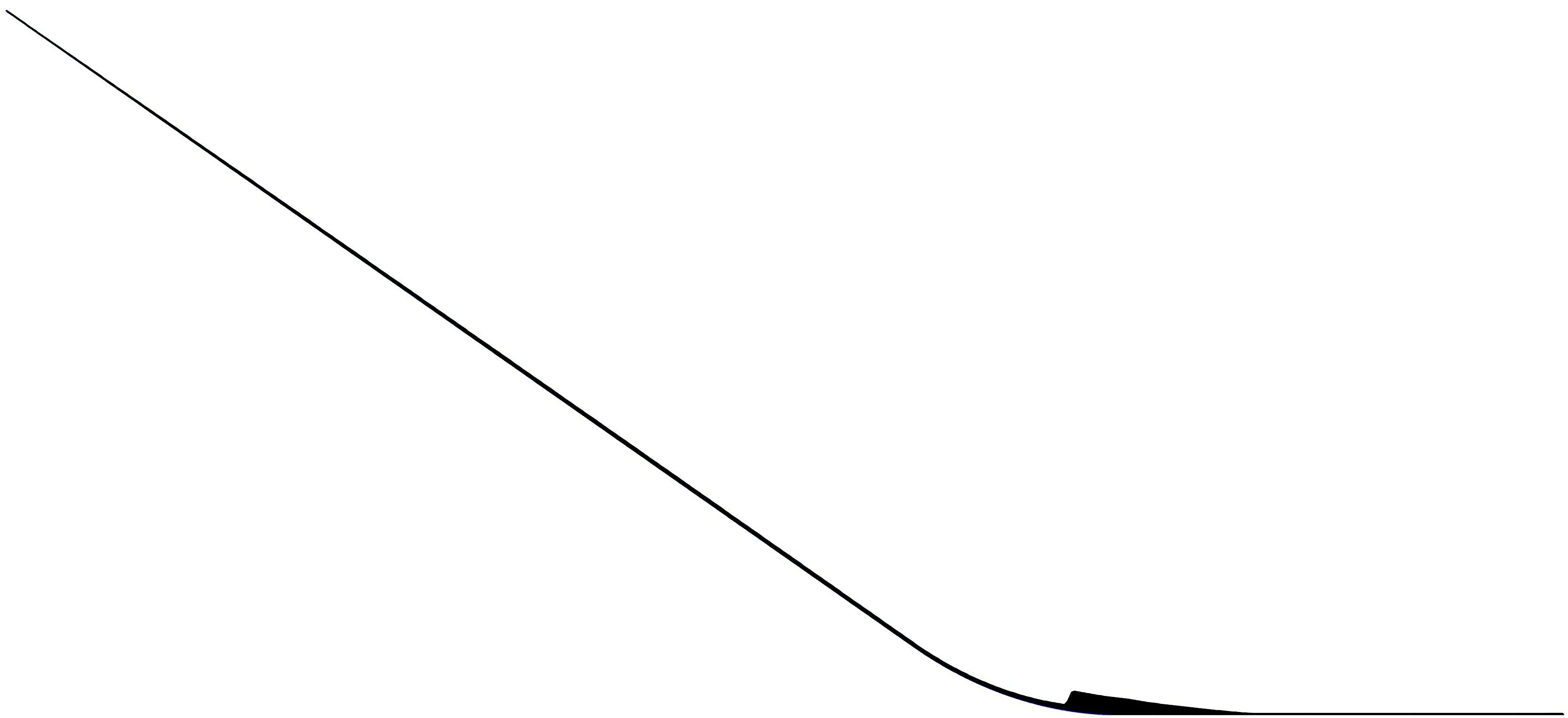

Avalanche on an inclined channel

- Deposit phase

$$t = 18$$

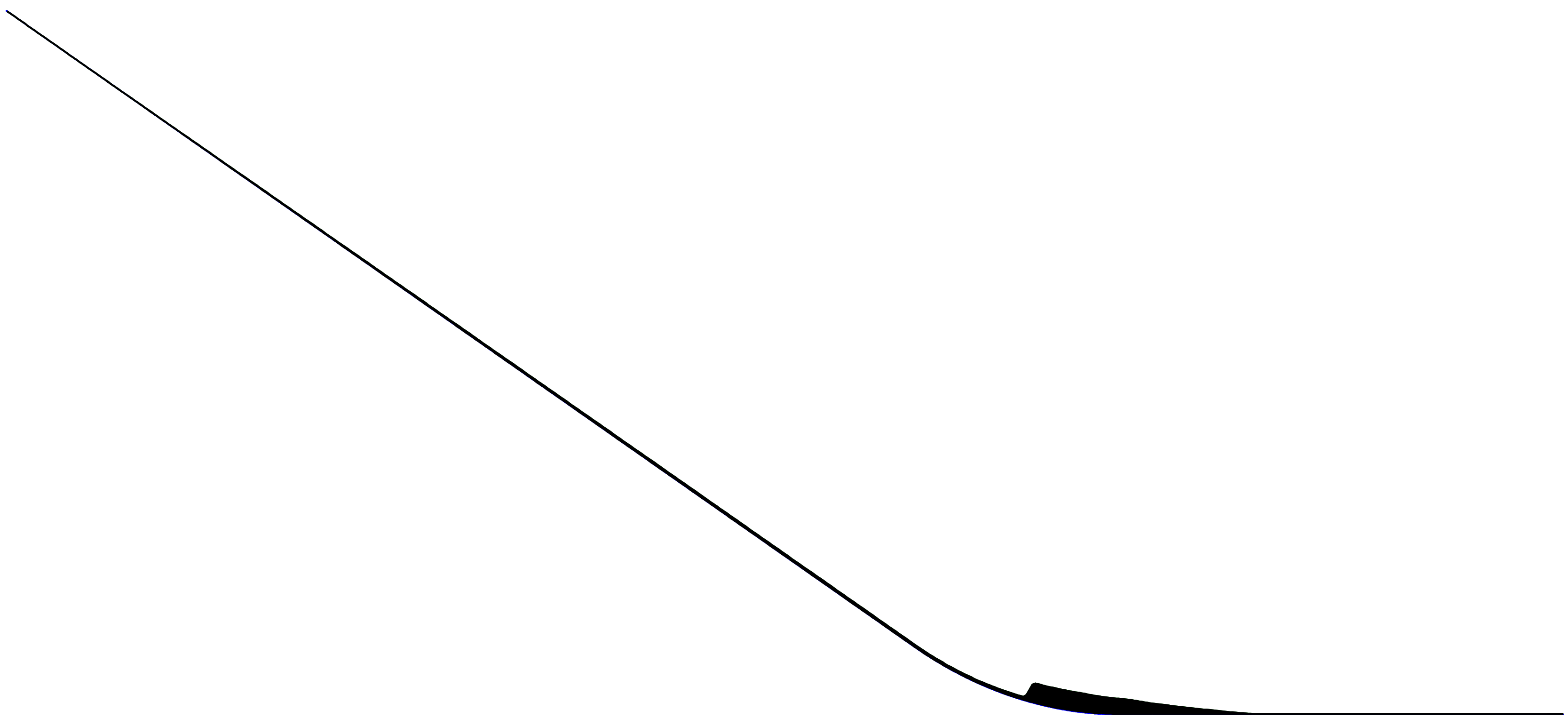

Avalanche on an inclined channel

- Deposit phase

$$t = 21$$

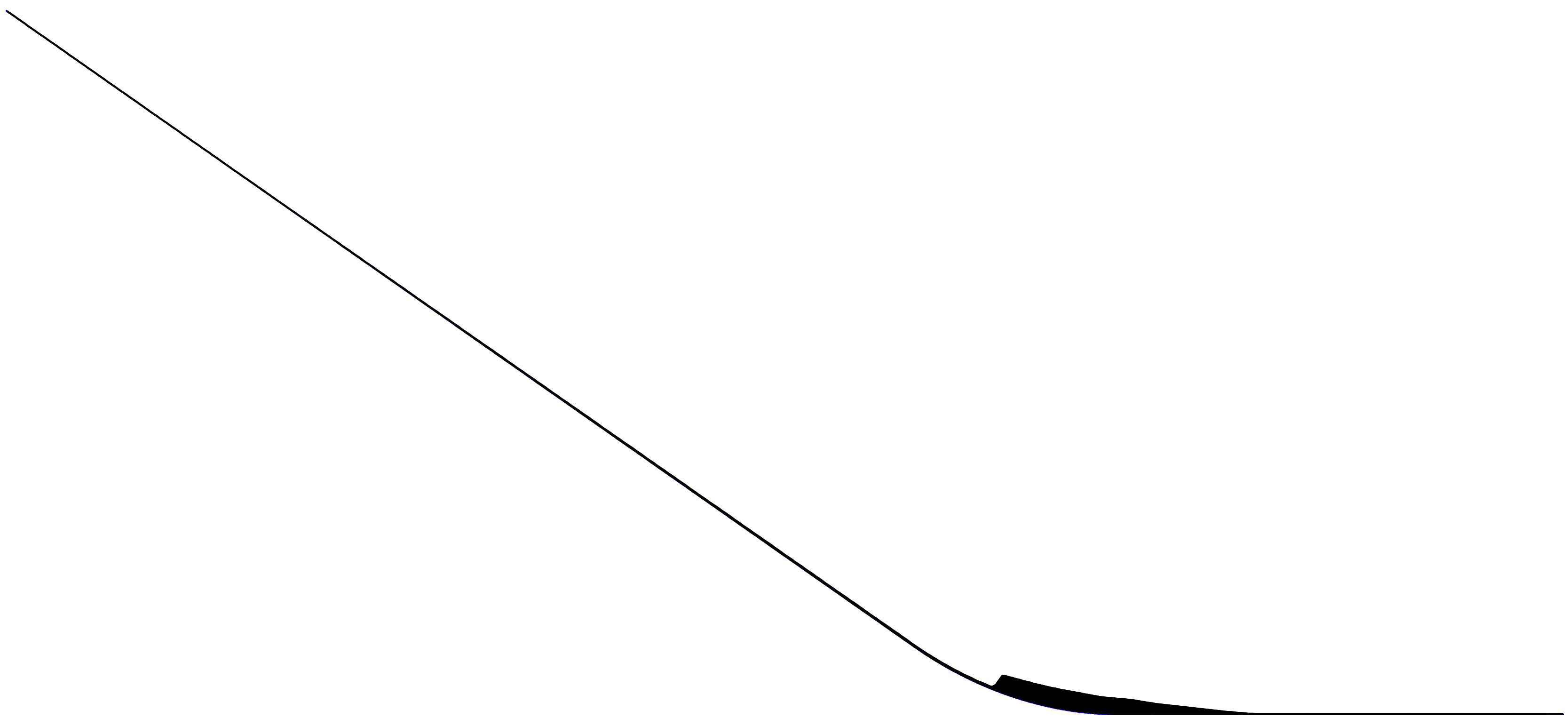

Avalanche on an inclined channel

- Deposit phase

$$t = 24$$

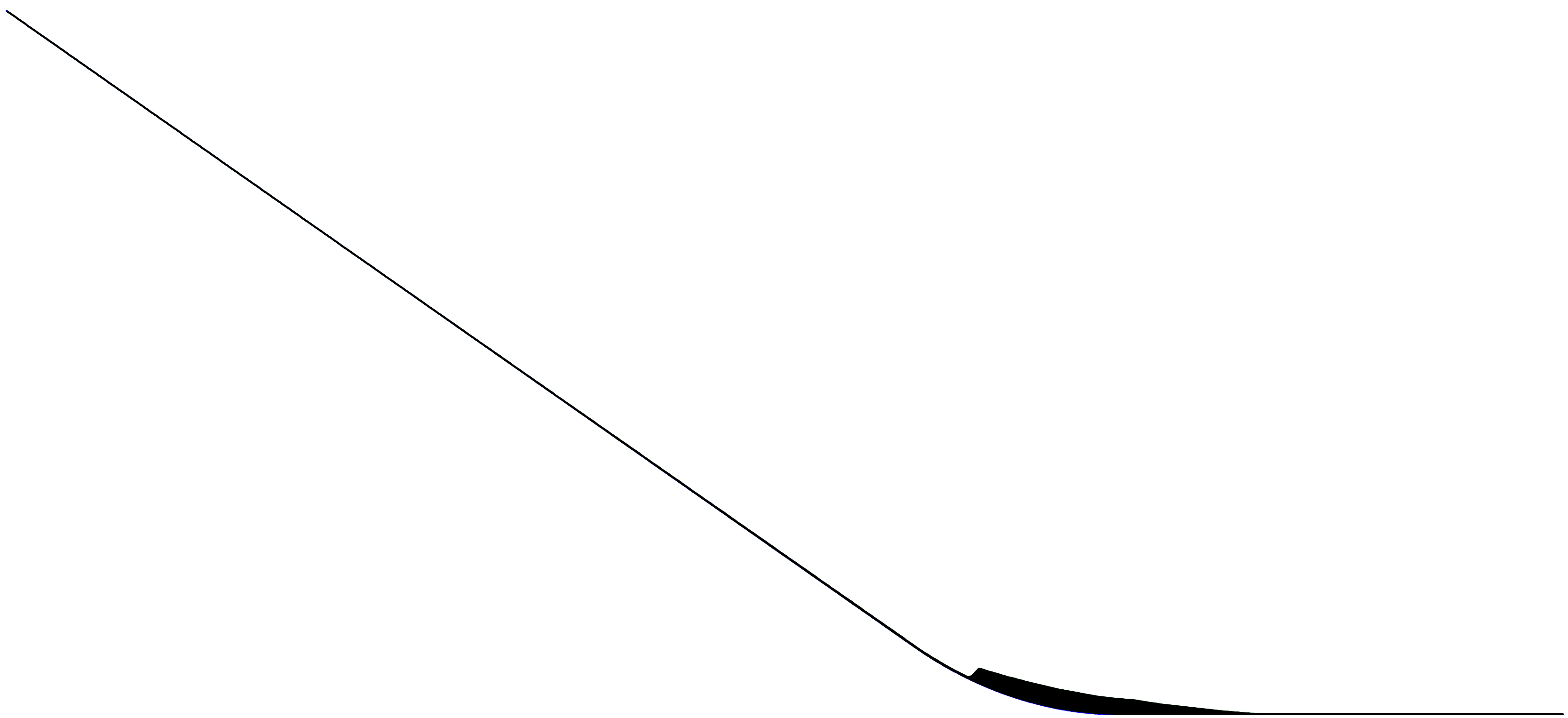

Avalanche on an inclined channel

- Hemispherical granular material
- Parameters: $\zeta = 35^o$, $\phi = 40^o$, $\delta = 30^o$

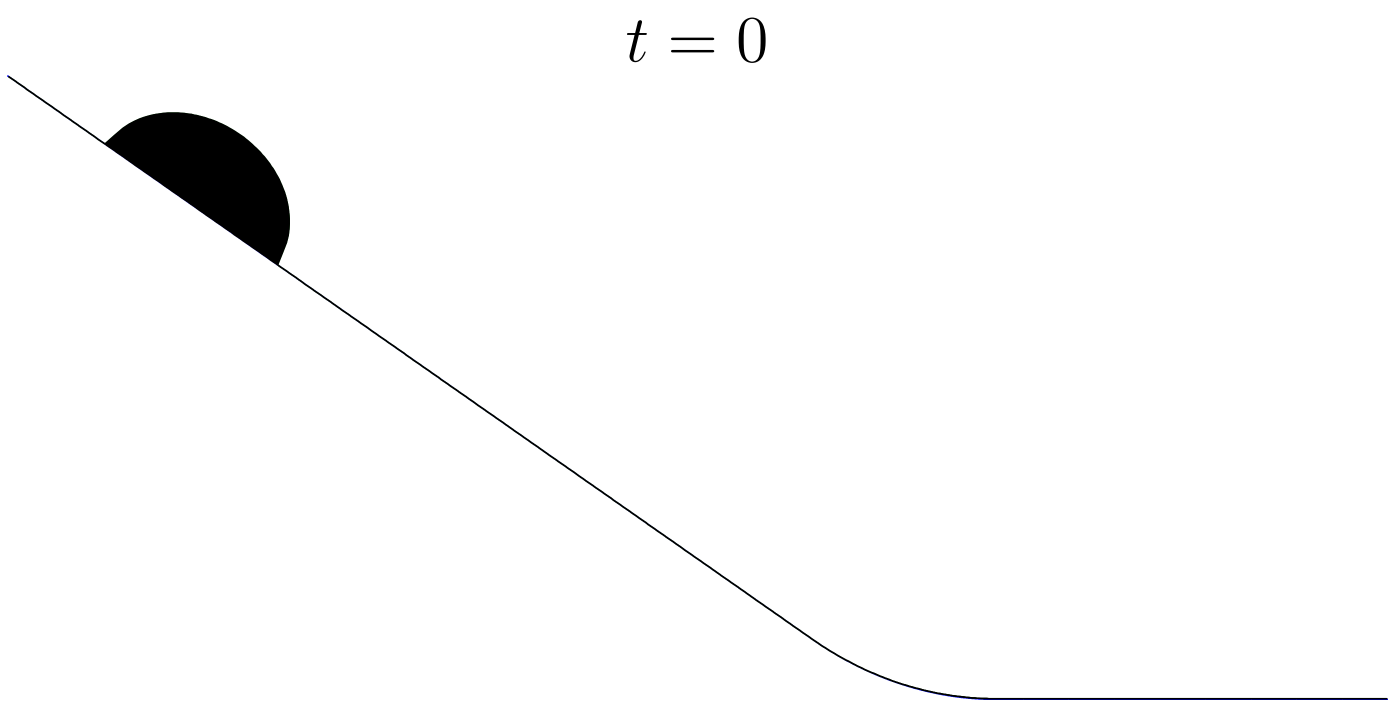

Avalanche on an inclined channel

- Contour plots for granular height (normal to channel)

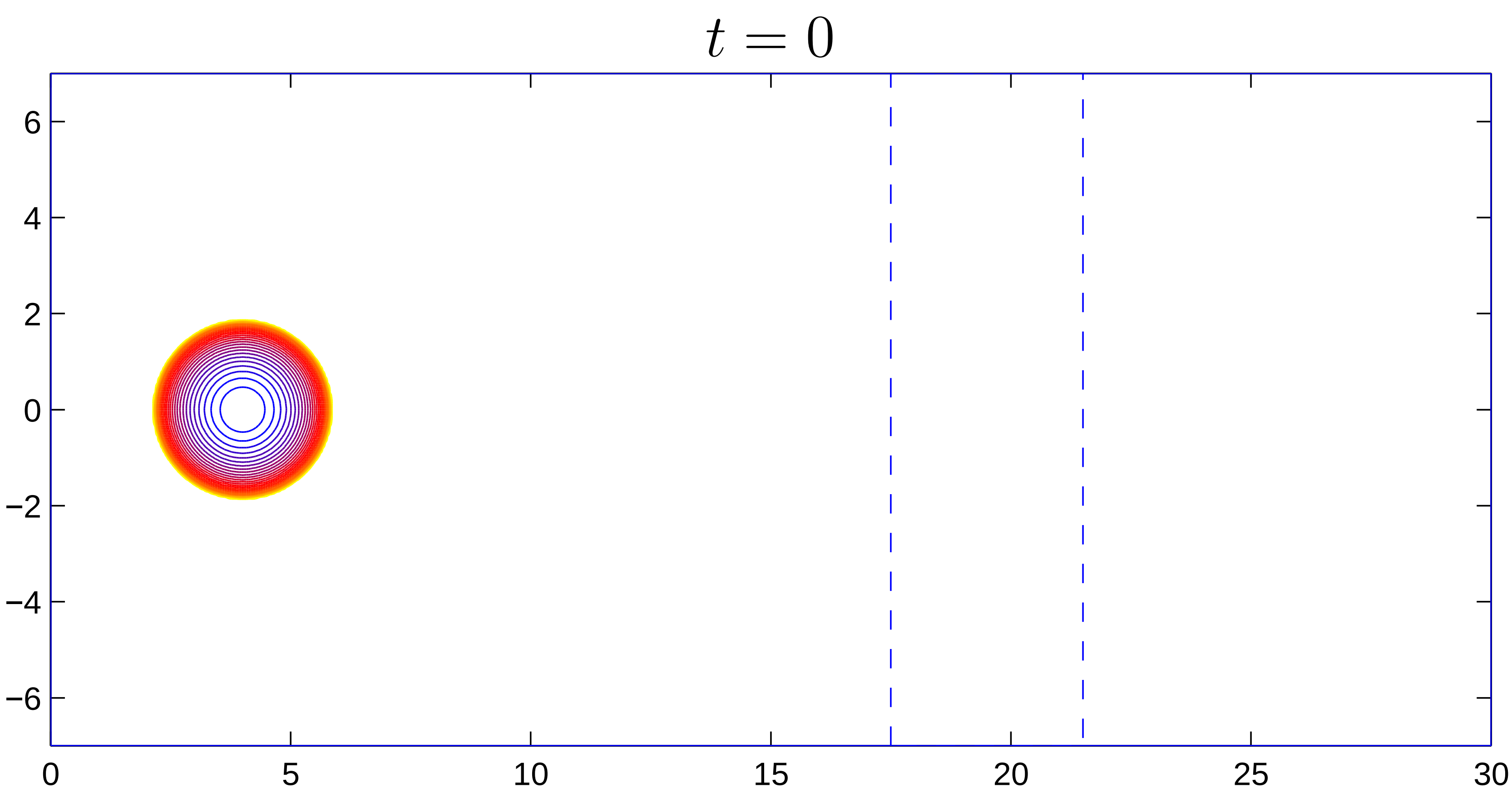

Avalanche on an inclined channel

- Down-flow phase

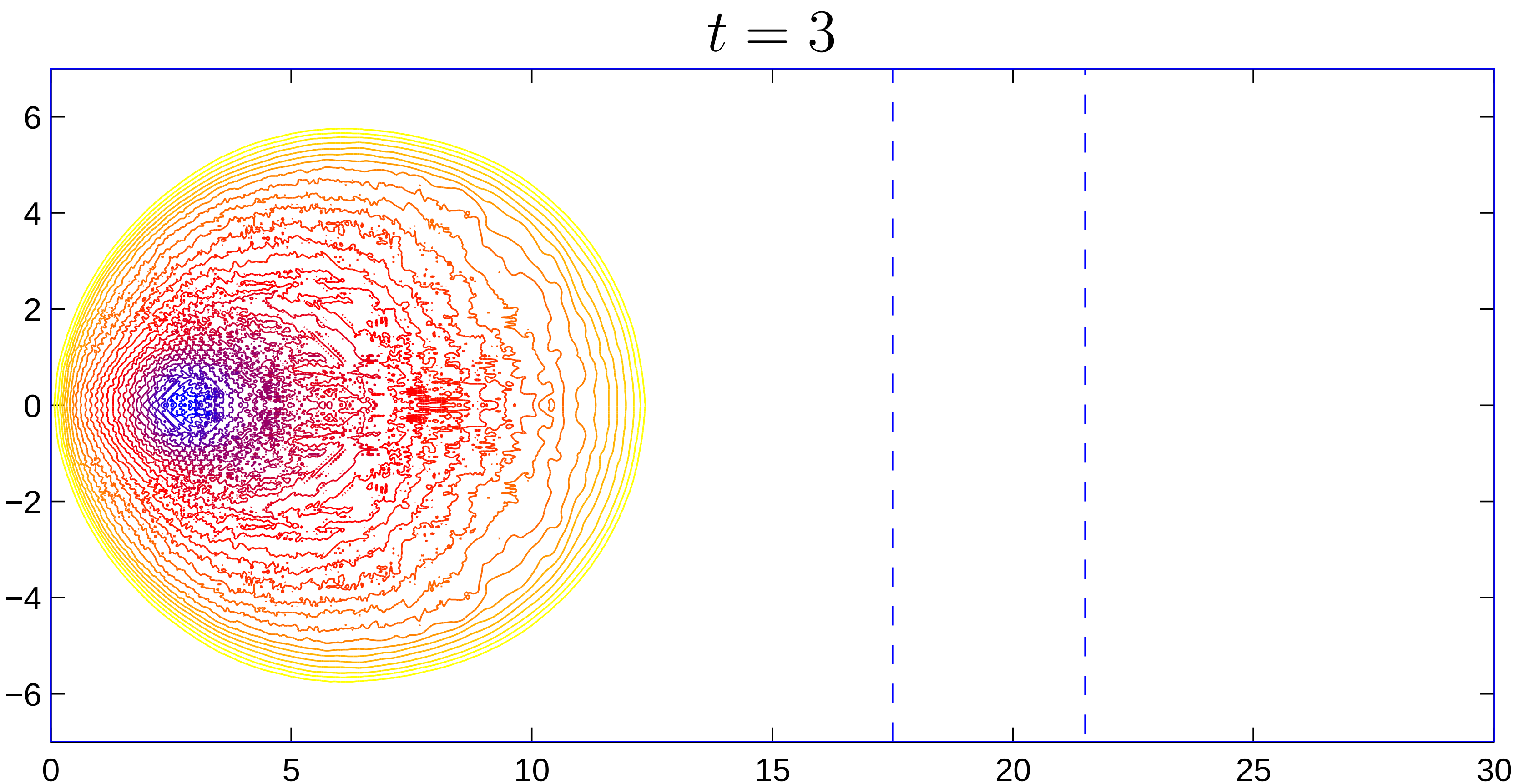

Avalanche on an inclined channel

- Down-flow phase

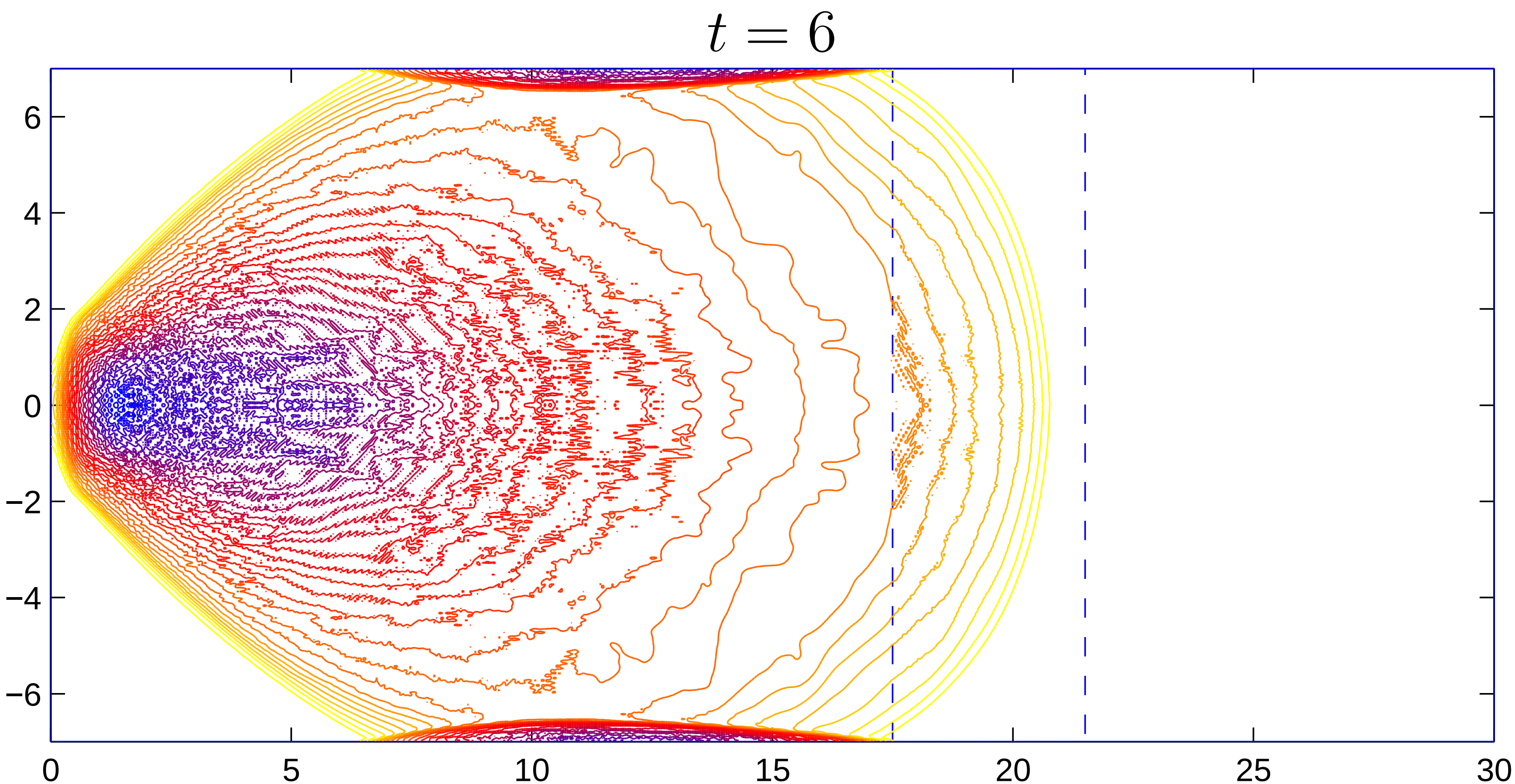

Avalanche on an inclined channel

- Down-flow phase

$t = 9$

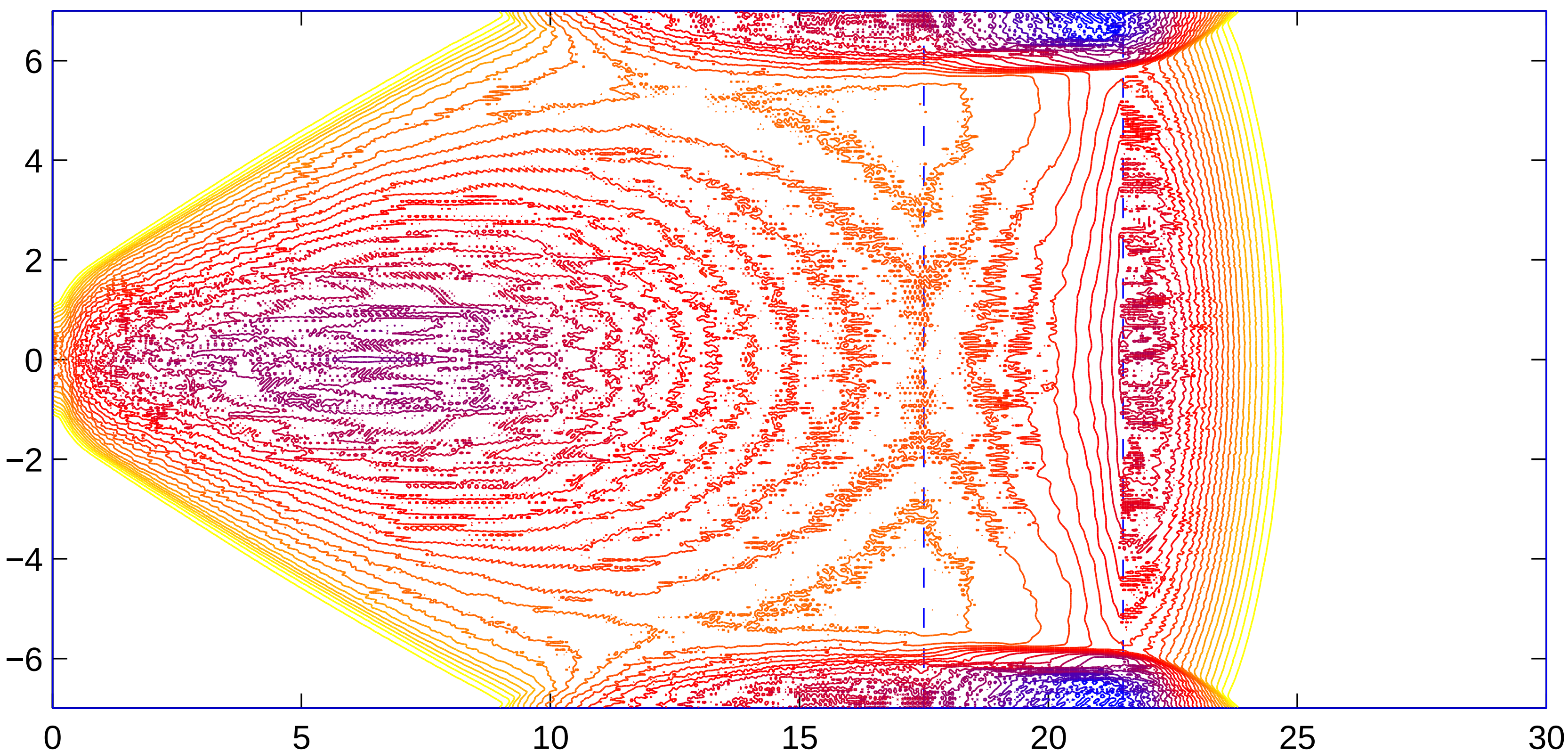

Avalanche on an inclined channel

- Deposit phase

$t = 12$

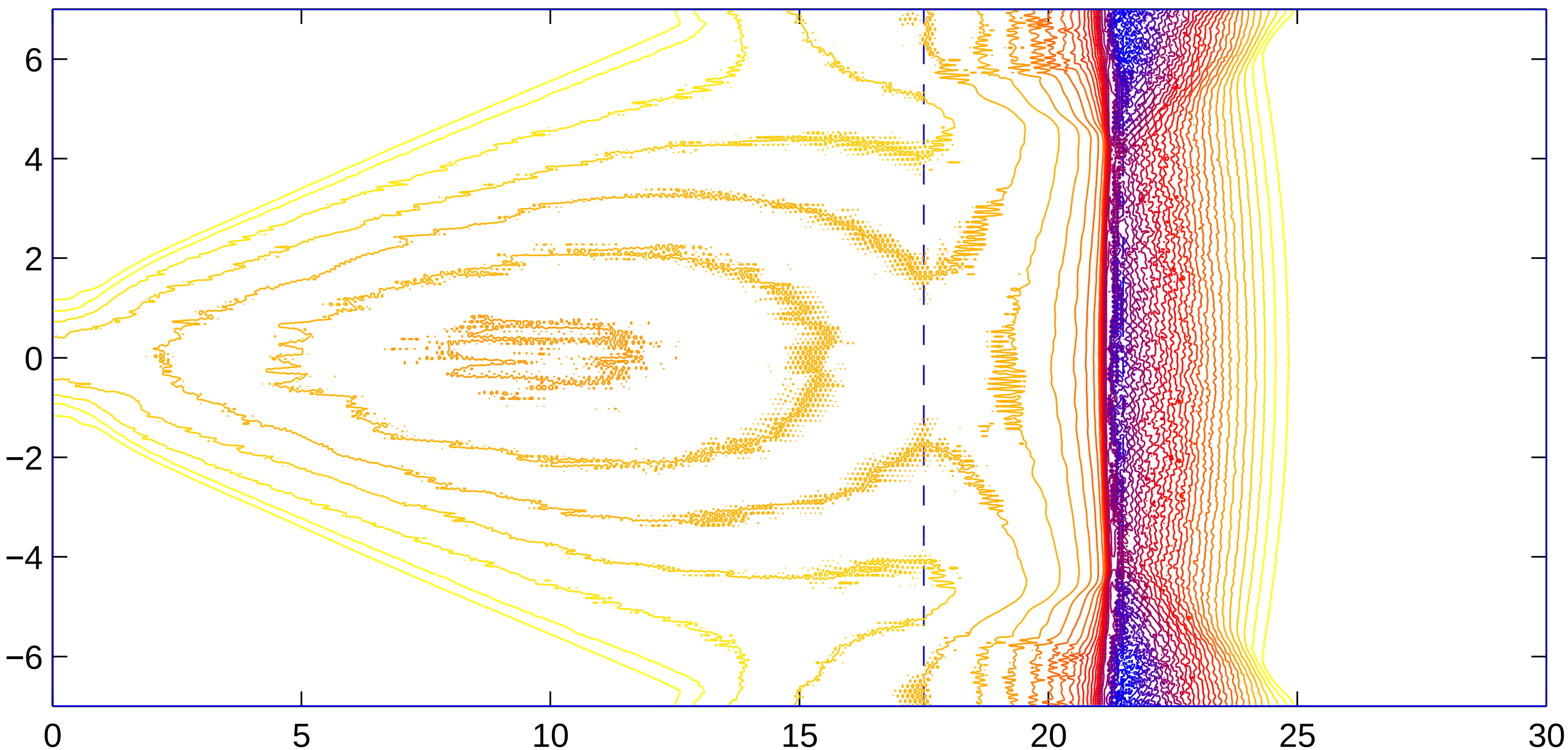

Avalanche on an inclined channel

- Deposit phase

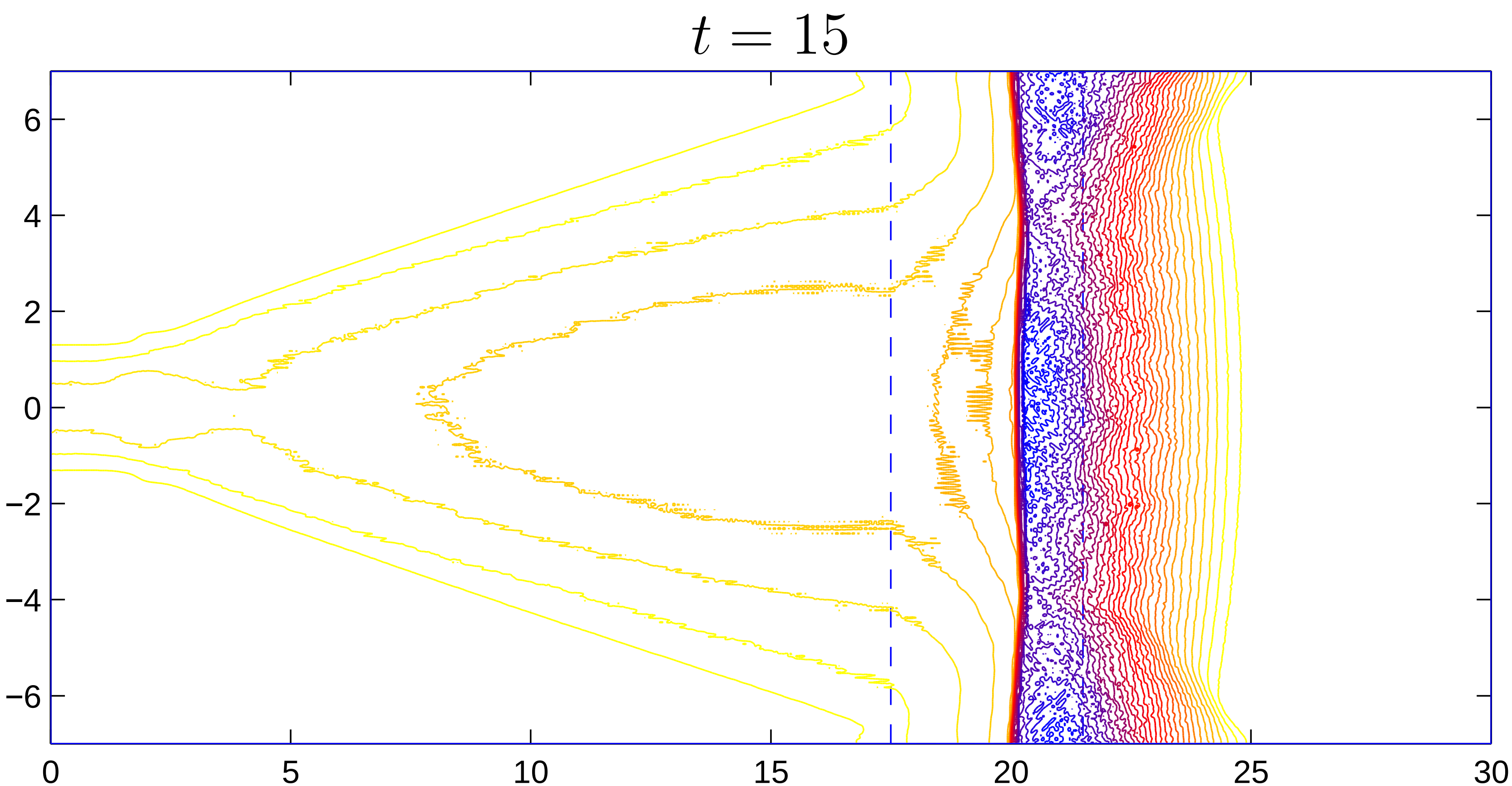

Avalanche on an inclined channel

- Deposit phase

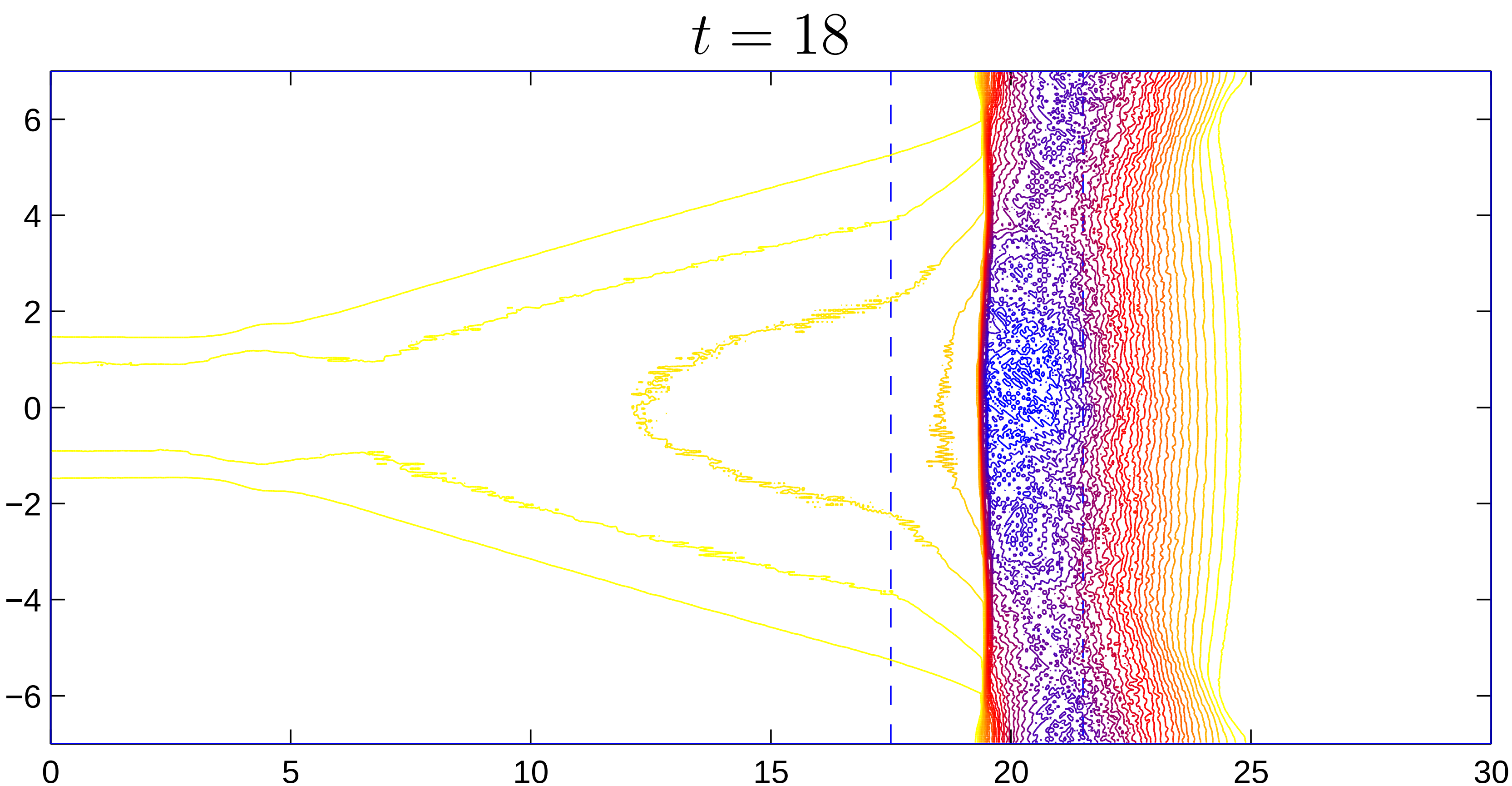

Avalanche on an inclined channel

- Deposit phase

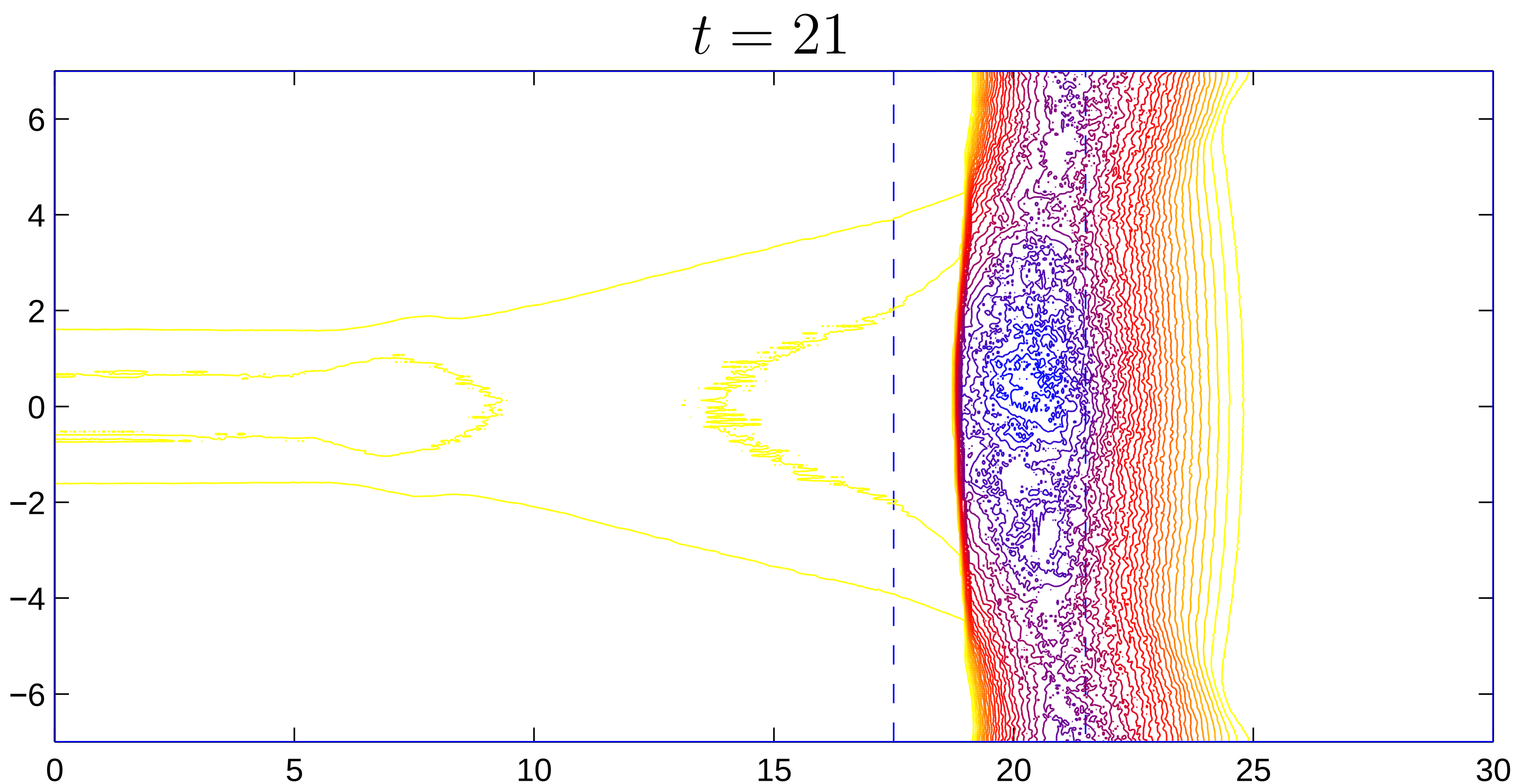

Avalanche on an inclined channel

- Deposit phase

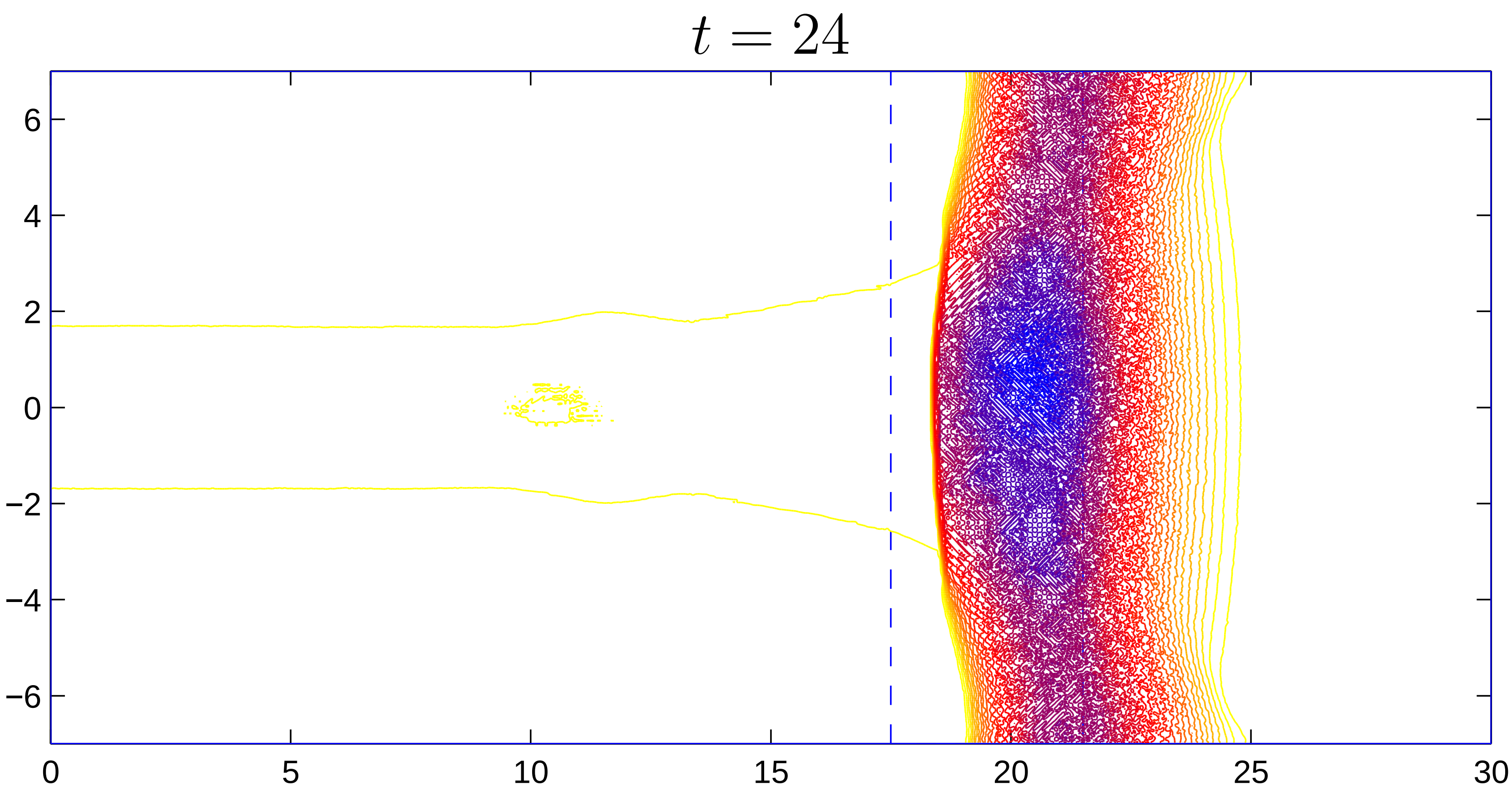

Avalanche on an inclined channel

- Cross-sectional plot along the channel

$$t = 0$$

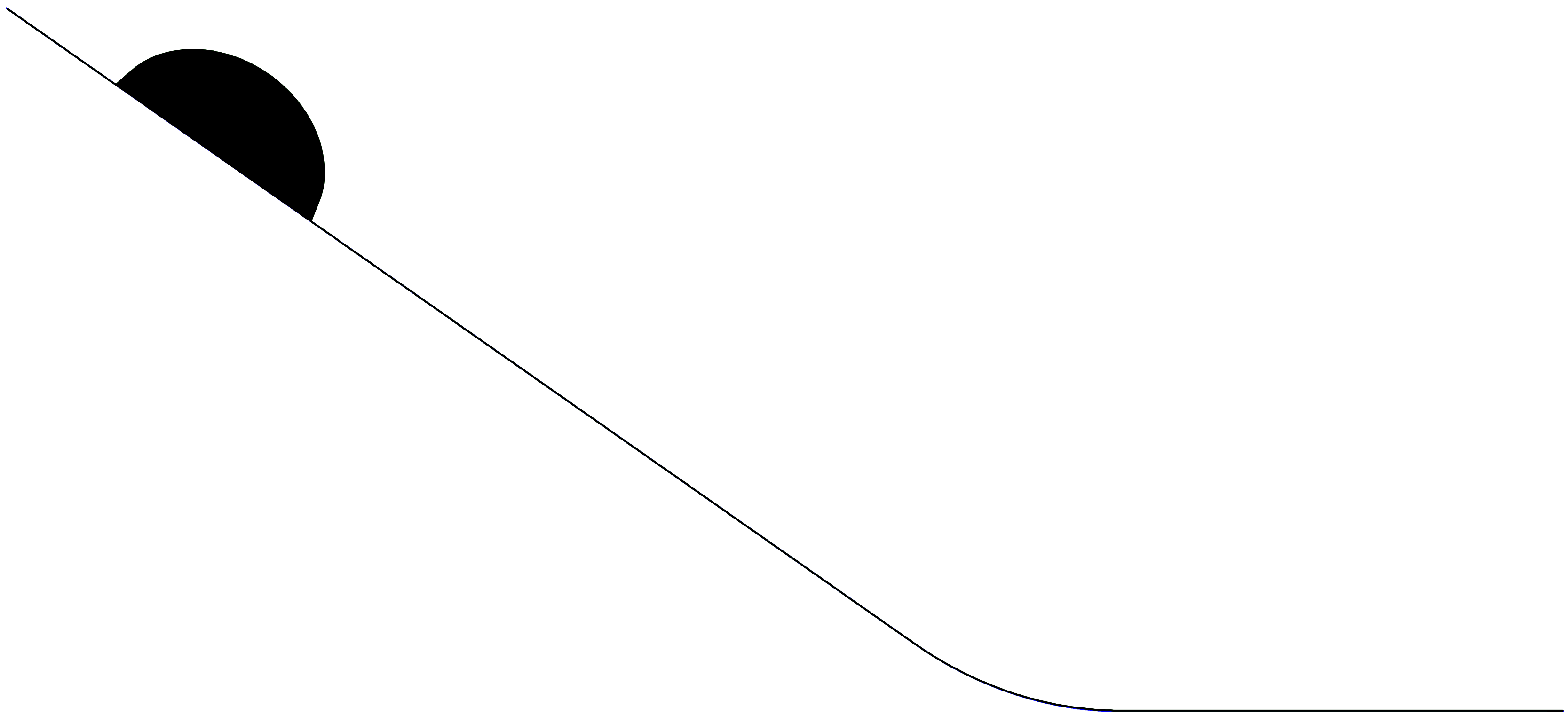

Avalanche on an inclined channel

- Down-flow phase

$$t = 3$$

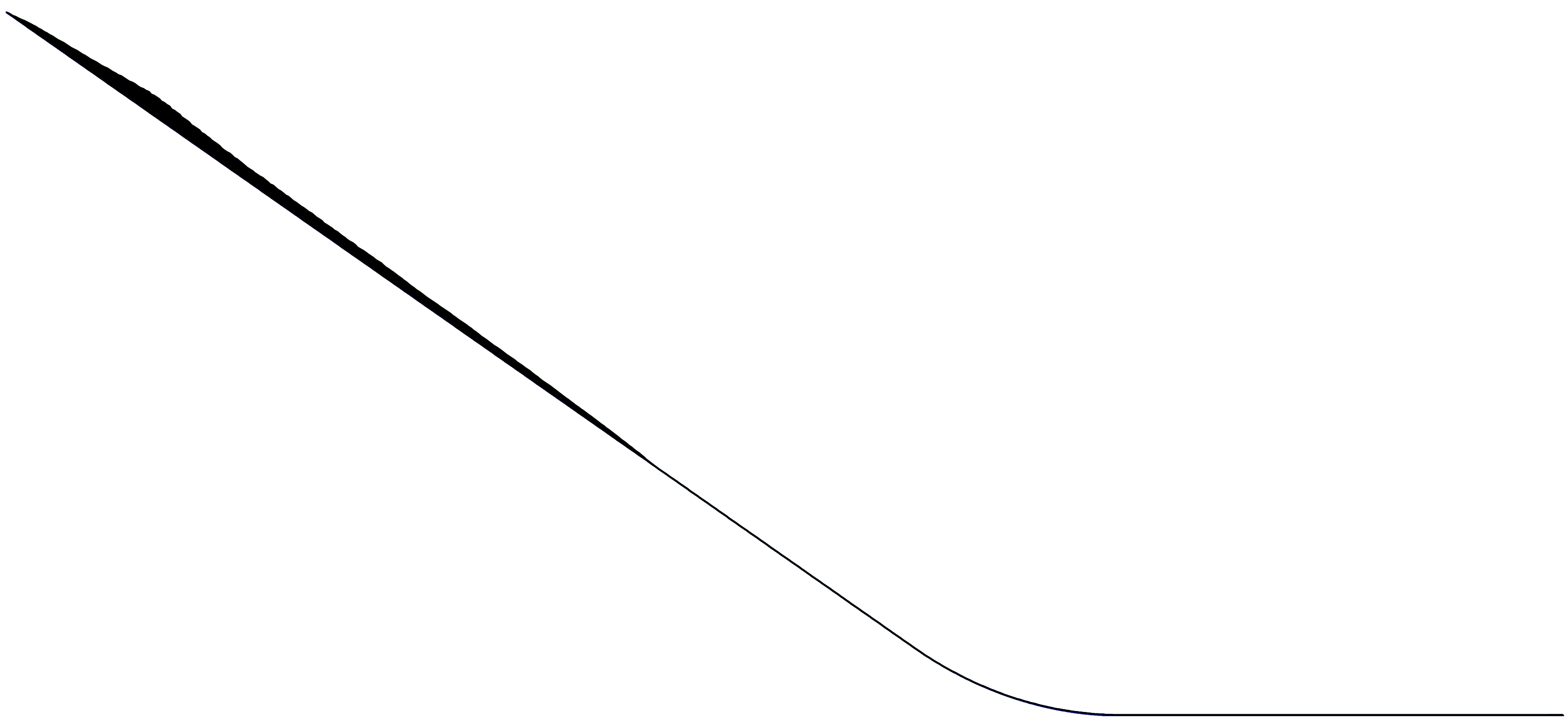

Avalanche on an inclined channel

- Down-flow phase

$$t = 6$$

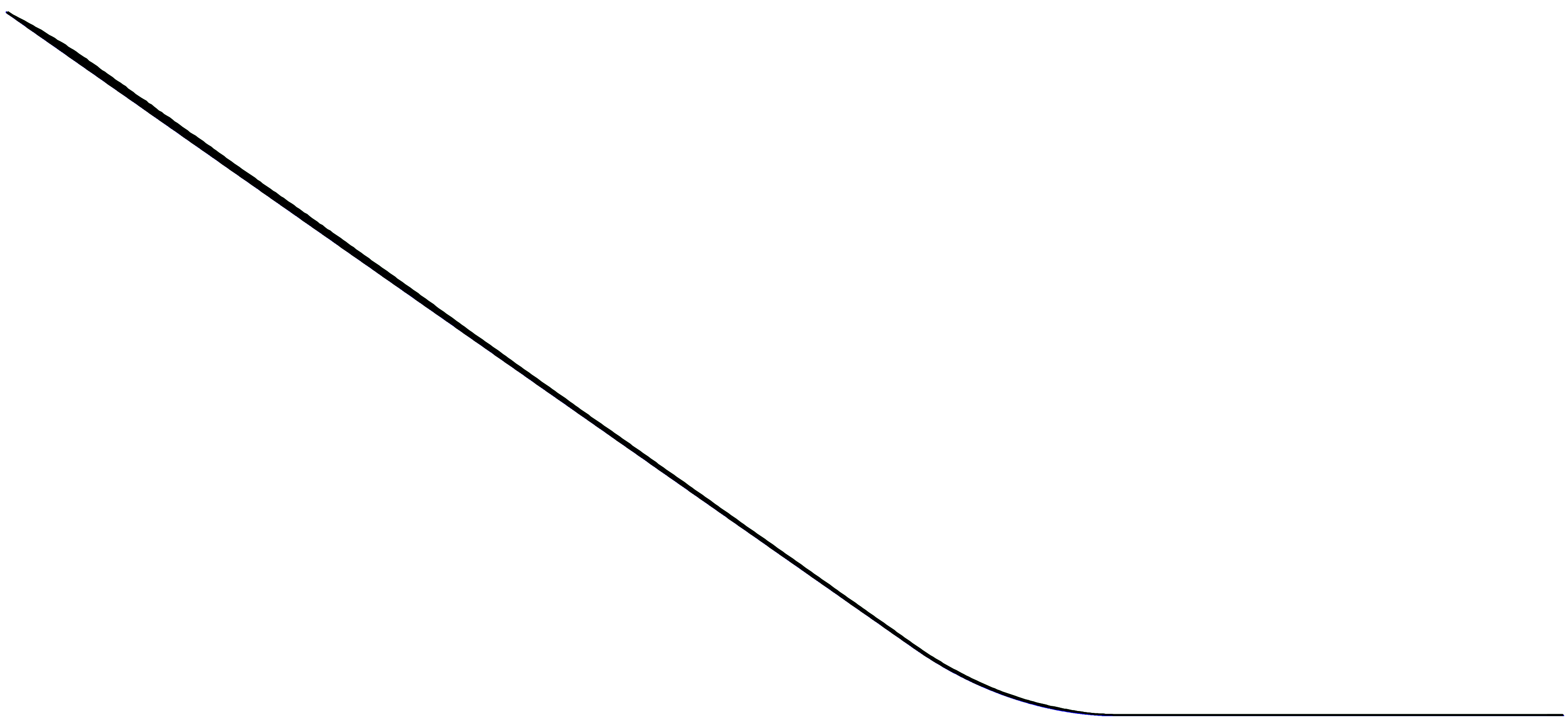

Avalanche on an inclined channel

- Down-flow phase

$t = 9$

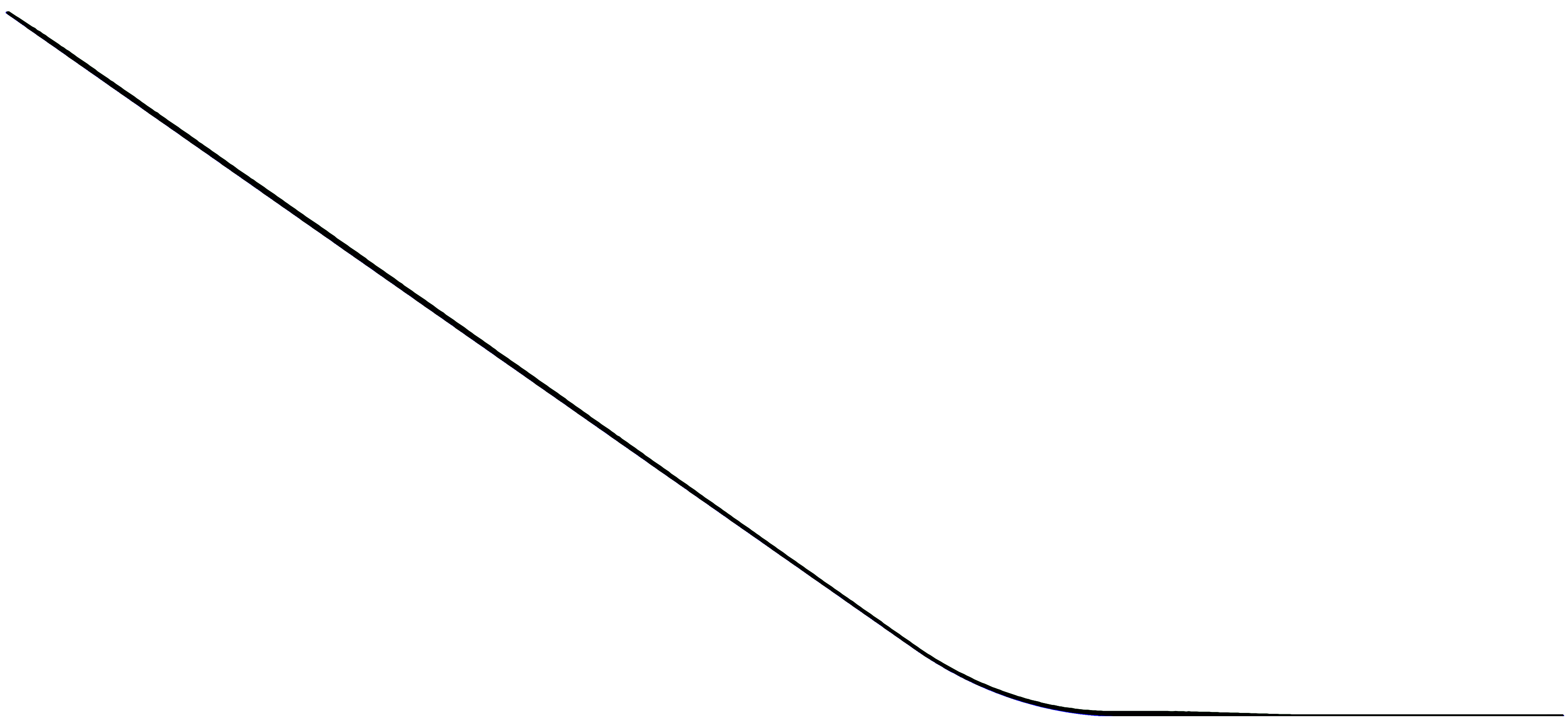

Avalanche on an inclined channel

- Deposit phase

$$t = 12$$

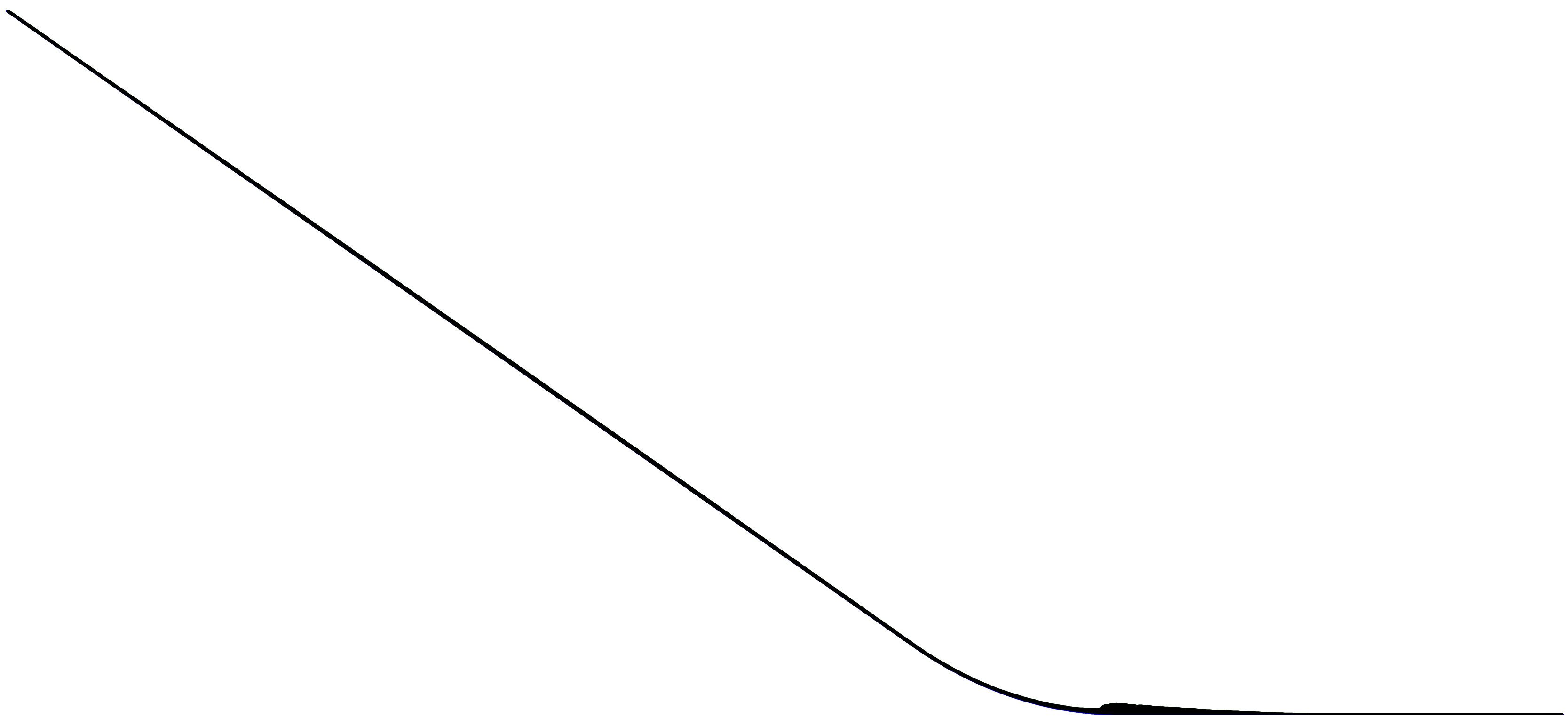

Avalanche on an inclined channel

- Deposit phase

$$t = 15$$

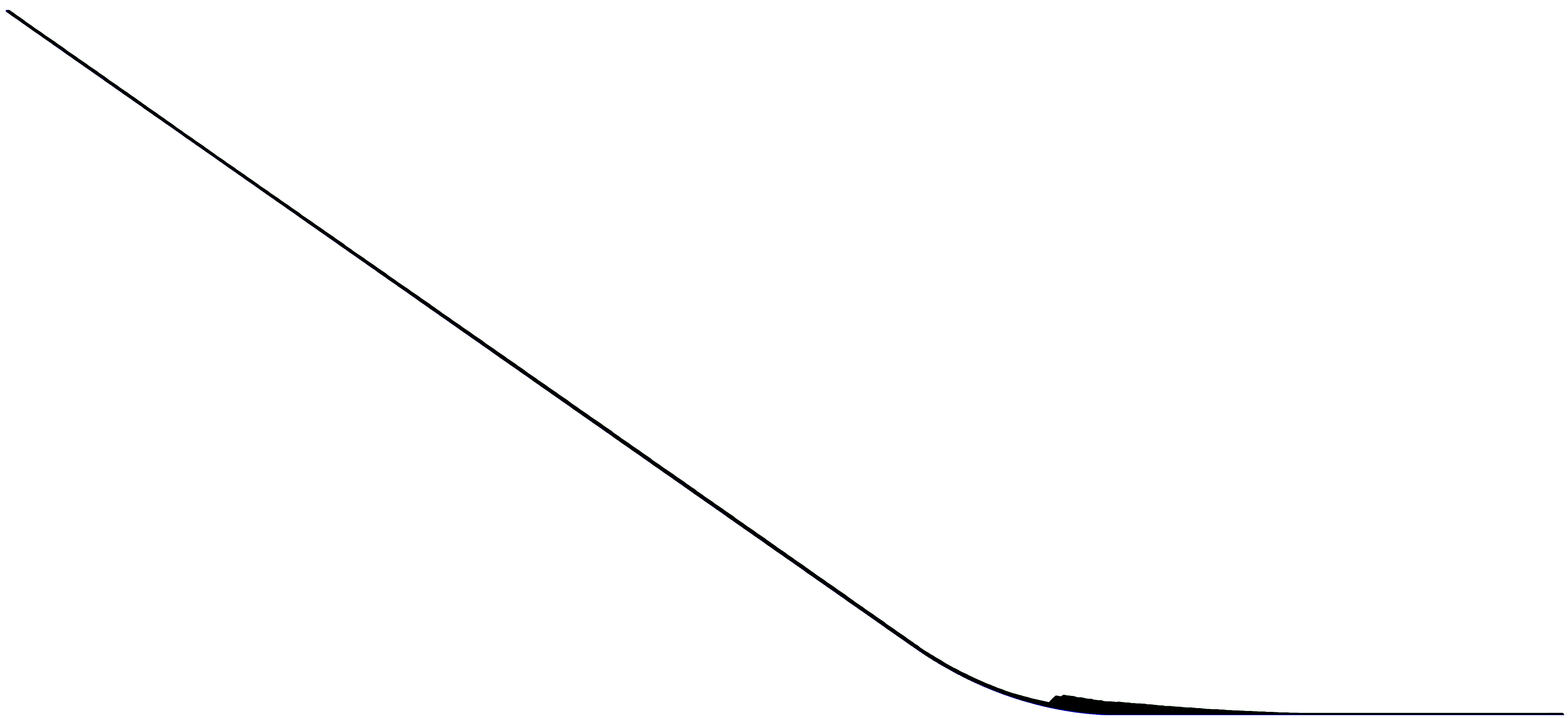

Avalanche on an inclined channel

- Deposit phase

$$t = 18$$

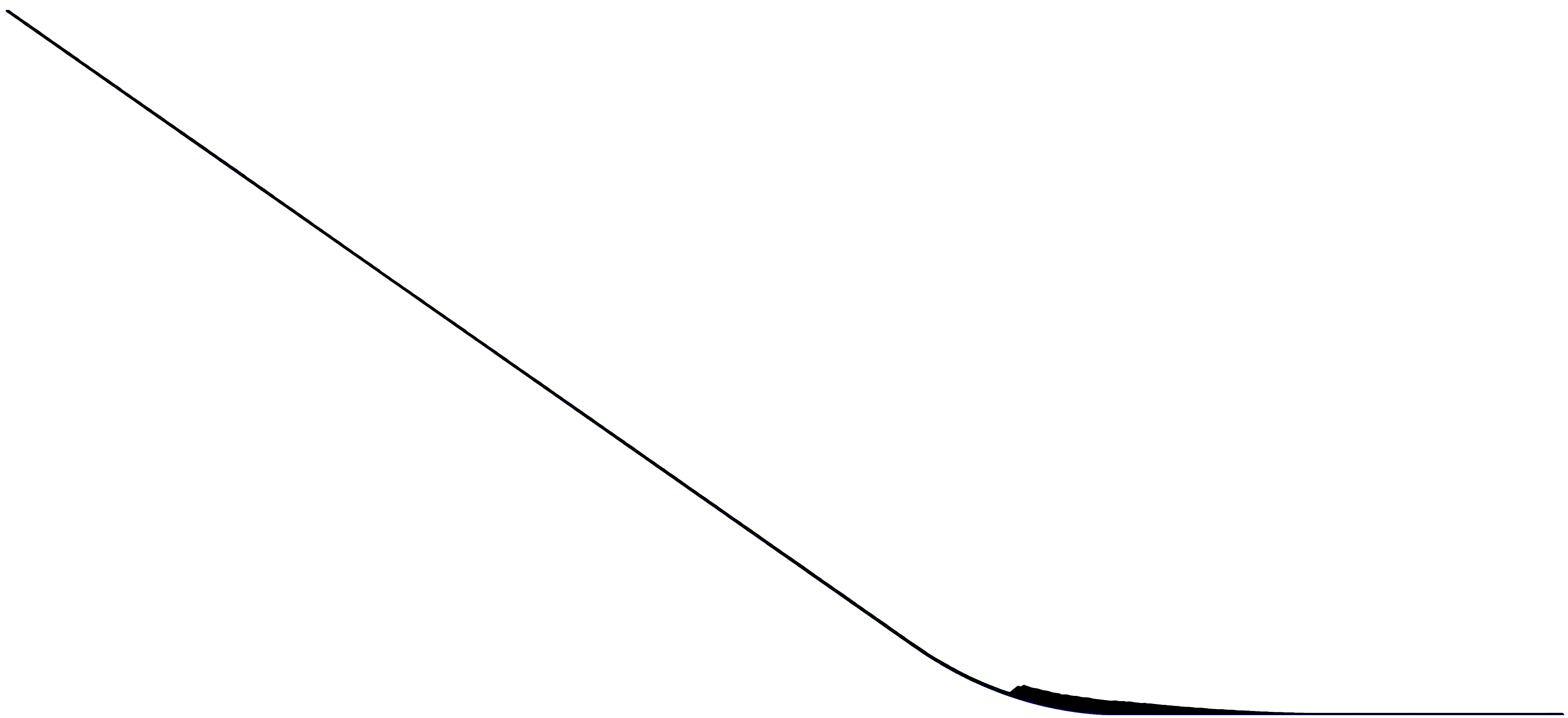

Avalanche on an inclined channel

- Deposit phase

$$t = 21$$

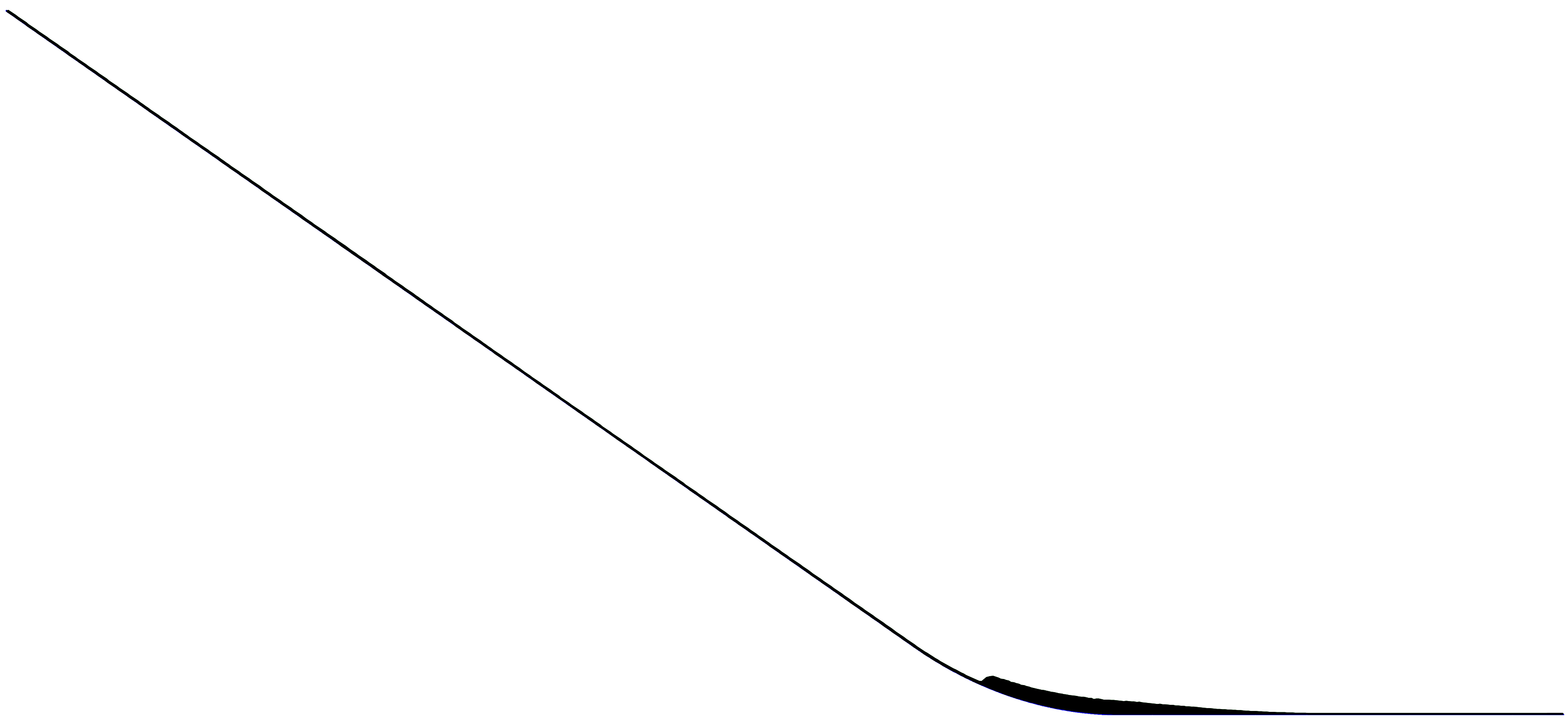

Avalanche on an inclined channel

- Deposit phase

$$t = 24$$

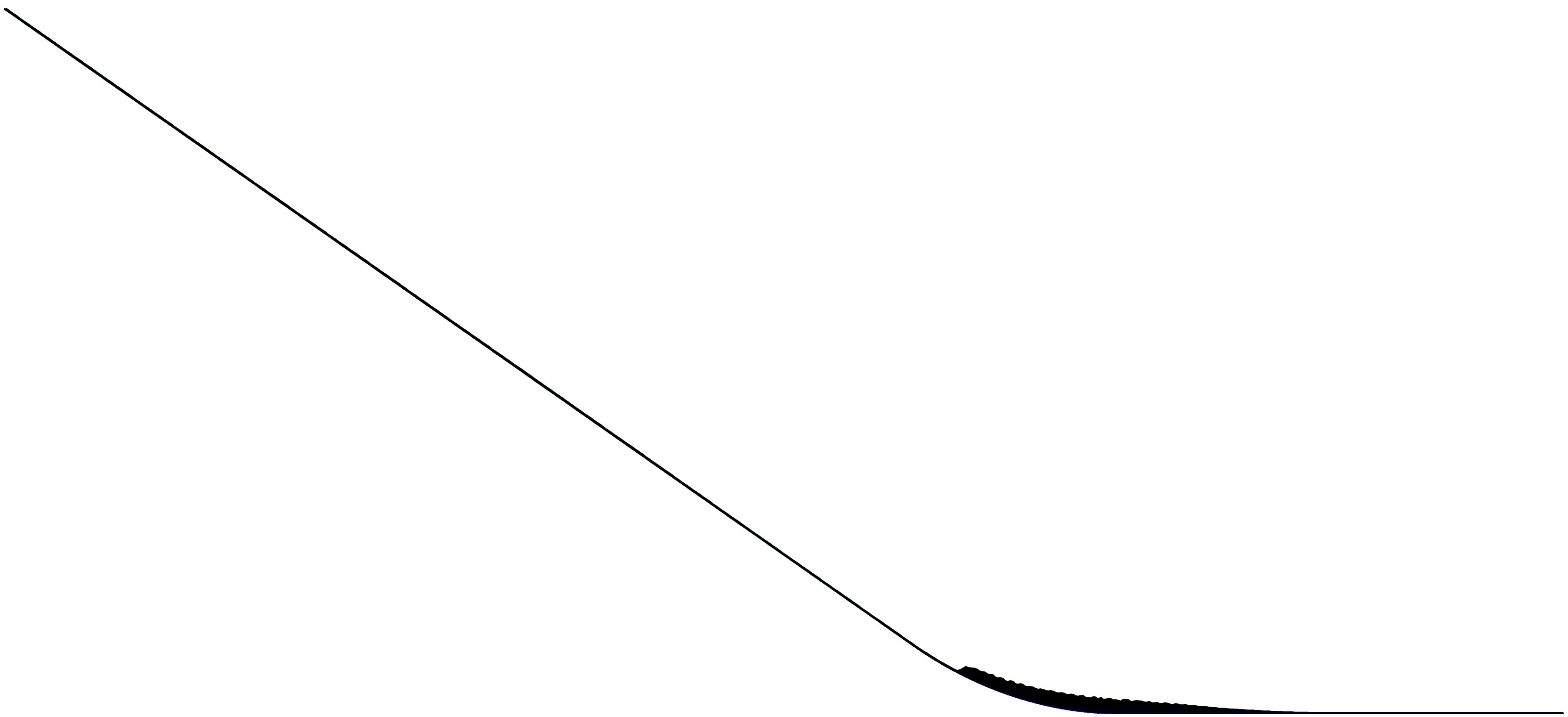

Avalanche on an inclined channel

- Pseudo colors of velocity divergence: Down-flow phase

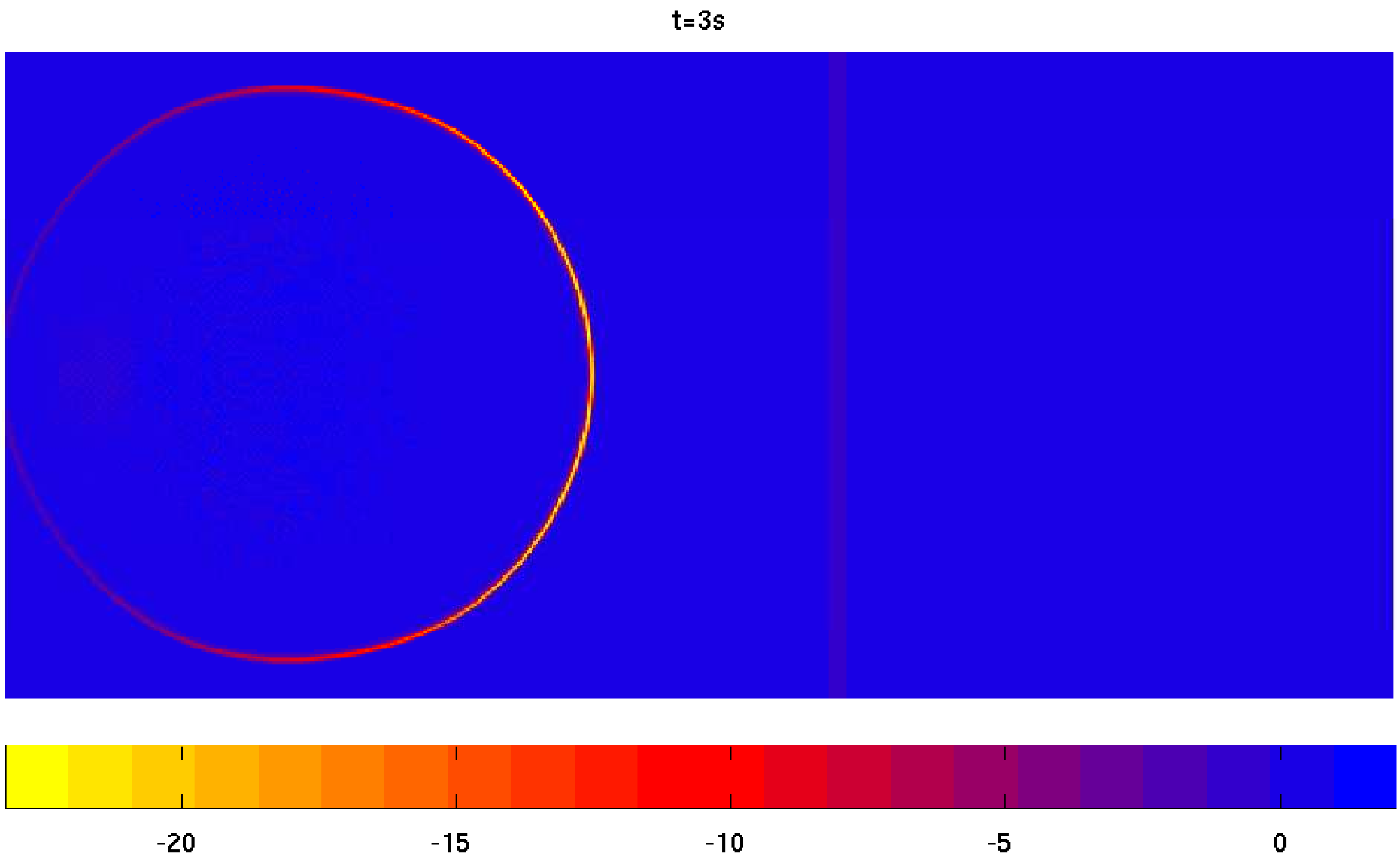

Avalanche on an inclined channel

- Pseudo colors of velocity divergence: Down-flow phase

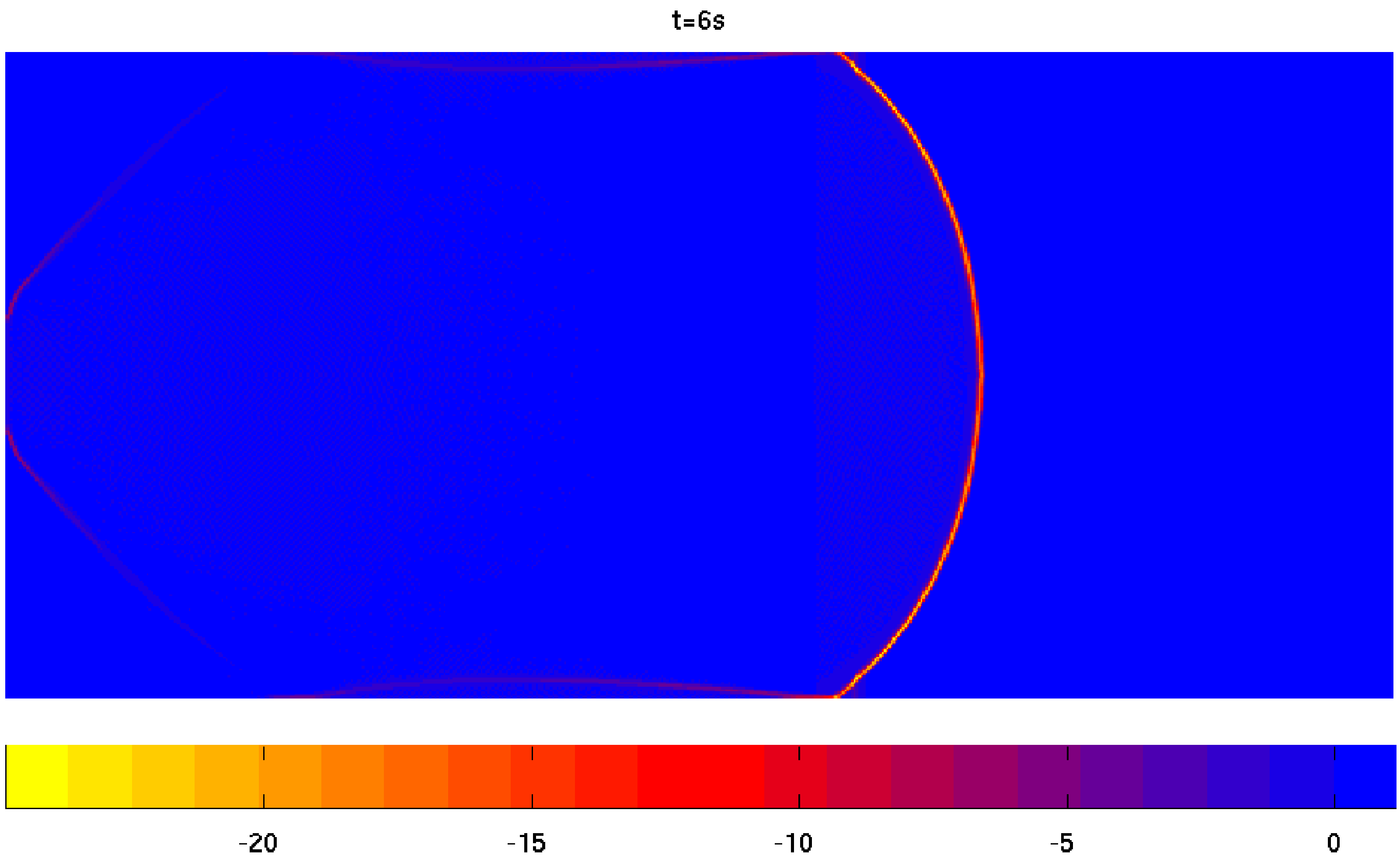

Avalanche on an inclined channel

- Pseudo colors of velocity divergence: Deposit phase

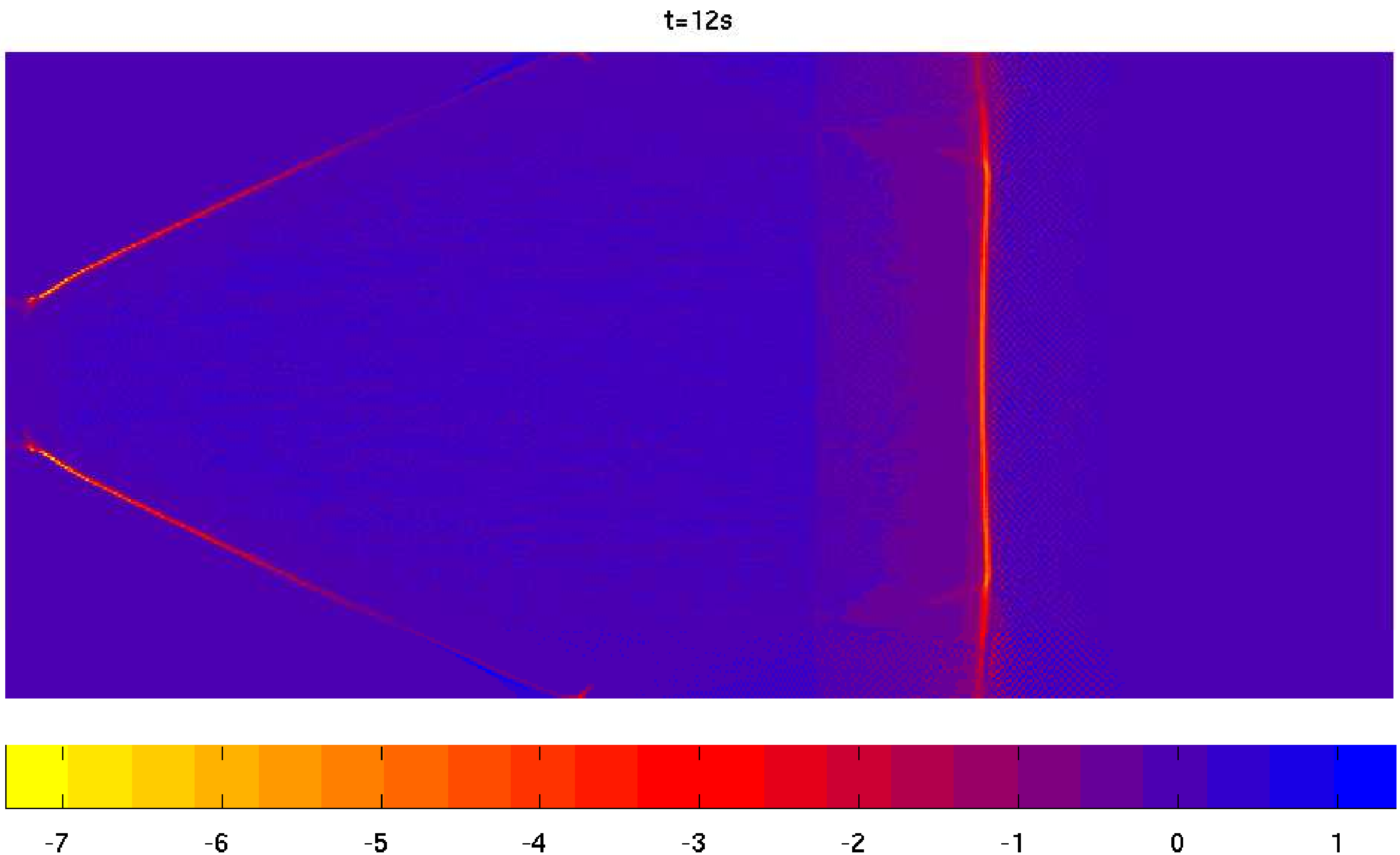

Avalanche on an inclined channel

- Pseudo colors of velocity divergence: Deposit phase

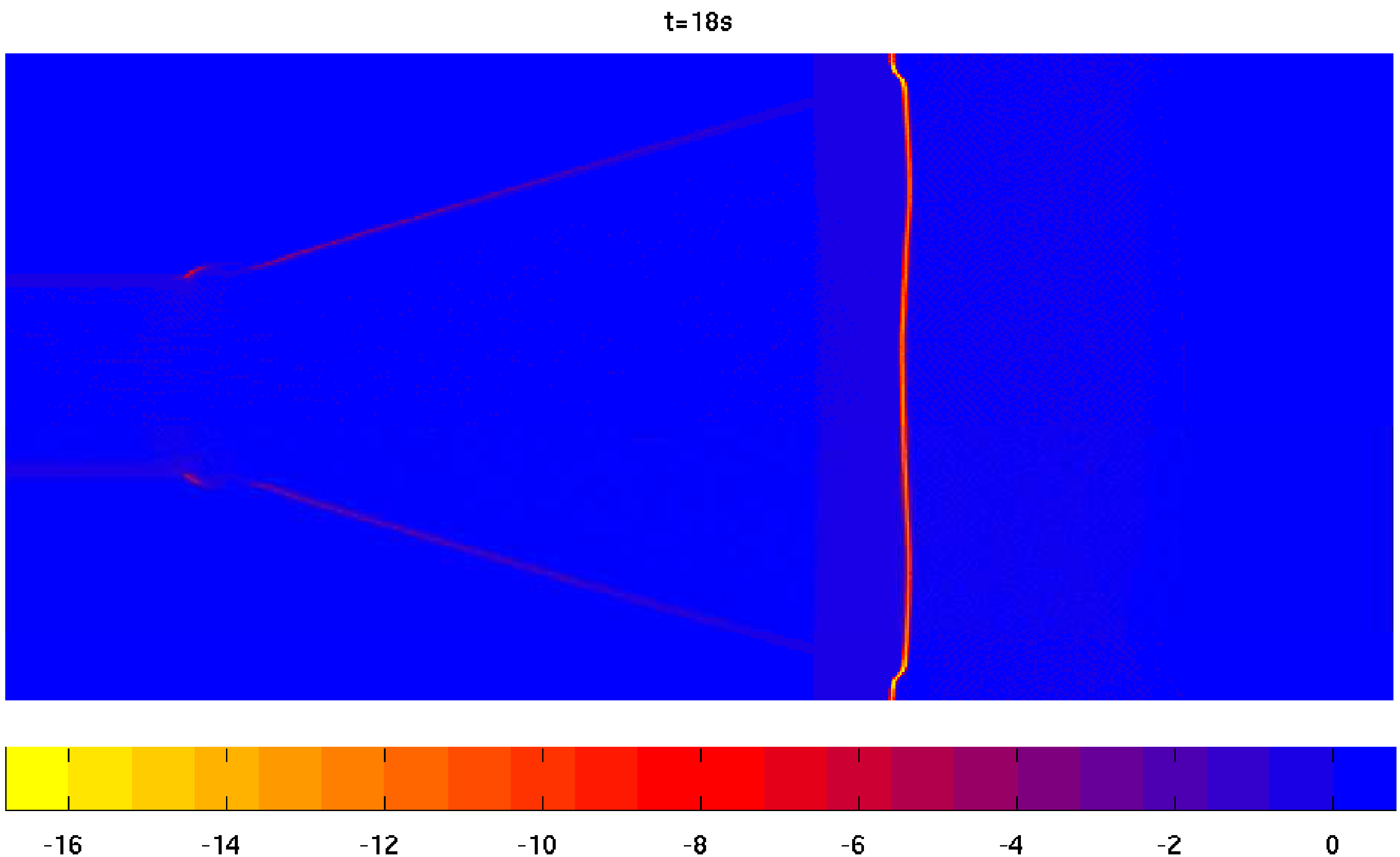

Steady state ramp computation

- A Froude 7 shallow granular flow over a 24.9^o ramp
- Parameters: $\zeta = 32.6^o$, $\phi = 38^o$, $\delta = 31^o$

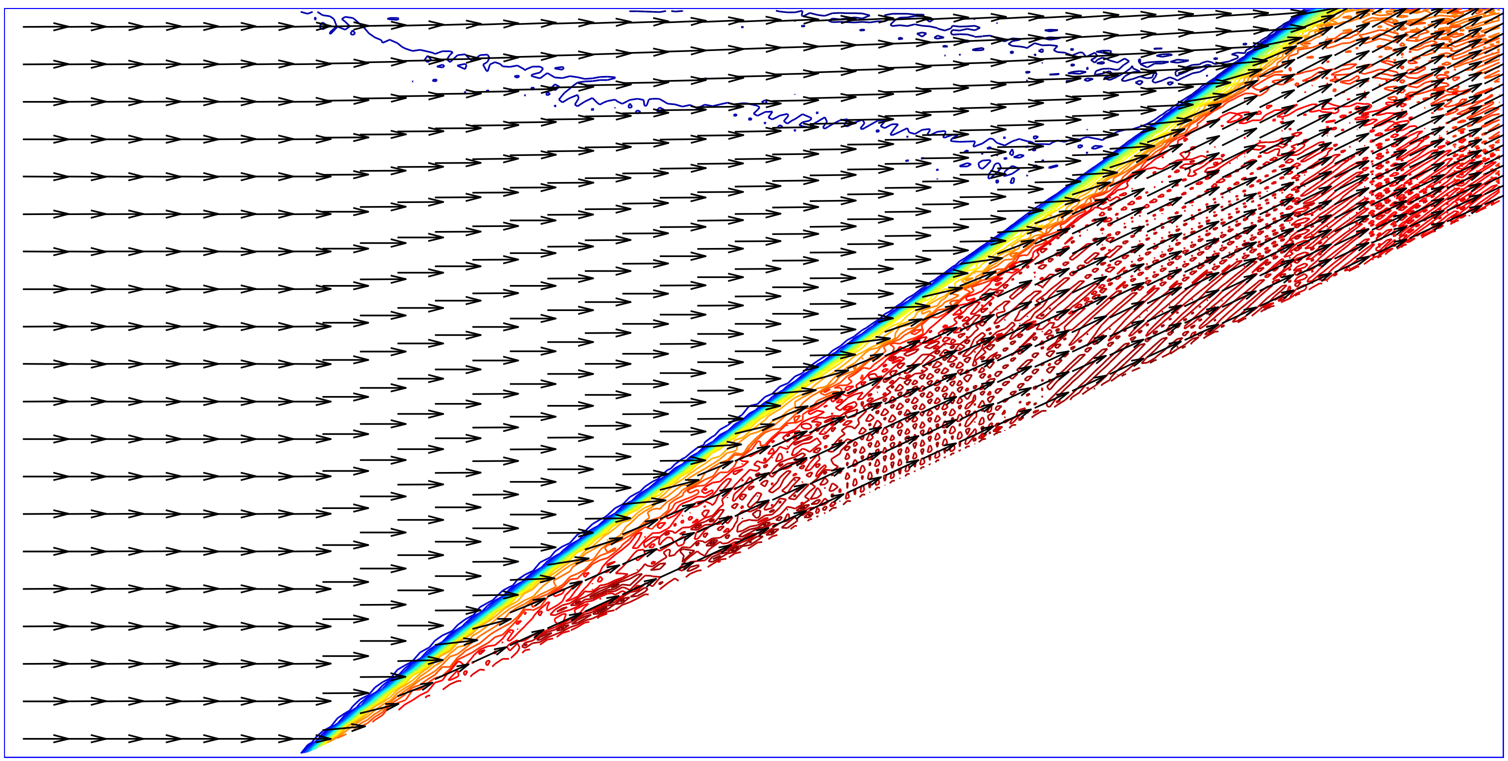

Steady state ramp computation

- A Froude 7 shallow granular flow over a 24.9^o ramp
- Parameters: $\zeta = 32.6^o$, $\phi = 38^o$, $\delta = 31^o$

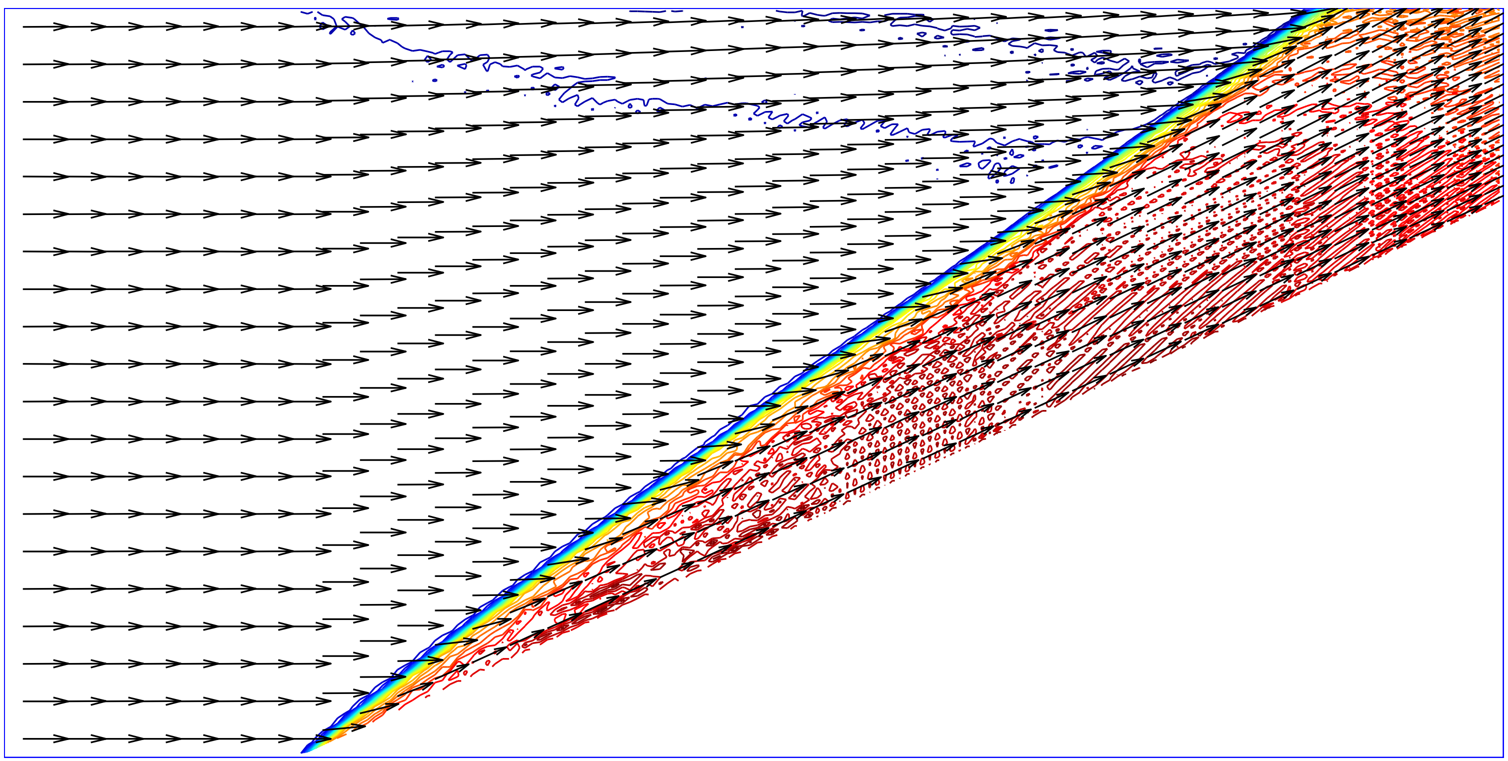

Steady state ramp computation

- Cross-sectional plot along ramp with three different ϕ

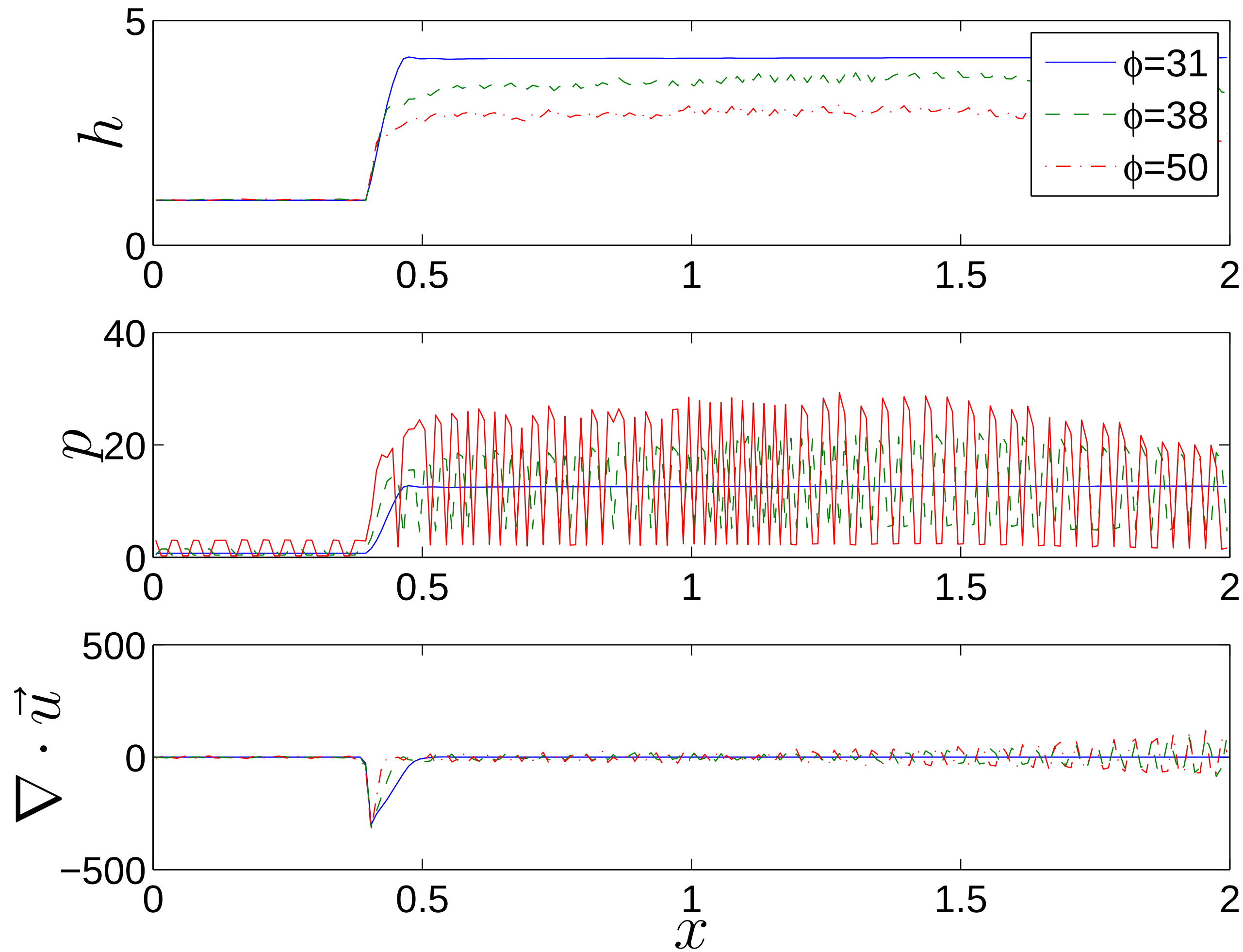

Future direction

- Numerical methodology
  - Vacuum (dry) state treatment
  - Flux & source terms well-balanced
  - Interface sharping by techniques such as Lagrange-like moving mesh or front tracking
  - $\cdots$
- Applications
  - Relaxation model as applied to more practical cavitation problems
  - General depth-average models to granular flows
  - $\cdots$

Future direction

- Numerical methodology
  - Vacuum (dry) state treatment
  - Flux & source terms well-balanced
  - Interface sharping by techniques such as Lagrange-like moving mesh or front tracking
  - $\cdots$
- Applications
  - Relaxation model as applied to more practical cavitation problems
  - General depth-average models to granular flows
  - $\cdots$

Thank You